IRAM Annual Report 2013

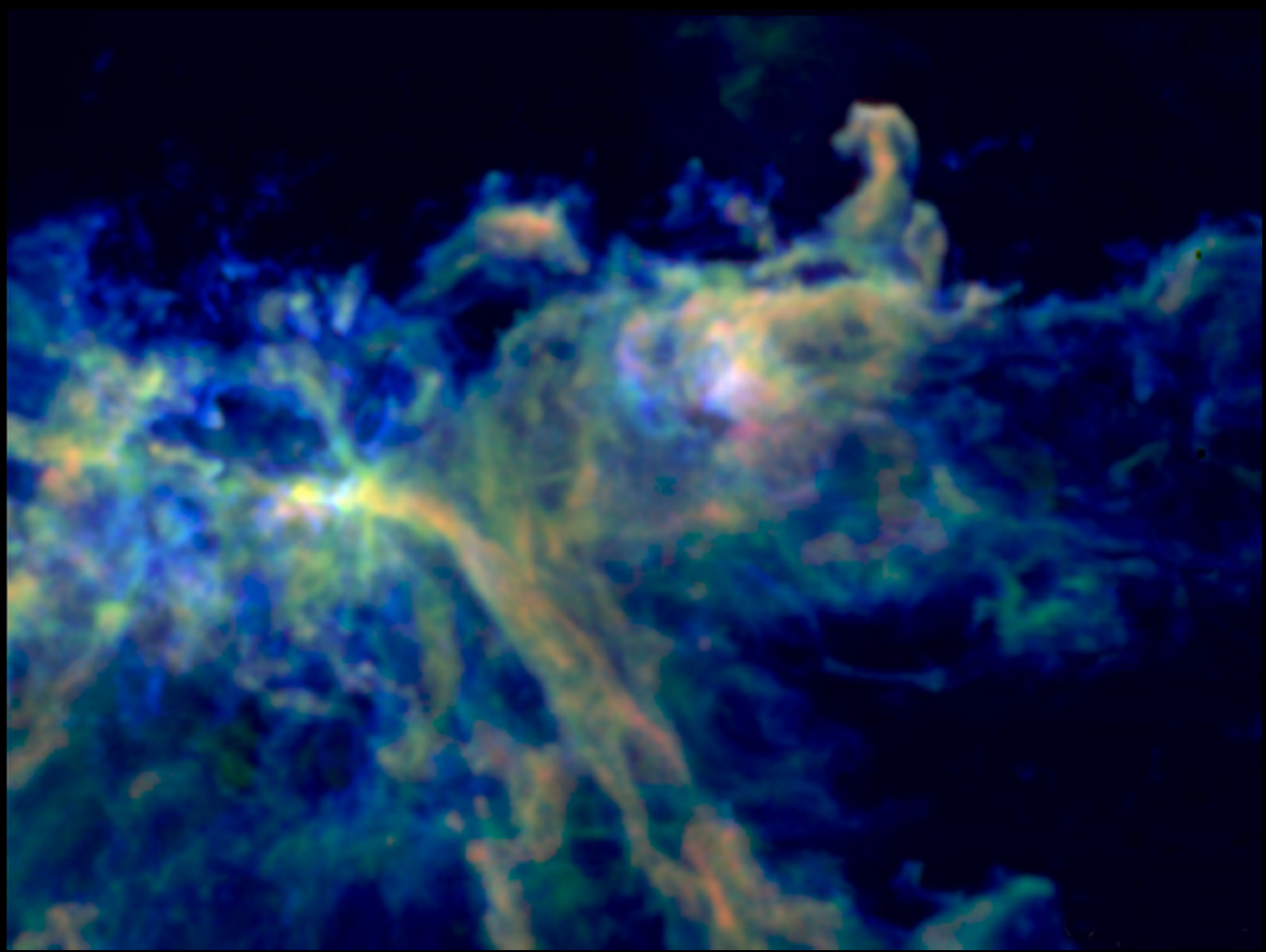

CO emission from the western edge of the prototypical Orion B molecular Cloud. The famous Horsehead pillar and the NGC 2023 and 2024 HII regions can easily be recognized on this false color image of the ^{12}CO (blue), ^{13}CO (green), and C^{18}O (red) line peak brightness temperature. These 3 CO isotopologues enable to distinguish between diffuse and dense gas. (Pety et al. in prep.).

iram
Institut de
Radioastronomie
Millimétrique

IRAM Annual Report 2013

Published by IRAM © 2013
Director of publication Karl-Friedrich Schuster
Edited by Melanie Krips, Catherine Berjaud and Karin Zacher

With contributions from:
Sébastien Blanchet, Walter Brunswig, Isabelle Delaunay, Bertrand Gautier, Frédéric Gueth, Carsten Kramer, Bastien Lefranc, Alessandro Navarrini, Santiago Navarro, Roberto Neri, Juan Penalver, Karl-Friedrich Schuster, Marc Torres

Contents

Introduction 5

Highlights of research with the IRAM telescopes in 2013 6

The observatories 14

The 30-meter telescope 14

Plateau de Bure interferometer 19

Grenoble headquarters 24

Frontend group 24

SIS group 30

Backend group 31

Mechanical group 33

Computer group 35

Science software activities 36

IRAM ARC Node 38

Administration 39

List of staff members 40

Annexes 42

Annex I - Telescope schedules 42

Annex II - Publications in 2013 51

Annex III - Committee Members 61

Introduction

The year 2013 has witnessed some of the most intense levels of activities since the foundation of IRAM.

During 2013 the NOEMA project has started real assembly work on the first antenna (Ant 7) with the antenna mount completed and a successful axes alignment. With intensive preparation work in 2013, reflector assembly is foreseen for the first half of 2014 with subsequent commissioning and operation of the antenna in the interferometer for winter 2014/15. Laboratory work to develop and construct the receivers and the backend has continued at high pace and a wide range of details of progress can be found in the specific sections of this annual report.

The construction of the new Plateau de Bure cable car is progressing well with all the pylons and two the stations now built. Operation is foreseen for the end of 2014.

At the IRAM 30m telescope, EMIR has received its final upgrade with the 2mm channel finally also providing 8GHz 2SB dual polarization operation. This receiver with its dual band capabilities is now by far the most powerful millimeter wave spectroscopy receiver available anywhere. At the same time the continuum camera development program has been pursued very successfully. The NIKA I prototype instrument has explored new solutions for the KID technology and GISMO, the 2mm TES based visiting instrument, has been successfully offered to the community with stunning results in galactic and extragalactic research. Developments for NIKA II, the future large FOV dual band continuum facility camera, have entered its critical phase and the cryostat is actually tested as this text is edited.

After a long and complex process, the IRAM partners have agreed in December 2013 on the new statutes, which were necessary to comply with the evolution of French legislation. More important, however, the partners have agreed to extend their engagement in IRAM at least up to 2024. This horizon allows IRAM to plan securely for the ongoing and upcoming projects, and the evolution of the institute. Finally the partners CNRS, MPG and IGN could agree on a revised funding scheme to compensate for the very difficult economic situation in Spain. This all but easy agreement has enabled IRAM to pursue with its ambitious projects without jeopardizing the fundamentals of successful operation.

Science progressed with many outstanding results from both observatories. In particular the IRAM large programs continued to generate a number of statistically significant data sets that allow researchers to explore the complex mechanisms at work during galaxy and star formation, as well as in the chemical networks of interstellar matter. This underlines the potential of upcoming NOEMA as a unique survey instrument.

The IRAM user community and the IRAM staff are now eagerly looking forward to see the first NOEMA results as soon as the 7th Antenna has been commissioned.

Karl-Friedrich Schuster
Director

Highlights of research with the IRAM telescopes in 2013

CATCHING THE SIGNATURE OF EARLY FRAGMENTATION IN IRDC18310-4

Because of their short evolutionary time-scales, the earliest stages of high-mass star formation prior to the existence of any embedded heating source have barely been characterized until today. Current questions in the field are: Does a single fragment dominate high-mass clumps or do we witness already strong fragmentation during the earliest evolutionary stages? What are the kinematic properties of the gas? Are the clumps sub- or super-virial? To address these and other questions, Henrik Beuther (MPIA/Germany) and collaborators embarked on a program to investigate the fragmentation and dynamical properties by means of PdBI and Nobeyama 45m single-dish data of IRDC 18310-4, a Herschel identified, massive gas reservoir that remains FIR-dark up to 100 µm.

The clump fragments at spatial scales of ~18,000 AU in four cores. Comparing the spatial extent of this high-mass region with intermediate- to low-mass starless cores from the literature, Beuther and collaborators find that linear sizes do not vary significantly over the whole mass regime. However, the high-mass regions squeeze much more gas into these similar volumes and hence have orders of magnitude larger densities. The fragmentation properties of the presented low-to high-mass regions are consistent with gravitational instable Jeans fragmentation. Furthermore, they find multiple velocity components associated with the resolved cores. Recent radiative transfer hydrodynamic simulations of the dynamic collapse of massive gas clumps also result in multiple velocity components

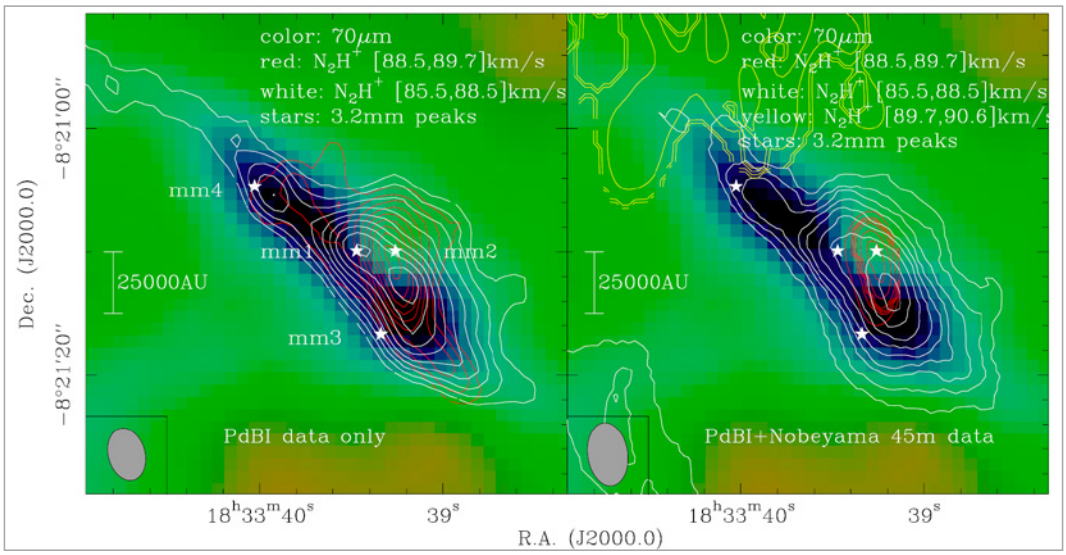

PdBI only (left panel) and merged PdBI plus Nobeyama 45m N_2H^+ (1–0) data (right panel). The color-scale shows the 70 µm extinction feature, and the contours present the integrated N_2H^+ (1–0) emission of three different velocity components as indicated in the figure. Work by Beuther et al. 2013, A&A, 553, A115

along the line of sight because of the clumpy structure of the regions. This result is supported by a ratio between viral and total gas mass for the whole region of <1.

This apparently still starless high-mass gas clump exhibits clear signatures of early fragmentation and dynamic collapse prior to the formation of an embedded heating source. A comparison with regions of lower mass reveals that the linear size of star-forming regions does not necessarily have to vary much for different masses, however, the mass reservoirs and gas densities are orders of magnitude enhanced for high-mass regions compared to their lower-mass siblings.

EARLY STAGES OF CLUSTER FORMATION

Most stars form in clusters rather than in isolation and thus the understanding of cluster formation is intimately related to the understanding of star formation. One of the results found from statistical studies of clusters at optical/infrared wavelengths, carried out for mass sensitivities as low as 0.1–0.5 $M_{\odot}$ and spatial resolutions of ~1000 AU, is that there is a correlation between the mass of the most massive star in the cluster and the number of members in the cluster. However, it is not clear what is the physical reason for this correlation: it could be the result of the initial mass function, it could also indicate that the most massive stars need a rich cluster to be formed, or that the most massive stars are inducing the formation of new stars.

To answer these questions and characterize clusters in the very first stages of their formation, Aina Palau (CSIC-IEEC/Spain) and collaborators observed 4 massive dense cores in the 1mm continuum and ^{12}CO(2-1) line with the ~0.4″ resolution of the IRAM PdBI. The sensitivity achieved in the continuum was sufficient to study their fragmentation down to a mass sensitivity of 0.3 $M_{\odot}$. According to Palau et al., the fragmentation levels are very different among the 4 cores. By combining them with 14 additional cores from the literature they concluded that there is no trend between the numbers of condensations in a cluster and its bolometric luminosity, but there is a weak trend between the mass and the bolometric luminosity of the strongest mm-source, which suggests a picture in which cores fragment to protostars. The study suggests the core formation efficiency is proportional to the density of the massive dense core, which provides support to the idea that gravity dominates as density increases. It also shows a correlation between the number of detected condensations and the number of infrared sources, indicating that different episodes of star formation keep the same fragmentation level with time.

Overall, the observations suggest that the optical/infrared correlation previously found between the mass of the most massive star of the cluster and the number of members in the cluster is not set at the early stages of cluster formation but probably arises as a result of cluster evolution.

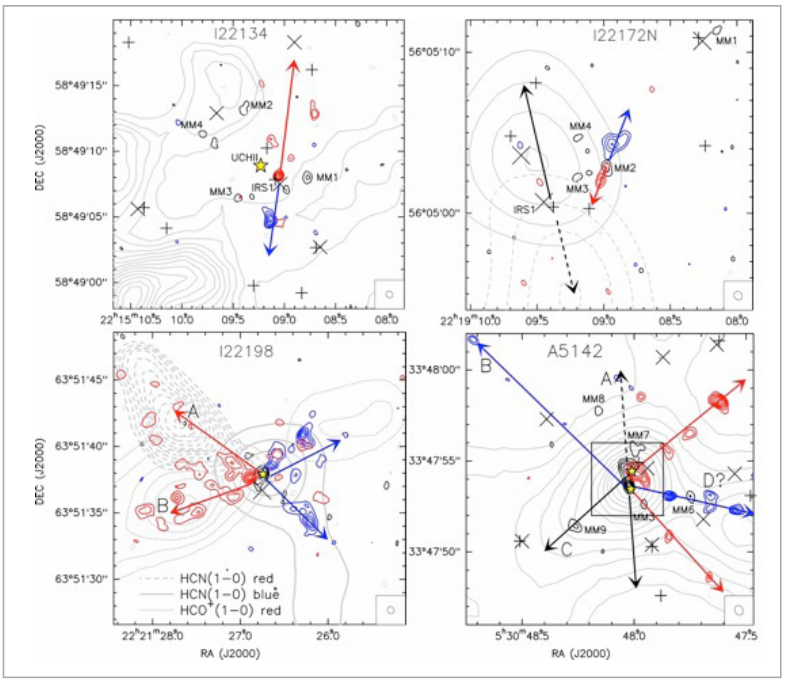

IRAM PdBI 1.3mm continuum maps of I22172N, I22134, I22198 and A5154 at ~0.4″ resolution, with blue-shifted (blue contours) and red-shifted ^{12}CO(2-1) line emission overlaid. Labels identify sources detected down to a sensitivity level of ~0.3 $M_{\odot}$. Work by Palau, 2013, ApJ, 762, 19

DISSECTING AN INTERMEDIATE-MASS PROTOCLUSTER IN ORION

The vast majority of stars in our Galaxy form in clusters. In particular, our Solar System likely formed within a large cluster containing massive stars. Understanding its birth should therefore involve investigating high-mass protoclusters in our Galaxy. However, these are typically located at large distances (>1kpc) and have a complex morphology, which altogether hinders their observational study. Intermediate-mass (IM) protoclusters, on the other hand, are commonly less crowded and can be found at smaller distances. They contain future IM stars, which have the ability to photo-dissociate and ionise the surrounding gas, as their high-mass counterparts. IM protoclusters thus represent

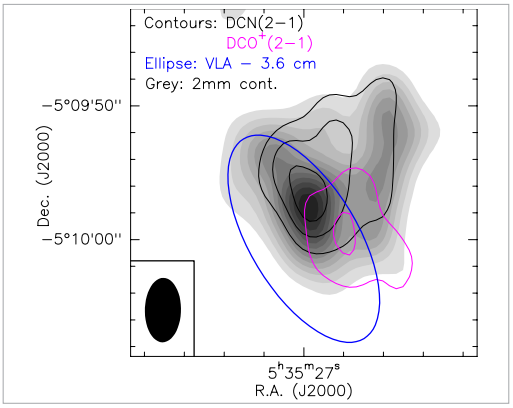

PdBI molecular line contour maps overlaid on the 2-mm continuum emission (grey scale). The blue ellipse marks the position and size of the VLA 3.6 cm emission. Work by López-Sepulcre et al. 2013, A&A, 556, A62

excellent laboratories for studying clustered star formation at almost the full range of stellar masses.

OMC-2 FIR 4 is an IM star-forming region located in the Orion A molecular complex, at a distance of 420 pc. It is one of the targets of the Herschel guaranteed-time Key Programme CHESS, which has provided an almost complete spectrum between 480 and 1910 GHz. In addition, broadband spectral surveys of this region at 1, 2, and 3 mm have been obtained with the IRAM 30-m telescope. High-angular resolution observations are therefore a crucial tool to help disentangle the information hidden in the often-complex line profiles of the single-dish spectral surveys.

Using the IRAM Plateau de Bure Interferometer, Ana López-Sepulcre (IPAG/ France) and collaborators observed the continuum emission and several molecular lines in OMC-2 FIR 4 with an angular resolution of ~4" (~2000 AU), the best one achieved so far for this region. The PdBI maps reveal the clumpy nature of OMC-2 FIR 4, indicating that it is not a single IM protostar, as previously believed, but a whole cluster of low- to intermediate-mass protostars. López-Sepulcre and co-authors identified three spatially resolved sources, of one or several solar masses each, with hints of further unresolved substructure. Two of these sources are associated with dust continuum emission peaks, thus likely containing at least one molecular core each. One of them also displays radio continuum emission, as seen with the Very Large Array (VLA), which may be attributed to a young B3-B4 star that dominates the overall luminosity of the region. The third identified source displays a DCO^+(2–1) emission peak and weak dust continuum emission, suggesting a lower temperature, and hence its possible association with either a younger low-mass protostar or a starless core.

W43 HERO - ON THE ENVIRONMENTS OF MASSIVE STAR FORMATION

Massive stars play a crucial role in star formation and in the mass and energy balance of the interstellar medium, yet in spite of this importance the formation of massive stars remains a largely unknown process. To develop a better understanding on the sites of high-mass star formation, on how giant molecular clouds and cloud ridges are assembled, and environments with different properties can change pathways to massive star formation, Frédérique Motte (AIM/CEA/ France) and Peter Schilke (Uni.Cologne/Germany) have established an international collaboration to embark on W43 HERO (Hera/EmiR Observations), a Large Program at the IRAM 30m telescope. The aim of W43 HERO is two-fold: study the dynamics of the molecular gas over a square degree region centered on W43 with unprecedented spectral resolution (~0.1 km/s) using the ^{13}CO(2-1) and C^{18}O (2-1) line transitions (Carlhoff et al. 2013), and investigate the physical and chemical conditions of the densest clouds at the center of the complex using the spectral signatures of molecular high-density tracers (Nguyên-Lu'o'ng et al. 2013). The survey covers a large range of spatial scales, between 0.3 and 140pc.

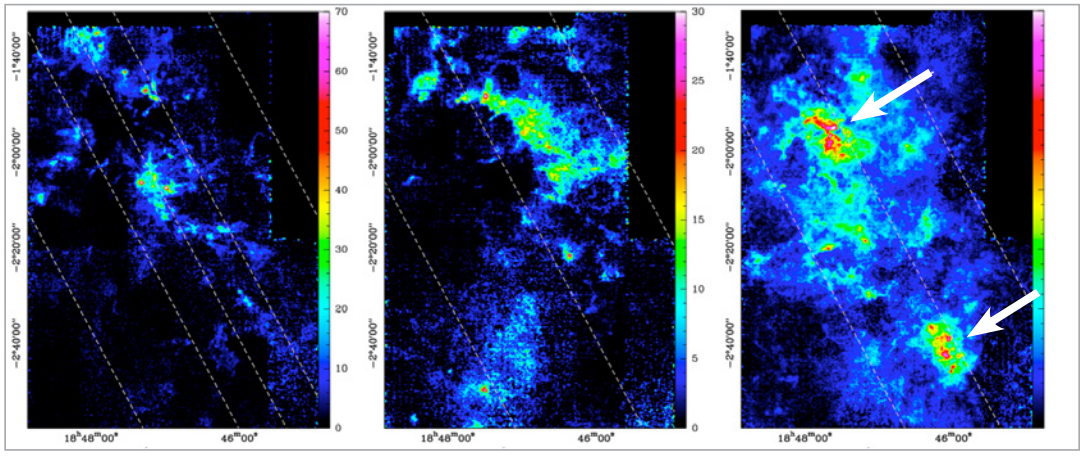

Velocity integrated ^{13}CO(2–1) maps over the range 35 to 55 km.s^{-1} (left), 65 to 78 km.s^{-1} (middle) and 78 to 120 km.s^{-1} (right; white arrows identify the two main clouds, W43-Main and W43-South). The white stripes mark the Galactic plane and the planes 30 pc above and below it for the molecular complexes at 4 and 12 kpc (left), 4.5 kpc (middle) and ~6 kpc (right). Works by Carlhoff et al. 2013, A&A, 560, A24 and Nguyên-Lu'o'ng et al. 2013, ApJ, 775, 88

W43 is located at the connection of the Galactic spiral arms and bar, where circular and elliptic orbits intersect and molecular clouds are expected to collide. First results presented by Carlhoff and collaborators confirm that W43 is one single connected molecular cloud complex, with a molecular gas mass (>10^2 cm^{-3}) of 2.10^6 $M_\odot$. The molecular complex is found to encompass some 20 molecular subclouds of 10-20 pc size and molecular gas masses of several 10^4 $M_\odot$. The shear parameter in W43 is likely to be too low to suggest that shearing forces in the galactic disk will affect the clouds further evolution. Nguyên-Lu'o'ng and collaborators suggest the low-velocity shocks observed in the SiO (2-1) line emission along two prominent high-density elongated clouds ("ridges") in W43-Main are formed through the gradual merging of several flows, which by themselves could feed the gas reservoirs for star formation for the next 10^6 yr. These findings thus support the general picture by which accretion flows from a surrounding filamentary network are considered necessary to create the star formation sites for the vast majority of massive stars.

UNBIASED SPECTRAL SURVEYS TOWARDS SGR B2(N) AND (M)

The discovery of amino acids in meteorites fallen to Earth and the detection of glycine, the simplest of them, in samples returned from a comet to Earth strongly suggest that the chemistry of the interstellar medium is capable of producing complex organic molecules and that they may be widespread in our Galaxy. The challenge of a team led by Arnaud Belloche (MPIfR/Germany) was to investigate the degree of chemical complexity that can be reached in the interstellar medium, in particular in dense star-forming regions.

Belloche and collaborators performed an unbiased, spectral line survey toward Sgr B2(N) and (M), two regions where high-mass stars are formed, with the IRAM 30 m telescope at 3 mm. Partial surveys at 2 and 1.3 mm were performed in parallel. The spectra were analyzed with a simple radiative transfer model that assumes local thermodynamic equilibrium but takes optical depth effects into account. About 3675 and 945 spectral lines with a peak signal-to-noise ratio higher than 4 were detected at 3 mm towards Sgr B2(N) and (M). This represents an increase by about a factor of two over previous surveys of Sgr B2. About 70% and 47% of the lines detected towards Sgr B2(N) and (M) are identified and assigned to 56 and 46 distinct molecules as well as to 66 and 54 less abundant isotopologues of these molecules, respectively. The team also reports the detection of transitions from 59 and 24 catalog entries corresponding to vibrationally or torsionally excited states of some of these molecules, respectively, up to a vibration energy of 1400 cm^{-1} (2000 K). The rotation temperatures of the detected complex molecules typically range from ~50 to 200 K. Among the detected molecules, aminoacetonitrile, n-propyl cyanide, and ethyl formate were reported for the first time in space based on this survey, as were five rare isotopologues of vinyl cyanide, cyanoacetylene, and hydrogen cyanide. The team also reports the detection of transitions from within twelve new vibrationally or torsionally excited states of known molecules. Absorption features produced by diffuse clouds along the line of sight are detected in transitions with low rotation quantum numbers of many simple molecules and are modeled with ~30–40 velocity components with typical linewidths of ~3–5 km s^{-1}.

Although the large number of unidentified lines may still allow future identification of new molecules, the authors expect most of the lines to belong to vibrationally or torsionally excited states or to rare isotopologues of known molecules for which spectroscopic predictions are currently missing. Significant progress in extending the inventory of complex organic molecules in Sgr B2(N) and deriving tighter constraints on their location, origin, and abundance is expected in the near future. The present single-dish survey will serve as a solid basis for the line identification and analysis of future interferometric surveys.

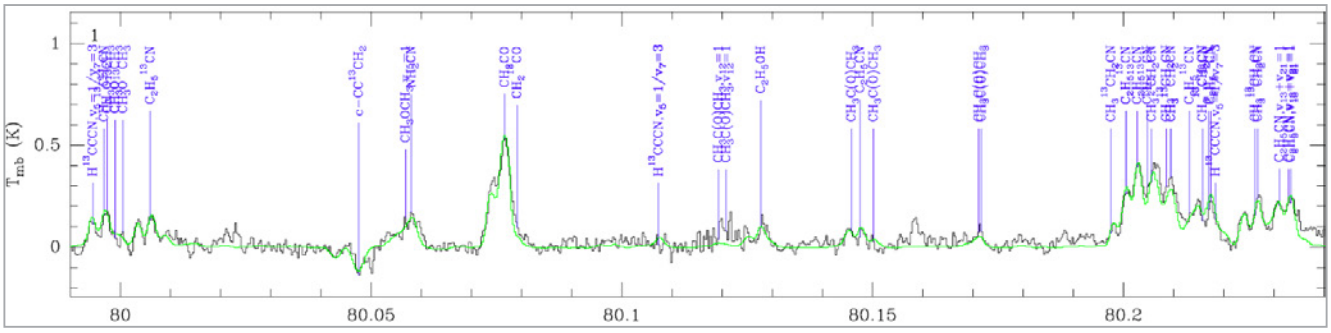

A 250 MHz slice of the 3mm spectrum observed towards Sgr B2(N) with the IRAM 30m telescope, with a best-fit model (green) and the most relevant lines (blue). The full 3mm spectrum covers the 80 to 116 GHz range. Work by Belloche et al. 2013, 559, A47

PATHS TO INORGANIC DUST FORMATION AROUND A RED SUPERGIANT

Understanding the processes of nucleation, growth and formation of dust particles in the molecular envelopes of stars on the Asymptotic Giant Branch (AGB) is undoubtedly one of the key research areas in late stellar evolution. While dust particles in circumstellar envelopes of carbon-rich stars are formed by the nucleation of aromatic hydrocarbons, inorganic processes are presumably responsible for the formation of dust particles in the envelopes surrounding oxygen-rich stars. Although the processes by which inorganic dust particles start to form and grow are largely unknown, chemical models suggest that molecules like TiO and TiO_2 must be key to their formation.

In a joined-up effort to provide the ever first millimeter detections of TiO and TiO_2, Tomasz Kamiński (MPIfR/Germany) and his collaborators directed the IRAM and SMA interferometers towards the oxygen-rich envelope of VY CMa. Embedded in a forest of molecular lines from many species, they successfully identified and dynamically resolved the chemical signature of the two molecules. The bulk of the TiO and TiO_2 emission was found to originate near the central star within 28 stellar radii, a size larger by a factor of 2-5 than the bounds predicted by the chemical models of Gail & Sedlmayr 1998. The authors derive column densities of N(TiO) = (6.7 ± 0.8) 10^{15} cm^{-1} and N(TiO_2) = (1.8 ± 0.2) 10^{15} cm^{-1}, which they translate to molecular abundances of log (TiO/H)= −8.6 and log (TiO_2/H) = −9.5. However, while Kamiński's measurements clearly indicate that these two molecules are formed close to the central star, they only provide the first necessary steps to answer the question as to how these molecules could nucleate to larger oxides and become the seeds for the formation of inorganic dust particles.

Kamiński and his team conclude that higher sensitivity and higher spatial resolution are necessary to address these questions. NOEMA and ALMA might in the long-term operate on resolving the chemical and dynamical signature of these and other titanium bearing molecules, and thereby help unveiling the formation pathway of inorganic dust particles in the envelopes of oxygen-rich late-type stars.

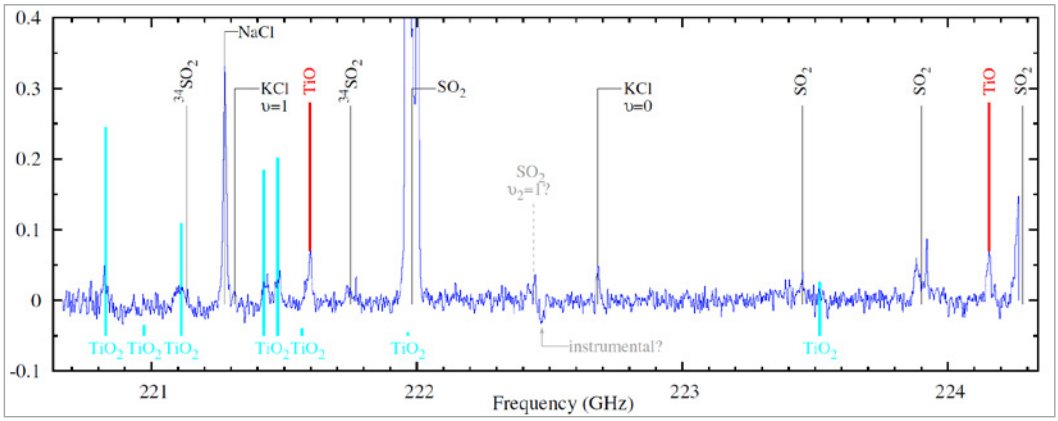

Spectrum obtained with the IRAM interferometer towards VY CMa. The height of the lines marking the TiO_2 (cyan) and TiO (red) positions corresponds to the relative intensities for LTE conditions at 300 K. The ordinate is the flux density in Jy/beam. Work by Kamiński et al. 2013, A&A, 551, 113

FIRST DETECTION OF A NITRIC OXIDE IN AN EVOLVED STAR

Yellow hypergiants (YHG) are post-red supergiants evolving blueward in the Hertzsprung-Russell diagram. One of the many remarkable peculiarities of these stars is that they expel half of their initial mass at a rate of 10^{-4} to 10^{-3} $M_{\odot}$/yr. Because of the short-lived nature of the mass ejection process, these stars are rare, and even more rare are the circumstellar envelopes around these stars that show prominent molecular line emission - among them is IRC+10420. Recent work suggests that most of the molecular material in the expanding envelope around IRC+10420 was expelled during the YHG phase. Although the molecular networks of evolved stars and YHGs in particular, testify to a high chemical richness and to high nitrogen and oxygen enrichment, no molecule containing nitrogen and oxygen was ever detected in an evolved star.

To explore the chemical network in IRC+10420 and address questions related to the relative under-abundance of molecules bearing oxygen and nitrogen atoms, an international collaboration group led by Quintana-Lacaci (CSIC-INTA/Spain) carried out a complete spectral line survey of the 3mm and 1mm bands with the IRAM 30m telescope. As a result, they reported the first detection of NO around an evolved star in the Π^{+} and Π^{-} bands of the J=5/2-3/2 transition, respectively with intensities of 1.6

K.km.s^{-1} and 1.4 K.km.s^{-1}. MADEX, the LVG radiative transfer code of Cernicharo (2012), was used to model the NO profiles and calculate abundances in the inner shell (~0.04 pc). The upper limits to the relative abundances of N/H (≥ 7.10^{-4}) and N/O (≥ 2) were found to be remarkably high and tend to confirm the N-enhancement predicted by the hot bottom burning process (HBB - hydrogen burning in the convective layers of the outer envelope) for massive stars. The calculations also suggest the nitrogen abundance has to be increased by a factor of 20 with respect to the values generally assumed in chemical models for standard O-rich stars.

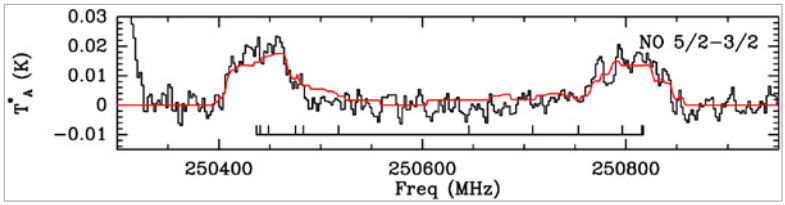

Observed profiles and results of model fitting (red) of the $^{14}N^{16}O$ J=5/3-3/2 Π$^+$ (left) and Π$^-$ bands transitions observed towards IRC+10420. The ticks in the line below the profile shows for each species the location of the hyperfine transitions.
Work by Quintana-Lacaci et al. 2013, A&A, 560, L2

PAWS RESHAPES ASTRONOMERS' VIEWS OF STELLAR BIRTHPLACES

One of the most fascinating aspects of galaxies in the local universe is the connection between CO emission lines as tracer of the molecular hydrogen mass, and star formation. Understanding how the hydrogen gas mass is distributed throughout a galaxy using CO, how it condenses into giant molecular clouds (GMCs), how it collapses to form new stars in a galactic disk, and predicting the star formation efficiency and lifetime of GMCs, are one of the many challenges in today's galaxy formation and evolution studies. CO line emission observations of GMC populations in nearby galaxies offer the best way to address many of these unknowns, and PAWS (PdBI Arcsecond Whirlpool Survey), a combined IRAM interferometer and 30m telescope Legacy Program led by Eva Schinnerer (MPIA/Germany), took up the challenge.

PAWS mapped with ~1″ resolution the ^{12}CO(1-0) emission from the central ~9 kpc of M51a (NGC1594), a massive grand-design spiral galaxy, to allow for the study of the molecular gas properties as a function of galactic environment at the scale of GMCs (~40pc). Recent results based on the PAWS dataset include the finding that on cloud-scales the correspondence between CO emission and tracers of the cold ISM (e.g. optical extinction, PAH emission) is excellent and even holds for radio continuum emission while the correspondence to star formation tracers ranges from excellent to absent (strongly depending on galactic environment. Schinnerer et al. 2013). Detailed analysis of the molecular gas structure reveals an additional thick molecular gas disk (Pety et al. 2013), a strong environmental dependence of the molecular gas structure function (Hughes et al. 2013a) as well as the properties and distribution of the GMCs (PhD thesis, Colombo 2013). Careful comparison to GMC properties in two local low-mass galaxies underlines the strong environmental dependence of GMC properties and identifies pressure as an important factor for GMC formation (Hughes et al. 2013b), in particular dynamical pressure is playing an important role in the dramatic changes observed (Meidt et al. 2013).

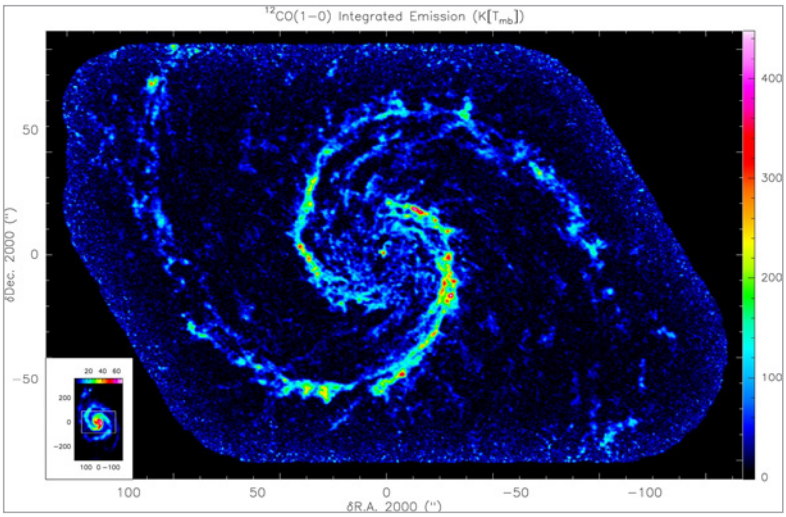

The ^{12}CO(1-0) line emission in the central ~9 kpc of M51a as observed by the PAWS project. The image results from the joint deconvolution of the IRAM interferometer and 30m telescope data sets. The image inserted at the bottom left is the ^{12}CO (1–0) integrated emission of the full M51 system (NGC1594 and NGC1595) as observed by the IRAM 30 m telescope.
Works by Schinnerer et al., Pety et al., Hughes et al., Meidt et al., all in 2013, ApJ, 779

A NEW TAKE ON THE CO/H$_2$ CONVERSION FACTOR

Molecular hydrogen is the most abundant molecule and a basic building block for star formation, but is also one of the most elusive tracers of mass. As a result, the most common means of tracing star formation is observing a ^{12}CO line and the conversion of its intensity into a molecular gas mass via a suitably estimated CO/H$_2$ conversion factor. Despite uncertainties in the physics of this factor, the observability of the CO molecule at low and high redshift makes it a widely used molecular gas

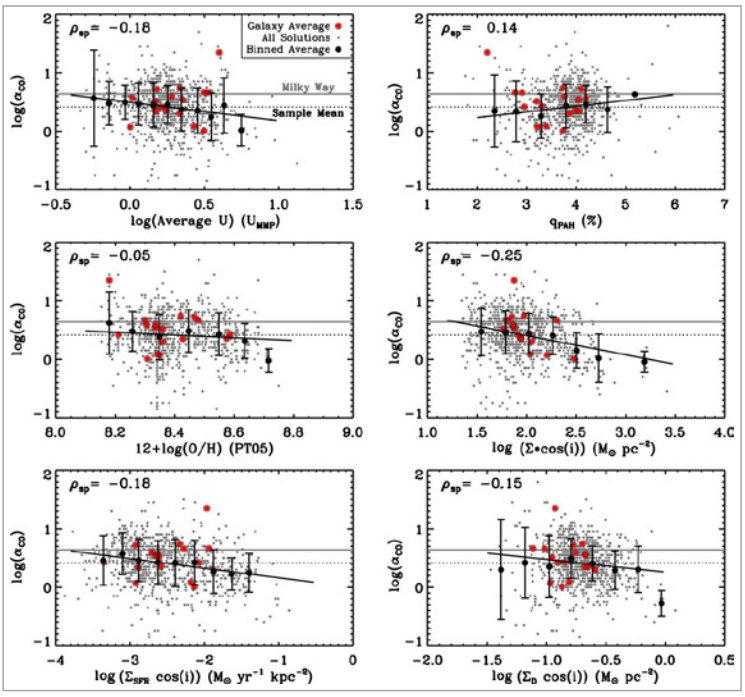

Derived CO/H_2 conversion factor for a sample of 17 nearby galaxies (mean values in red) as a function of the radiation field intensity and PAH fraction (top), metallicity and stellar mass surface density (middle), SFR surface density and dust mass surface density (bottom). The solid gray line shows the Milky Way and the dotted black line shows the sample average $CO/H_2 = 2.6\ M_\odot\ pc^{-2}/(K\ km\ s^{-1})$. A linear fit to the measurements is shown with a black line.
Work by Sandstrom et al. 2013, ApJ, 775, 33

tracer. While the factor is not varying significantly in the Galaxy, there are good reasons to believe that it depends on the galactic environment. To address the question of how the CO/H_2 factor varies on sub-galactic scales, Karin Sandstrom (MPIA/Germany; NRAO/USA) and collaborators performed a systematic study that made use of high-resolution dust and gas observations of 26 nearby galaxies from the HERACLES (IRAM 30m, Leroy et al. 2013), KINGFISH (HERSCHEL, Kennicutt et al. 2011), SINGS (Spitzer, Kennicutt et al. 2003) and THINGS (VLA, Walter et al. 2008) surveys.

Sandstrom and collaborators made use of the sensitive survey data to trace dust and gas mass surface densities on ~kpc-scales. They find that reliable estimates of the CO/H_2 factor can be obtained for ^{12}CO intensities above 1 K.km.s^{-1} and inclinations above 65°. The average CO/H_2 conversion factor of 782 sub-galactic ~kpc-sized cells is 2.6 $M_\odot\ pc^{-2}/(K\ km\ s^{-1})$ with an error of 0.4 dex. The factor is weakly dependent on galactocentric distance but is on average ~2x lower in the central region, and in several galaxies ~5-10 lower than the average Galactic value. While the results suggests the CO/H_2 factor is correlated most strongly with the stellar mass surface density, thereby raising the possibility of different properties/influences on the molecular medium, they also suggest it does not depend on metallicity. The global picture suggests the average CO/H_2 conversion factor in the disks of nearby galaxies is lower that the Galactic value (4.4 $M_\odot\ pc^{-2}/(K\ km\ s^{-1})$) and mainly constant over the disks, while the galaxy centers appear to show lower CO/H_2 values, indicating the onset of a different regime.

It is to expect that NOEMA and ALMA will further a better understanding of how the conversion factor may vary on the size scales of giant molecular clouds.

MOLECULAR SUPER-WINDS IN THE LOCAL MERGER NGC6240

One of the most important and still largely unsolved questions in cosmology is the combined evolution and growth of galaxies and their central super massive black holes (SMBH). Questions are about how galaxy and SMBH growths are being self-regulated by feedback processes, how feedback could be related to Active Galactic Nuclei (AGN) fueling and how it could terminate star formation in massive galaxies. According to the current picture, feedback processes are associated to AGN and outflows from supernovae or starbursts, which heat up the interstellar medium, expel it from the galaxy and thereby inhibit the formation of new stars.

In the framework of a systematic study of massive outflows, a team led by Chiara Feruglio (IRAM/France) mapped NGC6240 using the IRAM interferometer. NGC6240 is one of the nearest ULIRGs undergoing a merger event between two gas rich galaxies. Each of the remnants is hosting an AGN with a black hole (BH) mass exceeding $10^8\ M_\odot$ and is highly obscured by gas and dust. NGC6240 is also of interest as it displays multi wavelength evidence of ionized outflows and of expanding motions, and has the brightest line emission from hot molecular hydrogen among all LIRGs. The huge luminosity of H_2 is due to two main processes: the expanding motion of a shell-like structure around the southern nucleus (super-wind) and cloud-crushing at the interface of the two merging nuclei, where the super-wind is interacting with the central concentration of molecular gas. Herschel/PACS also recently observed a massive outflow in the blue-shifted absorption spectrum of OH at 119 µm.

The IRAM observations revealed low surface brightness $^{12}CO(1\text{-}0)$ emission on kpc-scales, and over a broad velocity range (~1600 km/s), thus excluding that this gas component is related to the molecular disk. Long baseline observations could locate the origin of the outflow in the southern active nucleus of the system, thus confirming that

the complex flow is associated to an AGN driven outflow. The joint analysis of Chandra X-ray and millimeter interferometric data is finally suggesting that the X-ray emission associated to the molecular outflow is produced by shock heating.

These observations, complementary to Herschel/PACS observations, allowed assessing that AGN feedback is at its maximum efficiency in the phase of a late stage merging, infrared luminous galaxy, hosting obscured but powerful AGN activity, in agreement with several models of galaxy-AGN co-evolution. This result also demonstrates the power of mm-interferometry for studying outflows.

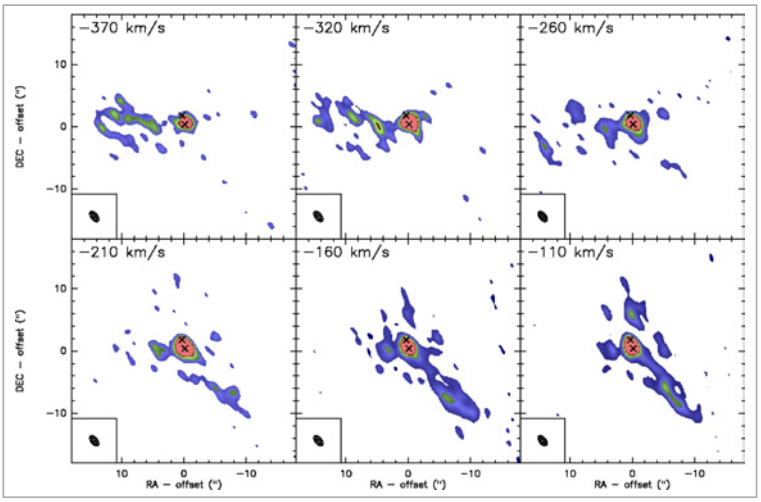

^{12}CO(1–0) maps of NGC6240 from extended (A) and compact (D) configuration data. Crosses show the positions of the two AGN nuclei.
Work by Feruglio et al. 2013, A&A, 549, A51

A DUST-OBSCURED MASSIVE MAXIMUM-STARBURST GALAXY AT Z=6.34

Massive present-day early-type galaxies probably gained the bulk of their stellar mass and heavy elements through intense, dust-enshrouded starbursts in the most massive dark matter halos at early epochs. However, it remains unknown how soon after the Big Bang such massive starburst progenitors exist. The measured redshift distribution of dusty, massive starbursts has long been suspected to be biased low in redshift owing to selection effects, as confirmed by recent findings of systems out to redshift z~5. Dominik Riechers (Cornell Univ./USA) and collaborators reported the identification of HFLS3, a massive starburst galaxy at redshift 6.34 through a submillimeter color-selection technique. They unambiguously determined the redshift from a suite of molecular and atomic fine structure cooling lines.

The team's measurements revealed a total molecular gas mass of ~10^{11} $M_\odot$ of highly excited, chemically evolved interstellar medium (ISM) in this galaxy, which constitutes at least 40% of the baryonic mass. A maximum-starburst is converting the gas into stars at a rate of ~2,900 $M_\odot$/yr, a rate among the highest observed at any epoch and more than 2,000 times that of the Milky Way. Despite the overall downturn of cosmic star formation towards the highest redshifts it seems that environments mature enough to form the most massive, intense starbursts existed at least as early as 880 million years after the Big Bang. From the spectral energy distribution and the intensity of the CO and [CII] emission, Riechers and collaborators find a dust mass of 1.3 10^9 $M_\odot$ and total molecular and atomic gas masses of 1 10^{11} $M_\odot$ and 2 10^{10} $M_\odot$, respectively. These masses are 15-20 times those of Arp 220, and correspond to a gas-to-dust mass ratio of ~80 and a gas depletion timescale of ~36 Myr. According to the authors, at the current star formation rate of HFLS3, this level of carbon enrichment could have been achieved through supernovae on a timescale of ~10^7 yr. The gas is distributed over a 1.7 kpc radius region with a high velocity gradient and dispersion. This suggests a dispersion-dominated galaxy with a dynamical mass of 2.7 10^{11} $M_\odot$.

Galaxies like HFLS3 are unlikely to dominate the star formation history of the Universe at z>6, but they trace the highest peaks in SFR at early epochs.

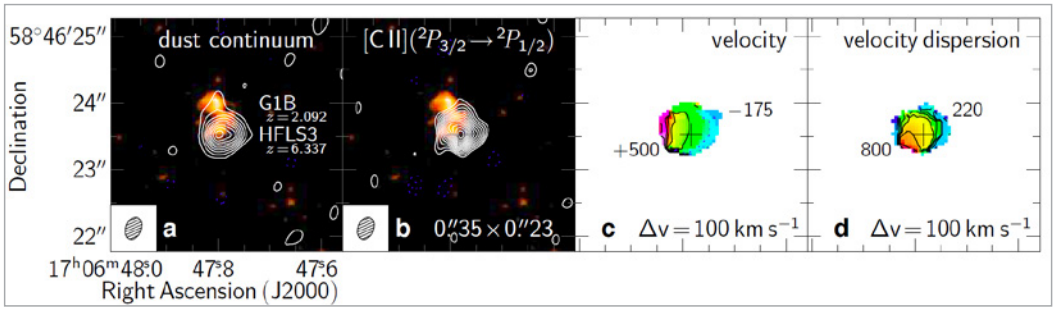

(a) ~0.3" maps of the 158-μm continuum in HFLS3, (b) velocity integrated [CII] line emission, (c) isovelocity field and (d) velocity dispersion map obtained with the IRAM interferometer in A-configuration, overlaid on a Keck/NIRC2 2.2-μm adaptive optics image (rest-frame UV/optical light).
Work by Riechers et al. 2013, Nature, 496, 239

The 30-meter telescope

Inside view of the 30-meter parabola structure capable of achieving a surface precision of within 55 microns.

OVERVIEW

With more than 180 scheduled observing projects and 160 astronomers visiting the telescope to conduct and support these projects, 2013 was a busy year. The highly successful EMIR receiver was upgraded, to now offer 16GHz of instantaneous bandwidth in two polarisations also with the 2nd band of the four EMIR bands, the 2mm band. The NIKA dual-band prototype continuum camera featuring kinetic inductance detectors continued to make rapid progress e.g. with regard to its sensitivities, stability, reliability, and data processing, as is shown in a series of publications submitted towards the end of 2013, together with a first open call for observing proposals issued in September. In addition, the year 2013 saw a strong increase in preparatory work for the future new facility camera at the 30m, NIKA2, with its 5000 pixels and 6.5' field-of-view.

In September 2013, the Eight MIxer Receiver EMIR was upgraded with tunerless dual-sideband mixers for the 2mm band. In addition, the upper frequency range of the 0.8mm band was slightly extended. These changes required upgrades of the distribution of intermediate frequencies (IF), of its control software, as well as an update of the paKo/NCS observing software. Astronomical commissioning was successfully conducted directly after the installation and included testing of all important EMIR band combinations using the Fast Fourier Transform Spectrometers (FTS) at 200kHz and at 50kHz resolution. A shallow 2mm line survey of the nearby carbon-rich evolved star IRC+10216 covered the entire frequency range of the 2mm band, between 125 and 186 GHz. Its line intensities compare well with the previous survey of Cernicharo et al. (2000) when taking into account improved telescope beam efficiencies. To calibrate data taken near the atmospheric water line at 183.3GHz, the reduction software allows to fix the amount of precipitable water vapor or the sky opacity.

A good knowledge of the beam pattern at a given frequency is important to calibrate the observed line intensities and to derive the spatial resolution of the observed data. The beam pattern of the 30m telescope was investigated at five frequencies between 86 and 340GHz, using total power scans of the limb of the Moon taken under best conditions. The beam patterns were derived down to a level of -30dB and to a full width of upto 2000". Relative to the numbers derived by Greve et al. (1998), the main beam efficiencies have been improved significantly, leading to a corresponding reduction of the power contained in the errorbeams. The main beam efficiencies, for example, at 145GHz and 230GHz are now 74% and 59%, respectively. The two-dimensional structure of the beam pattern will in the future be studied with the new continuum cameras.

The prototype GISMO 2mm continuum camera of the NASA Goddard Flight Center has been offered to the 30m community since the winter semester 2011/12. In 2013, two more pooled observing sessions were scheduled in April and in October/November, over a total of 5 weeks. This camera has a field-of-view of 1.8'x3.7' with a resolution of 17" and about 100 healthy pixels. A total of 270 hours

were spent on-sky, limited only by the daily Helium refilling and recycling intervals and the weather. For GISMO, the telescope control software was operated with a fast rate of 8Hz, which allows to conduct Lissajous scanning patterns, in addition to zig-zag patterns while taking data on-the-fly. For atmospheric calibration the opacities continously measured by the IRAM 225GHz taumeter are used. The telescope, instrument, and the highly automated NEXUS/crush data pipeline worked very stable with a flux stability of better than 8% and a final pointing accuracy of better than 3″ rms. One science highlight has been a deep continuum survey centered on the Hubble Deep Field. The 1σ sensitivity reached in the innermost few arcminutes of the map is 135μm/beam, which allowed to directly identify 12 sources. About half of these sources have known (sub)millimeter counterparts. Most of the sources without shorter wavelength counterparts must lie at high redshifts larger than z~3 and must have high intrinsic luminosities of a few 10^{12} L_{sun}.

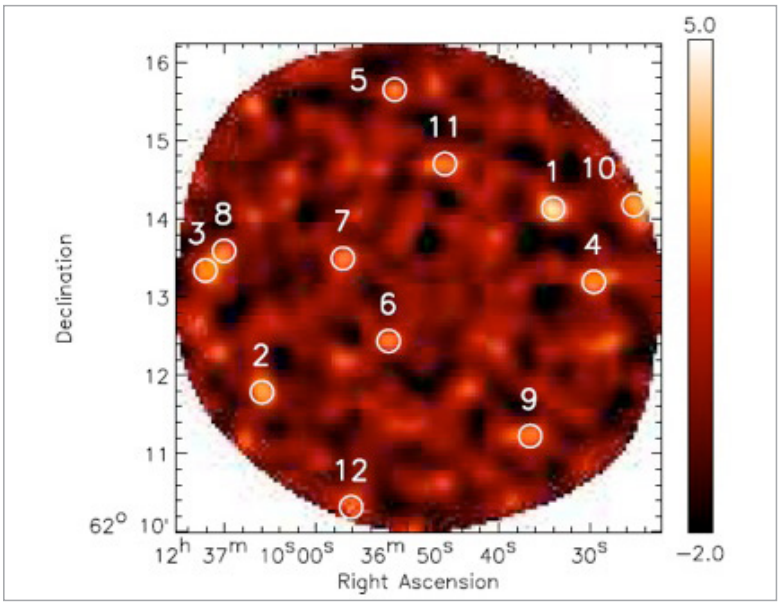

Map of the S/N ratio of the GISMO deep field. The circles mark the sources with S/N > 3 (Staguhn, Kovacs et al. submitted).

Lissajous scans with the 8Hz telescope control loop, have also been made available for NIKA. Refinement were made in the observers pako control software to allow for skydips to measure the sky opacity with tune subscans for NIKA, as well as for standard skydips for GISMO and NIKA.

While GISMO uses super-conducting transition edge sensors as detectors, the NIKA prototype continuum camera uses a new detector technology, super-conducting kinetic inductance detectors (KIDs). In 2013, two NIKA test runs were conducted at the telescope. Performance and integration into the observatory system progressed significantly, which allowed to offer NIKA to the community for the winter semester 2013/14. Using a dichroic, NIKA allows simultaneous dual-polarisation observations at 2mm and 1mm, with ~114 and ~136 healthy pixels, respectively. Its field-of-view is about 2′. NIKA uses a closed cycle ^{3}He-^{4}He dilution fridge, with a work temperature of 100mK, and allowing for continuous observations. To correct for the atmospheric absorption, skydips are conducted once per day establishing KID scaling factors which are then used together with the total power detected prior to each on-source scan in order to derive the atmospheric opacity. A data pipeline built by the Neel Institute in Grenoble was successfully tested. Among the first science highlights are maps at 1 and 2mm of the Horsehead Nebula in Orion B at ~450pc distance and a 2mm map of the Sunyaev-Zel'dovich (SZ) effect toward the bright X-ray cluster of galaxies at a redshift of z=0.45.

The total power flux monitoring program for time-variable quasars in the list of pointing and focus calibrators has been continued. Results are available online to IRAM users for the planning of their observations. They include plots of the recent time evolution of the fluxes and a source file which can be used with sky charting tools like XEphem to display the pointing sources with a symbol size corresponding to their most recently measured flux, in addition to primary and secondary calibrators, and the science targets.

ASTRONOMICAL PROJECTS

During the year 2013, a total of 183 projects were scheduled at the 30m telescope. This number includes 4 Large Programs, 11 Director's time projects, and 5 VLBI projects. About a quarter of these programs was scheduled in observing pools, including the continuum pool with the GISMO 2mm camera. During the scheduling year, 159 astronomers visited the telescope, 39 of which came to support the observing pools. About 15% of the

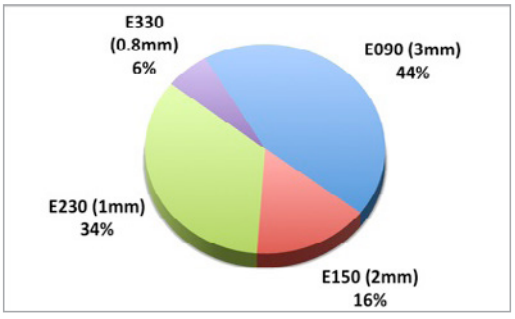

Usage of EMIR bands in 2013

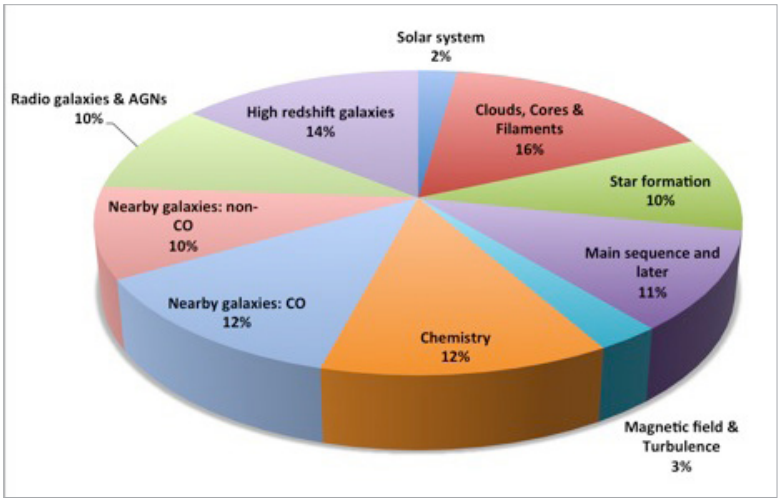

scheduling units, mainly the shorter ones (< 10 hours), were observed remotely.

Over three quarters of the scheduled projects used EMIR. The remainder was made up by HERA (7%) and GISMO (16%). Half of the scheduled proposals (50%) were for Galactic research, including a small fraction (2.5%) of solar system targets. Almost a quarter of the total time was devoted to nearby galaxies, and another quarter of the time to more distant extra-galactic objects.

.

Time distribution of science categories observed in 2013

TELESCOPE OPERATION

In 2013, about 66% of the total time was used for observations. Similar to previous years, the total time lost due to adverse meteorological conditions was about 25%. The time lost due to technical problems was 1.25% or 80 hours, only. About three quarters of this time was lost due to ball bearings which had to be replaced by Desch engineers in September in the upper part of one of the Azimuth gearboxes. Careful tests did not reveal any further malfunction, and as one of the resulting measures we improved the procedure to exchange the telescope motors.

Following a detailed work plan, preparation intensified to prepare for the arrival of the large field-of-view NIKA-2 1mm/2mm continuum camera in 2015. The cable spiral to connect the moving parts of the telescope with the pedestal has been cleared of obsolete cables, the electrical power capacity available inside the receiver cabin has been increased, and the upper blind above the vertex has been covered with a new armaflex protection improving the water tightness of the cabin.

Below right: Monthly time distribution of observing time (U.Observ.), technical projects (U.T.T.), maintenance (U.Mainten.), time lost due to high wind speeds (U.Wind), or other adverse metheorological conditions (S.Meteo), or technical problems (S.Techn.).
Below left: Distribution of the total time in 2013.

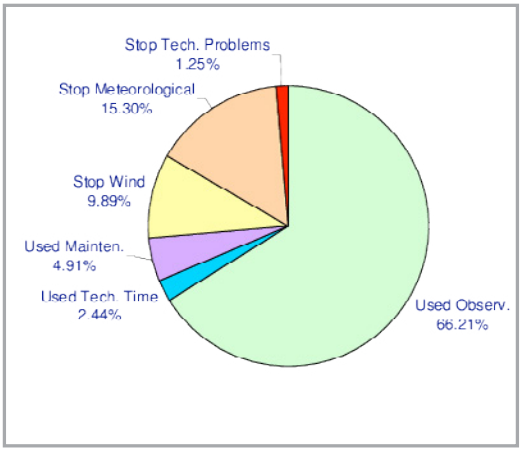

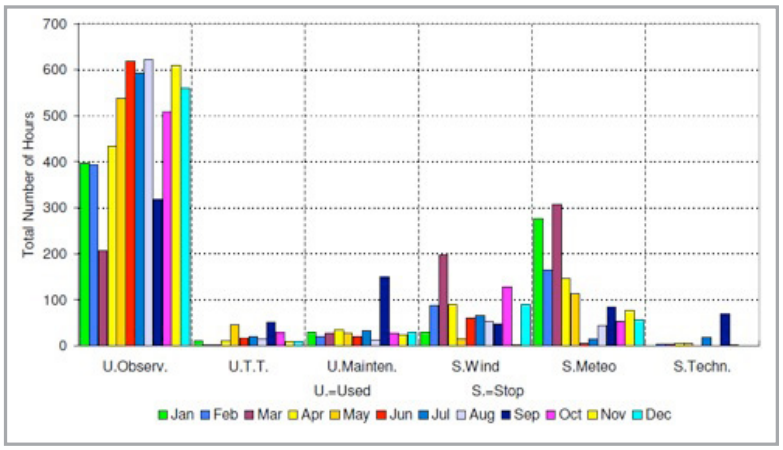

FRONTENDS AT THE 30M TELESCOPE

The planned installation of large field of view cameras at the 30m telescope will require the modification of the existing receiver optics, including the Nasmyth mirrors and all the associated elements. During 2013, much time has been spent in close collaboration with IRAM/Grenoble on designing a new scheme to accommodate the bigger optics. As a first step, the old vertex window has been replaced by a much larger window of 1.4m in diameter.

A significant step forward in improving the performance of EMIR was taken in September 2013 when its 2mm band E150 was upgraded with new dual sideband (2SB) mixers. The IF switch unit was modified to allow observers to use E150 like any of the other three EMIR bands which now all have 2SB mixers.

A new way of measuring the receiver image band rejection by injection of artificial lines has been investigated. Early results obtained with the present spectrometer backends show that the method could be used to calibrate the receiver image band rejection at the telescope.

The 225GHz taumeter has been working stable during the entire year, providing the observers continuous, online information of the zenith sky opacity. The local oscillator and some of the electronic boards have been replaced by more sturdy units. The outside housing has been completely redesigned providing now a much better protection against adverse weather conditions, while maintaining a good accessibility from the observers room.

COMPUTERS & SOFTWARE

Due to the large increase of the amount of data and of the data rates, owing to the increased bandwidths of EMIR and the Fast Fourier Transform Spectrometers (FTS), the informatics system to conduct backups and to store the data has been further and significantly improved. For backups of the observer data, and also for system backups, magnetic tapes are used. Each of the LTO-6 Ultrium cartridges holds up to 2.5 terabyte of data, and the two tape robots which are currently installed at the observatory store a total of up to 100TB . These robots allow to conduct routine backups running in the background, without manual intervention. The disk space at the observatory has been extended to a total of also about 100TB. For ongoing observing projects ~30TB of disk space are provided, while supporting a maximum data rate of 1TB per day. About two thirds of the total disk space are used to keep the observational data in a dedicated set of disks, the IRAM-internal project archive. In 2013, the project archive was moved to a network attached storage system (NAS), which allows for easy extension. An increase of storage space of about 30TB per year is expected.

At present, the observatory computer network runs with 1Gbit/s. The connection with IRAM/Granada is conducted via a radio link of 100Mbit/s, and the internet connection from the offices in Granada via the Universidad de Granada at a speed of up to 10Mbit/s. The radiolink works via two independent lines, enhancing reliability. In 2013, the radiolink and also the connection to the internet worked reliably without any major interruptions during the whole year.

The online TAPAS data base which contains the scan header variables of the observations conducted at the 30m telescope has been extended to include the data taken with the continuum cameras GISMO and NIKA. Observers can now add comments to each scan online, to create a logsheet of the observations. Special online tools were developed for IRAM staff to monitor the observations, and critical parameters like the pointing and focus results or the receiver temperatures. These are now routinely used for example in the weekly reports of the astronomers-on-duty. In close collaboration with the pool managers, a web interface has been developed, to help observers and IRAM staff to organize pooled observations and schedule observations in a flexible, dynamical way, taking into account their ratings, visibility, sky opacity, and other parameters, and allowing to keep the balance between open time and guaranteed time projects.

A monitor has been installed at the observers desk to permanently show the tracking behaviour of the telescope after each scan of observations. Tracking deviations are the differences between commanded and true positions of the telescope in Azimuth and Elevation, which are usually only a small fraction of an arcsecond, i.e. much smaller than a tenth of the beam sizes. This monitor is useful e.g. when observing under high wind conditions near the limits of telescope operation, or, when conducting fast slewing motions like during Lissajous scans, i.e. in conditions when the tracking deviations will increase somewhat.

7TH IRAM 30M SUMMERSCHOOL

The 7th IRAM 30m summerschool was held in September 13-20, 2013. As usual, the meeting place was the small ski resort Pradollano in the middle of the Sierra Nevada, at only 15 minutes driving distance to the 30m telescope. The 40 participating students came from the IRAM partner countries France, Germany, and Spain, but also from the United Kingdom, The Netherlands, Italy, Serbia, Ukraine, Mexico, Argentina, Chile, Brazil, China, and Vietnam.

The school offered a series of lectures by 9 experienced and active 30m users centered on millimeter astronomy from sungrazing comets to high-*z* galaxies, which were complemented by dedicated presentations on millimeter instrumentation, observing techniques, and data processing. Two highlight presentations showed complementary recent observations conducted with the Stratospheric Observatory for Far-Infrared Astronomy (SOFIA) and with the Planck satellite. About 40hours of observing time were reserved for observations of short projects prepared and conducted by the students who presented their work on the last day of the school. These short presentations as well as the lectures have been made available online on the IRAM web portal. Visits to the Alhambra and Granada rounded-off the program on a long Thursday evening.

Financial support was received by the RadioNet3 program and the Junta de Andalucia.

Participants of the IRAM 30m summerschool of 2013.

Plateau de Bure interferometer

The Plateau de Bure interferometer caught in the icy drizzle of a winter storm. (Copyright Diverticimes)

Operation highlights this year are the successful integration of the new phase-referencing system to prepare for the arrival of NOEMA and successful intercontinental 1mm VLBI observations. The interferometer continued its efficient operation with almost no downtime due to hardware upgrades, maintenance operations, construction work on the cable car, and work in preparation of antenna 7. The antennas, receivers and digital correlators all worked well throughout the year.

The observatory continued to provide unique and exciting scientific results in 2013. Observations were performed in periods of excellent phase stability and atmospheric transparency in January and most of February. Observing conditions in spring were pretty unstable but allowed observations in the high frequency bands during short periods until beginning of May. Conditions were excellent again from the second half of November until the end of the year. The extended configurations (A and B) were scheduled from January 9 to April 4. The scheduling of the A configuration was readjusted shortly after the beginning of the winter scheduling period to optimize the observing of A-rated projects with respect to Sun avoidance limitations and weather constraints. All interferometric observations were performed exclusively in service mode.

As in previous years, the percentage of contiguous array-correlation-time scheduled for observing programs was on average 50% of the total time. This year a total of 170 days and nights were scheduled for science operations. Additional 20% have to be accounted for receiver tuning, array configuration changes, engineering and commissioning activities. The remaining 30% were lost because of precipitation, wind and poor atmospheric phase stability.

The Program Committee reviewed 217 proposals, including 8 VLBI proposals, and recommended the approval of 115 proposals corresponding to 296 individual projects. In total, more than 226 different projects were scheduled at the observatory in 2013, including 3 Large Programs, 8 proposals for Director's Discretionary time, 8 VLBI projects and the backlog of projects from 2012.

The interferometer supported a broad range of science areas in 2013. The weight on extragalactic

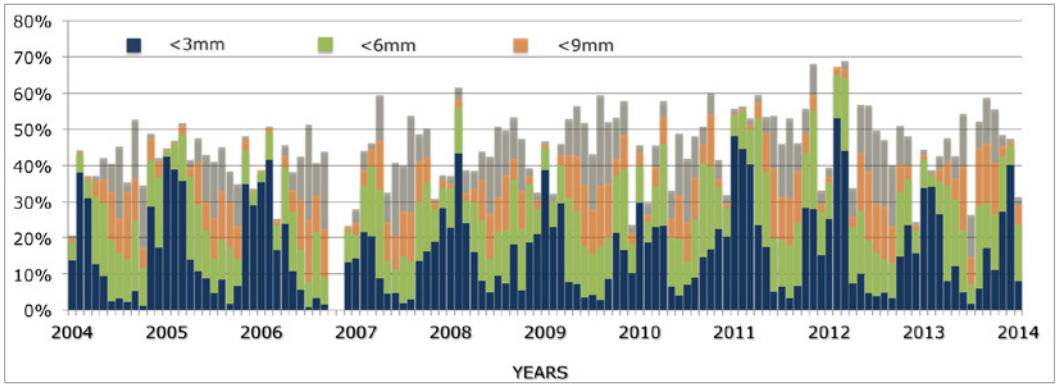

Plateau de Bure observing time and atmospheric water vapor statistics over the last ten years. The overall correlation time accounts for 47% of the total time in the year 2013. Band 3 (200 – 268 GHz) and band 4 (275 – 373 GHz) programs and observations in the most extended (AB) configurations are for the most part carried out in the winter months. The smooth increase in the observing efficiency over the years 2004-2012 results from a combination of weather statistics, technical improvements and reduced calibration overheads. Science operations were suspended in the autumn of 2006 for the installation of new receivers.

high-redshift research was considerable; the requested observing time was about 3-4 times higher than the time requested for each, nearby galaxies and young stellar objects. Also, a fairly large amount of observing time was invested in D-configuration between spring and fall in the detection of line-emission from molecular and atomic transitions in galaxies at high redshift. Annex I details all the proposals to which time was granted in the course of the year, and testifies to the high scientific return of the Plateau de Bure Interferometer.

ONGOING WORK AND ACTIVITIES

There were major developments, initiatives and infrastructure improvements during the year that deserve a special mention.

In the frame of the NOEMA project, we report the installation and commissioning of a new LO control system in September 2013. The new system was designed to provide two independent phase-reference signals for the 12-antenna NOEMA array, one for band 1, the other for one of the higher frequency bands. The capabilities of the new LO control system are being enhanced through the implementation of a built-in power meter to monitor the strength of the LO reference signals on their round-trip to the antennas, and through an innovative circuit design to provide ultra-low phase noise in the LO signals. The software was completely rewritten to address the LO control system directly over EtherCat. The performance of the new system was evaluated through a series of technical verifications, assessed over a period of several weeks through astronomical observations, and fully validated by the end of November.

To prepare for the arrival of the NOEMA antennas, it was decided to renovate part of the computer system. New workstations were bought to speed up the data processing and array calibration pipeline at the observatory. In parallel, the computer infrastructure was also improved to support work of visiting astronomers on mission at IRAM headquarters. Four powerful workstations are now available in Grenoble for data reduction and analysis. In the context of extending and improving the computer infrastructure for NOEMA, major and continuing efforts are planned in 2014 and 2015 to equip the observatory with even more powerful data servers and workstations, and modify the current network structure and topology of the observatory.

A particular effort was devoted to the reorganization of work and responsibilities of astronomers within the Science Operations Group to streamline operation procedures and services, and prepare for the upcoming challenges. Much of the group work was employed to ease the daily work of the AoDs and the scientific coordinator with respect to keeping track of the observational progress at the observatory. A software program was developed that automatically maintains a global database on the status of all projects scheduled for observations at the interferometer. This has been a real change from previous practice, where the project management was done manually. The upside is that automating this work has reduced the human work time, and reduced possible human error. We are now in the process of developing a view to sharing the database with other applications in the future.

As in previous years, the surface quality of all of the antennas was verified by means of holographic measurements at the end of the maintenance period. Surface panels were readjusted when deemed necessary. The final overall surface precision achieved by holography was better than 42µm for all antennas.

The 22 GHz radiometer systems equipping the antennas performed satisfactorily in 2013. Two units showed minor stability problems in one of the three monitoring bands; this effect was traced to a detector diode that showed signs of aging and was successfully repaired in the Grenoble receiver lab. On several antennas the water vapor radiometer performance is limited by the temperature variations of the receiver cabins. Detailed studies are underway to remedy this point. In order to keep an eye on the presence of man-made environmental interference in the 18-26 GHz receiver band of the radiometers, first tests were made with a broadband spectral scan on the radiometer of antenna 5. To complete the evaluation, a more performant spectral analyzer unit is awaiting its installation in 2014.

INFRASTRUCTURE

Most of the annual investment for the infrastructure and work at the IRAM Plateau de Bure Interferometer was spent preparing NOEMA. The most significant parts are listed in the following:

The construction of two rooms at the rear side of the hangar which are fire-protected during at least 2 hours was finished during this year. One of them is used for the storage of hazardous materials and equipped with electrical ATEX equipment (which can safely operate in explosive environments). The other one is used for storage of electro-technical equipment necessary for the construction of the future telescopes (cable drums, optical fibers, etc.). These two rooms are equipped with a fire detection system and an autonomous fire extinguishing system in order to ensure optimum safety. Toilets were destroyed during this operation, and completely new sanitary facilities were built and equipped nearby. A safety shower has also been added.

A new 16 tons driven hoist was set up by our technical staff, thus enabling the handling of heavy elements of the telescope. The initial hoist was not complying with safety regulations and was showing significant signs of decay.

As to ensure a good temperature uniformity in the hall during the phase of the reflector mounting, a big fan was installed at the top of the assembly hall that can constantly stir the 18000 m^3 of air in the hall. Given the large size of this fan (diameter of more than 8 meters), special care was taken to fix its various elements and avoid any of its pieces to fall down on the working areas.

The workshop has not changed, nor was it renovated for many years. Therefore, some investments were necessary to ensure the successful completion of NOEMA related works. A lathe and a milling machine were thus bought for mechanical adjustments of in situ components. A cutter, a folding machine and a plasma welding machine were also bought for the production of thermal insulation panels.

The two scaffoldings, fixed to the East and West side of the assembly hall, have been refreshed and changes were made that were necessary because of the evolution in State regulations and the need to carry out maintenance of existing telescopes while assembling new antennas. These evolutions allowed to guarantee more accessible and safe workspaces without the constraint of equipping them with working material otherwise necessary to ensure the security of working at height. In addition, a mobile scaffolding was under study and finally bought for the construction of the thermal insulation panels.

Access to the upper parts of the telescopes (either in maintenance or in construction) is achieved by means of a lift platform (type PEMP3B). As the current model is equipped with a diesel engine and an extensive use of this device is foreseen in the confined assembly hall, it has been necessary to change the model thus preferring an electric one (type NiftyLit). This new dual-energy model allows both internal and external use. The other platform (Manitou) was sold back.

Regarding the maintenance hall, a thorough check of the flatness and horizontality of the mounting station was carried out with the help of a geometer in order to ensure the correct position of the anchor ring. Only minor corrections were required to fall within the tolerances.

Finally, in order to answer the oncoming considerable needs for transfer of information and data between Grenoble and the Plateau de Bure Observatory, a call for tender was launched and carried out under project ownership of the Dévoluy region, for an optical fiber cable connecting the observatory to the station of SuperDévoluy through the slopes. This call is still ongoing and has not yet been assigned. Work is scheduled for summer 2015.

Excluding NOEMA, no infrastructure changes were made this year, most of our staff being focused on this new project. The most important change is the anemometer that could not be maintained anymore due to either the complete lack of spare parts or completely obsolete ones. Positive tests were performed with an ultrasonic anemometer which allowed to move from a cupola technology to a static measurement technology. In addition to merging the weathervane and the anemometer into a single device, it is also much less sensitive to frost and allows increased availability of the device. Finally, the implementation of this unit is a test for the future anemometers of the new cable-car.

MAINTENANCES

Despite the arrival of NOEMA maintenance of the existing 6 antennas was carried out exactly the same as in previous years, in order to maintain the antennas at their current performance level. The efforts made during the previous maintenance by the technical staff to follow the running procedures and maintenance notebooks were very helpful, and maintenance actions could thus be performed more efficiently.

Developments and upgrades on telescopes, as well as work on the buildings were on the other hand

minimal, in order to concentrate all the efforts on antenna 7.

It had been scheduled for long, and it is now operational on the entire site: the defrosting system using the dew point measurement has been completed and commissioned, in spite of the intense activity. It ensures the absence of moisture on the telescopes dish while ensuring at the same time a minimum power consumption. This point is now becoming essential given the increasing cost of energy. Other similar efforts are also planned for the future.

Finally, the old cable car was very busy throughout the summer period for the transportation of both antenna 7 components, and the new cable car elements.

USER SUPPORT

The Plateau de Bure Science Operations Group (SOG) is part of the Astronomy and Science Support Group, a group of astronomers and engineers with a wide range of expertise and technical knowledge in millimetre wave astronomy and associated techniques. The SOG is staffed with astronomers that regularly act as astronomers on duty (AoD) to optimise the scientific return of the instrument, directly on the site or remotely from Grenoble. The group also provides technical support and expertise on the interferometer to investigators and visiting astronomers for questions related to the calibration, pipeline-processing and archiving of Plateau de Bure data, interacts with the scientific software development group for developments related to the long-term future of the interferometer, performs the technical reviewing of the science proposals, collaborates with technical groups to ensure that operational requirements are being met, and keeps documentation up to date. Six astronomers on duty were appointed to the group at the beginning of 2013.

Work was also continued in the context of extending and improving the Plateau de Bure data calibration pipeline and the accuracy of the absolute flux calibration scheme. A major effort was made on measuring flux densities and modelling the spectral energy distribution of the optically thick core surrounding LkHa101. The overall aim is to calibrate its flux densities in all four bands to better than a few percent and thereby establish an alternative high-precision absolute flux calibration reference to MWC349.

The IRAM headquarters hosts a regular stream of visiting astronomers from all around the world that stay at the institute for periods between a few days and a few months. Some of the visiting astronomers come to reduce data from the Plateau de Bure interferometer, others are part of our Visiting Astronomers Program (VAP). The program aims at training research scientists and postgraduate students in interferometry concepts, instrumentation and data reduction, and at strengthening science collaborations. In 2013, advice and assistance was given to 33 investigators from Europe, and overseas, visiting IRAM Grenoble for a total of 128 days to reduce and analyze data from the interferometer. Support was also provided to 10 experienced astronomers from ICC/Durham, NASA/GSFC/ Greenbelt, MPIFR/Bonn, MPIA/Heidelberg, LESIA/ Meudon and IRAP/Toulouse for a total of 33 days to calibrate and analyze interferometer data remotely from their home institutes. Hands-on training was provided to one visiting astronomer from Brazil on a 7 months stay in the frame of the VAP. Assistance was provided to 43 science projects in total. IRAM astronomers collaborated on 60 projects in which they were directly involved.

Visiting astronomers reducing Plateau de Bure interferometer data with the assistance of IRAM staff astronomers.

In a continuing and successful, joined-up effort with the Centre de Données astronomiques de Strasbourg (CDS), data headers of observations carried out with the

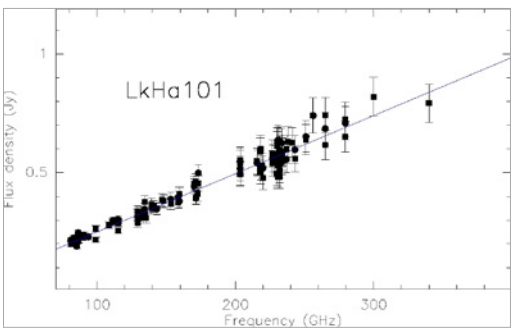

Spectral energy distribution of the optically thick core surrounding LkHa101 in the frequency range from 80 to 350 GHz.

Plateau de Bure Interferometer are conjointly archived at the CDS, and are available for viewing via the CDS search tools. In 2013, the archive contained coordinates, on-source integration time, frequencies, observing modes, array configurations, project identification codes, etc. for observations carried out in the period from January 1990 to September 2012.

The archive is updated at the CDS every 6 months (May and October) and with a delay of 12 months from the end of a scheduling semester in which a project was observed in order to keep some pieces of information confidential until that time.

VLBI NEWS

The year 2013 marks a significant technology advance in mm VLBI. A new generation of digital backends provides larger instantaneous bandwidths (up to 2 Gb/s) and better sensitivities (up to a factor of 2) at most VLBI stations.

Two Global 3mm VLBI Array (GMVA) sessions were scheduled in May and in September 2013 that included both IRAM observatories. However, due to exceptionally bad meteorological conditions at both observatories no data were acquired during the May session. Successful 1mm VLBI observations were conducted in March 2013. The participating stations included CARMA and for the first time the APEX antenna in Chile, besides the IRAM facilities. Fringes were detected on the Apex – IRAM 30M – CARMA baselines, while the data on baselines with the PdBI phased array require a more complex treatment due to their smaller bandwidth, and are still under analysis.

On Pico Veleta, VLBI was conducted during the first half of 2013 with a rented EFOS-21 maser (courtesy of MPIfR Bonn while our vintage EFOS-10 maser underwent a major revision at T4Science, Switzerland) and a new Mark5C recorder with increased bandwidth replacing the old Mark5A. The revised EFOS-10 maser was reinstalled at the 30m-telescope in August, and has been working well since then.

Plateau de Bure still operates with a Mark5A recorder (higher data rates will have to wait for the new NOEMA correlator and its high-capacity VLBI modules) but observations in a new integer backend frequency observing mode successfully provided fringes in "zoom-mode" at the MPIfR Bonn software correlator with stations recording at higher bandwidths. This means that the PdBI phased array stays compatible with stations recording in higher data rates.

RADIONET TRANSNATIONAL ACCESS (TNA)

IRAM is a member of RadioNet, an initiative to coordinate radio-astronomy facilities for the benefit of European astronomers. As in previous years, travel funds have been made available to RadioNet eligible astronomers from non-IRAM partner countries for expenses incurred during their stay at IRAM for observations with the 30m-telescope and for reducing data from the Plateau de Bure Interferometer. These funds, which were initially made available by the European Commission for the institutes participating in the FP6 TransNational Access (TNA) initiative, are today granted by the FP7 programme. Only expenses related to accommodation or travel were covered in 2013. Because of non-compliance with directives of the European Commission, financial support to astronomers visiting IRAM for reducing Plateau de Bure Interferometer data was closed from June to December.

The program committee received 29 TNA-eligible proposals for the 30m-telescope, and recommended 28 for observations (12 A-grades and 16 B-grades). Among those, 25 could be scheduled at the telescope for a total of 813 hours. Note that a fraction of this time was lost due to the bad weather at the observatory, and that the affected projects could not be completed. During the year, 13 European astronomers were granted travel support to Granada for observing their project.

For the same year, the program committee received 28 TNA-eligible proposals for the Plateau de Bure Interferometer and recommended 13 proposals (3 A-rated, 10 B-rated) for observations. Taking into account proposals accepted in 2012 but continued in 2013, time was allocated to 10 eligible proposals corresponding to a total of 12 projects and 136 hours of observing time.

User responses to questionnaires to the RadioNet management in Bonn show that IRAM continues to maintain an excellent reputation concerning the assistance and service given by scientists and support staff to visiting astronomers.

RadioNet observing time from 2010 to 2013 was allocated to eligible investigators from 12 European countries and with a well balanced distribution between senior scientists (53%), PhD students and post-doctoral researchers (47%).

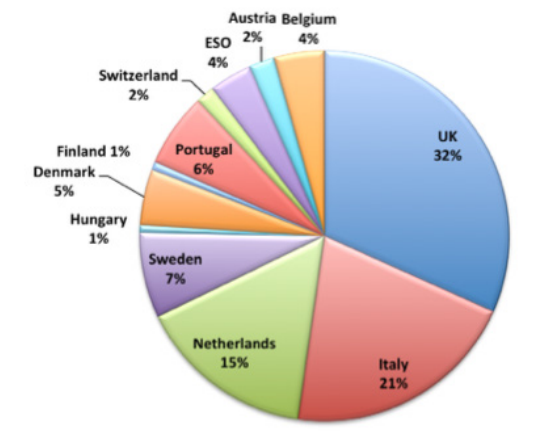

Grenoble headquarters

Frontend group

During 2013, the Frontend group was very busy with maintenance and development activities for both IRAM observatories. The focus was on the development of the new NOEMA receivers, on the upgrades of the EMIR receiver and of the laboratory instrumentation, as well as on the development and test of components for AETHER and ALMA Band 2&3. Also, SIS mixers were produced for other research institutes.

PLATEAU DE BURE INTERFEROMETER MAINTENANCE

The Sumitomo CSA-71A compressors of the PdB receiver cryogenerators were serviced on five antennas (1, 2, 3, 4 and 6) after seven years of continuous operation (60000 hours). The maintenance consisted in replacing the capsule compressor, the oil separator and some annexed parts.

In parallel, the maintenance of the Sumitomo cryogenerators, every 15000 hours of operation, was performed using the "hot-swap" method, where the active parts of the cold-heads were swapped without opening the cryostat and removing it from the receiver cabin. The cryogenerator maintenance was made on antennas 2, 4 and 5.

Three 18-26 GHz WVRs (Water Vapour Radiometers) were serviced and repaired.

UPGRADES AND NEW FRONTEND DEVELOPMENTS FOR THE 30 M TELESCOPE

New cryogenic module for EMIR E1

The 2 mm band (E1) of the dual-polarization EMIR receiver on the Pico Veleta telescope was upgraded from backshort-tuned Single Side Band (SSB) mixer delivering one band of 4-8 GHz to Sideband

New E1 (127-179 GHz) cryogenic optical module installed in EMIR in October 2013.

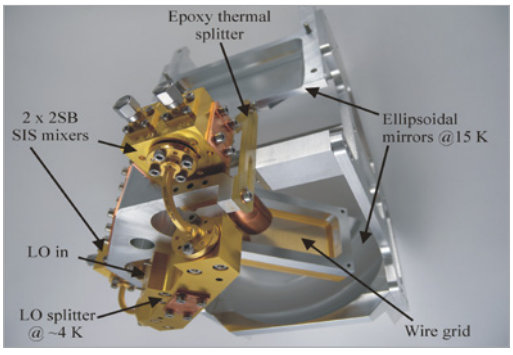

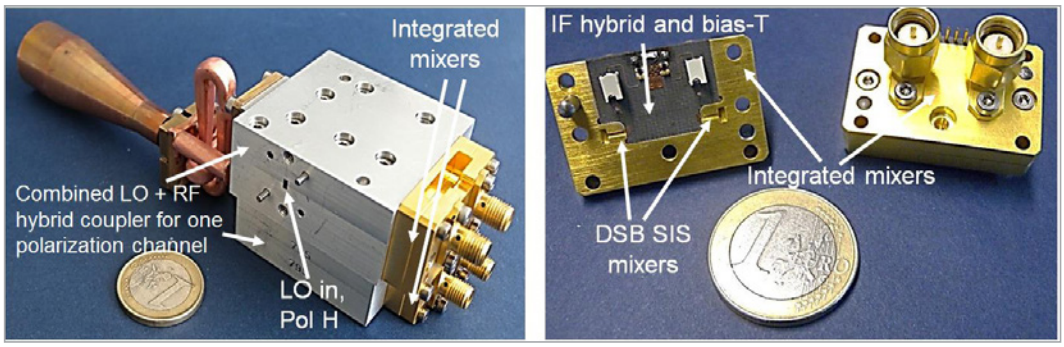

Prototype of single-pixel cryogenic module for the 3 mm band of the future multibeam receiver for the Pico Veleta radiotelescope.

Separating (2SB) mixer delivering two 4-12 GHz IF bands. The cryogenic module includes a new mechanical interface between the two ellipsoidal mirrors, the feed-horn flanges, and the wire-grid to improve the alignment on the sky between the two (linear) polarizations. The local oscillator is distributed to the two independent 2SB mixers through a waveguide local oscillator splitter and 90º waveguide bends thermalized at 4 K. The SIS mixer unit is a copy of the one adopted for NOEMA Band 2, which is described in a next section.

Electronically tuned YIG Local Oscillator for EMIR E3

The LO Gunn system of EMIR E3 was replaced by a spare LO system of PdBI Band 4 (283-365 GHz LO range) allowing extension of the upper edge of the observable sky frequency from ~358 GHz to ~373 GHz (which was not limited by the mixers or optics).

Prototyping of components for a 3 mm band multibeam receiver

A good progress was made on the design of a 5x5 pixel dual-polarization 2SB SIS receiver for the 3 mm band (70-116 GHz). A prototype of a single-pixel RF module for a 5-pixel linear array was built and characterized. The module includes a combined waveguide 90º hybrid coupler and LO injection coupler as well as an integrated mixer block which includes two DSB SIS mixers, a 90º IF hybrid and mixers bias-T. The two IF outputs of each polarization channels are connected directly to a cryogenic low noise amplifier without intervening isolator.

Characterization of panel painting for the Pico Veleta reflector

The paint of the reflecting surface of the 30-m radio telescope has degraded over the past years due to the thinning of the existing paint layer over a large part of the dish. The dish needs to be re-painted. In order to qualify different types of paint and determine their maximum thickness for minimum degradation of the antenna efficiency, several aluminum painted samples were characterized in the laboratory at mm-waves. The experimental results show that the excess noise due to the paint layer across 250-370 GHz increases dramatically for paint thicknesses beyond ~45 μm and is independent of the paint type. Electromagnetic modeling of the paint layer, combined with the experimental results, allowed to constraint the dielectric properties and to derive approximate values of the dielectric constant and tangent loss of the paint at millimeter wavelengths.

CONTINUUM DETECTORS FOR THE 30 M TELESCOPE

NIKA1 (prototype)

The 6th test run occurred in June 2013. The main upgrades were a new 2 mm array with bondings allowing the suppression of unwanted RF propagation modes, a new amplifier for the 1mm band, instrument control and data processing, and a better integration of NIKA in the telescope system, with the possibility to perform Lissajous scan patterns. The average Noise Equivalent Flux Density achieved during the run was:

- $NEFD_{150GHz}$ = 15 mJy×s$^{1/2}$ with 94% good pixels yield.
- $NEFD_{240GHz}$ = 40 mJy×s$^{1/2}$ with 85% good pixels yield.

Despite a leak in the cryostat and some problems with the data the main goals of the run were met so that the opening to the community occurred via IRAM's call for proposals, for a pool run in February 2014.

The cryostat was repaired at the Institut Néel in Grenoble in the summer, shipped back to Pico Veleta, and quickly tested on site in November. This test included a new polarizer prototype (LPSC – I. Néel), and 4-faced pyramids corrugated lenses, that were both tested in laboratory previously.

NIKA2 (instrument)

The NIKA2 instrument design was finalized in 2013 and a final review meeting occurred in April 2013. The cryostat will contain 3 channels for simultaneous observations: a 1000 pixels array for the 150 GHz band, and two 2000 pixels arrays for the 240 GHz band allowing the measurement of the linear polarization of the targeted sources. Each of these 3 arrays will fully cover a field of view (FoV) of 6.5' in diameter, all of them being cooled at 100mK using a 3He-4He dilution fridge. The fabrication of the cryostat has started.

The activity on the KID improvement for NIKA2 has increased at the Institut Néel and at IRAM where KID design and micro-fabrication is performed.

The KID will be read by the NIKEL electronics, which allows a multiplexed readout of up to 400 channels over 500 MHz bandwidth. 20 NIKEL boxes will be used in NIKA 2. The future location of the NIKA2 components in the telescope has been defined.

A workshop dedicated to the large programs that will be proposed by the NIKA consortium for the guaranteed time occurred in October 2013.

30 m cabin mirrors refurbishment

The study of the future large FoV optics for NIKA2 and heterodynes focal plane arrays (FPA) continued in 2013. Optics simulations confirmed that the maximum FoV available with the Nasmyth system is 7' (arc-minutes) diameter, and 11' for a tertiary mirror (M3) with 2 axes of rotation. The 7' option was chosen for the implementation. 3D modelling allowed to progress on the definition of the future mounts, attached to the roof for M3 and attached to the side wall for M4. The Grenoble mechanical group started structure studies. An installation of the new optics is foreseen in September 2014.

GISMO 1 & 2

GISMO has continued to be used on the same basis since 2012, with 2 pool runs in 2013. The median NEFD of 14 mJy$\times$s$^{1/2}$ is confirmed.

GISMO-2 will be a 2 band system using filled arrays of 1280 pixels at 250 GHz covering a 4'x5' FOV and 256 pixels at 150 GHz covering a 4'x4' FOV. The GISMO-2 optics has been finalized in March 2013, and its complete cryostat architecture in the following months. The fabrication of all the parts of the instrument (cryostat, detectors, optics, etc.) is ongoing. The delivery for first tests at the 30m telescope is foreseen for the autumn 2014.

NOEMA FRONTEND

The first NOEMA quadri-band heterodyne receiver, based on 2SB SIS mixer technology, is being built for installation on antenna 7. Successful developments were carried out for some of the key components of such receiver, including new 2SB SIS mixers, cryogenic optics modules and an electronically tunable LO for the 3 mm band, which were built and characterized. The Frontend design was completed and the purchasing of the parts for the production of the 11 NOEMA Frontends (10 + 1 spare) for NOEMA Phase A has started. The goal is to build four new receivers for the four new antennas and to upgrade the 7 (6 + 1 spare) existing PdBI receivers to the NOEMA specifications.

Fully integrated 2SB mixers with 3.8-11.7 GHz IFs for Bands 1 and 2

The design of a 90º IF hybrid coupler chip based on superconducting lines and employing three coupling sections to achieve low gain and phase imbalances allowed the development of a fully-integrated sideband separating (2SB) mixer. All components constituting the 2SB mixer, i.e. the 90º RF hybrid coupler, two DSB mixers, the in-phase LO splitter and the 90º IF hybrid coupler, are now combined into one mechanical block resulting in a very compact unit. Such mixers have been designed and fabricated for both Bands 1 and 2 of the NOEMA receivers. In the two bands, the new mixers yielded very good performances in terms of noise temperatures and image rejections. Furthermore, the RF bandwidth of the Band 1 mixer could be enlarged with respect to the previous generation allowing the NOEMA Band 1 receiver to cover the 72-116 GHz signal band.

Cryogenic optics modules for Band 1, 2 and 3

New cryogenic optics modules were designed, fabricated and tested for NOEMA Bands 1, 2 and 3. The modules share the same design philosophy, where two ellipsoidal mirrors thermalized at 15 K re-image the antenna sub-reflector into the apertures of the two independent single-polarization feed-horns. A polarization splitting wire-grid and the feed-horns, attached to the main frame of the module (made of

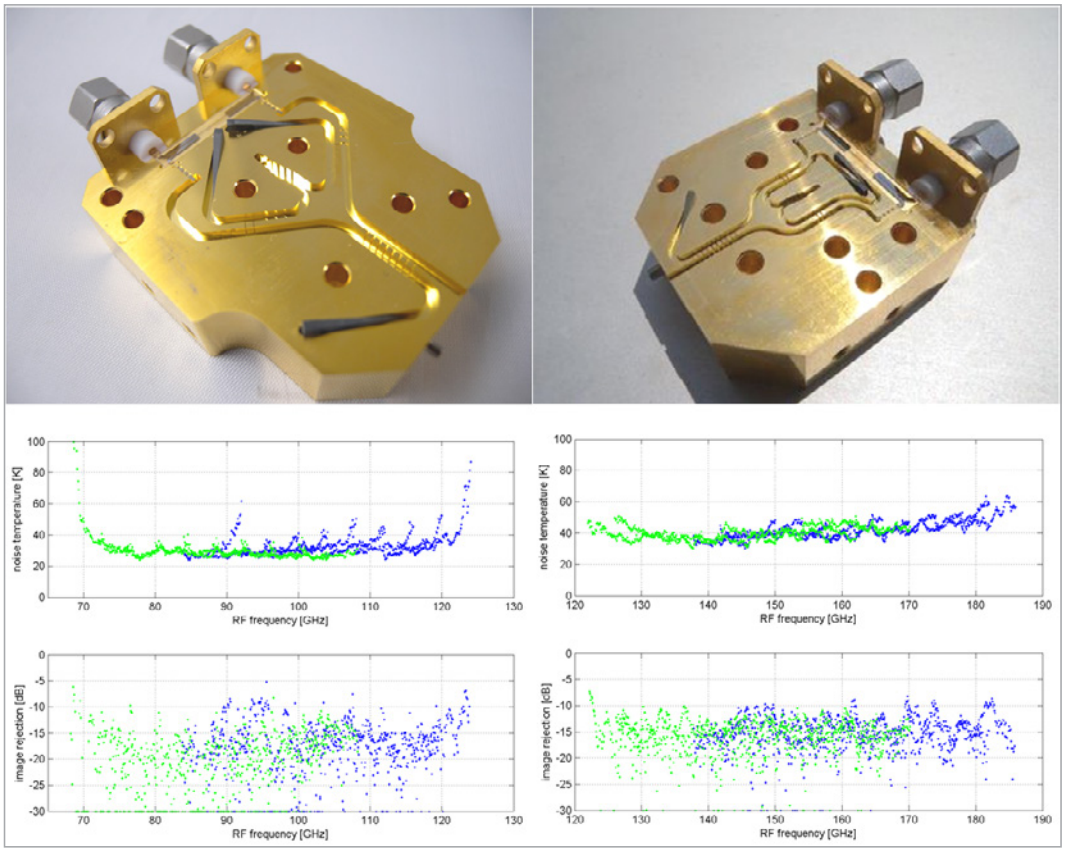

NOEMA Band 1 (72-116 GHz) and Band 2 (127-179 GHz) 2SB mixers: One half split-block of the fully-integrated 2SB mixers with SIS junctions, IF coupler chips, and loads (above) and typical performances of the mixers in terms of noise temperatures and image rejections (below, green: LSB measurements, blue: USB measurements). Bands 1 and 2 are shown on the left and on the right, respectively.

6060 aluminum), will be maintained at 4 K. Fiberglass tabs are used to thermally split the 15 K and the 4 K stages. The optics modules were tested at room temperature using the IRAM mm-wave antenna range and proved to work well, according to the prescribed specifications. The co- and cross-pol beam-patterns of each polarization channel were measured at the central RF frequency and at the band edges.

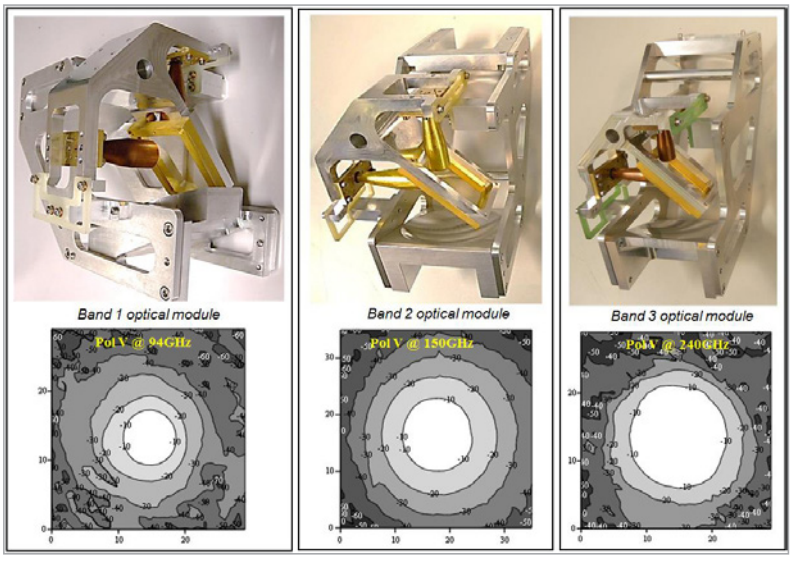

Cryogenic optics modules for NOEMA Bands 1, 2 and 3 (top panels) and Pol V copolar beam patterns measured with the antenna range at the central frequency of the respective RF ranges (bottom panels).

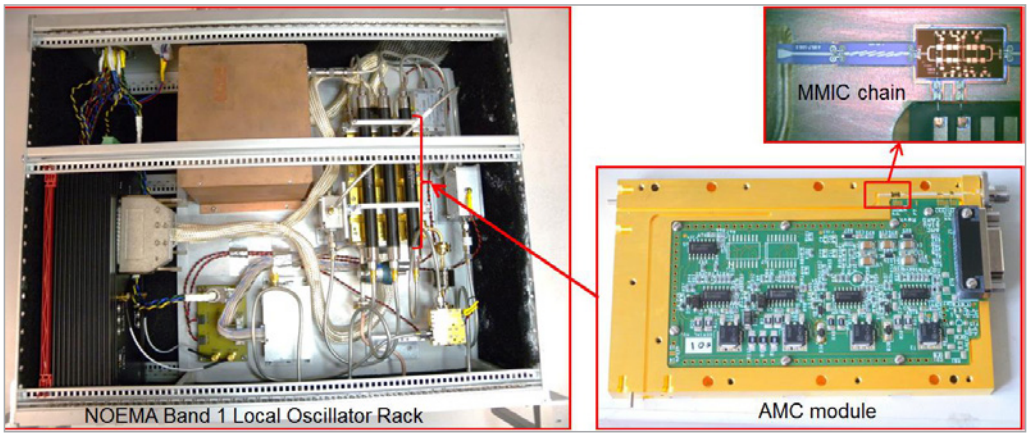

Electronically tunable NOEMA Band 1 Local Oscillator system showing the rack (left) and the AMC module with details of parts of the 3 mm band MMIC chain (right).

Electronically tuned Local Oscillator for Band 1

A new electronically tuned YIG-based Local Oscillator (LO) was designed, constructed and tested for NOEMA Band 1. The LO frequency can be phase-locked on the LO1ref PdBI reference signal (13.6-16.4 GHz) and tuned anywhere across the 83.7-108.3 GHz range. The new LO system will allow astronomy observations with the Band 1 2SB SIS receiver across the 72-116 GHz signal band with no noise degradation compared to that delivered by a Gunn oscillator pump. The LO output power is ~17dBm with Active Multiplier Chain (AMC) cascaded with a Power Amplifier (PA) module and ~10 dBm without PA (retained for the final use).

NEW LABORATORY TEST EQUIPMENT

A new 70-116 GHz probe-station was developed in-house to allow on-chip S-parameter measurements of mm-wave MMIC components and micro-circuits. The probe-station is interfaced with the IRAM mm-wave Vector Network Analyser (MVNA).

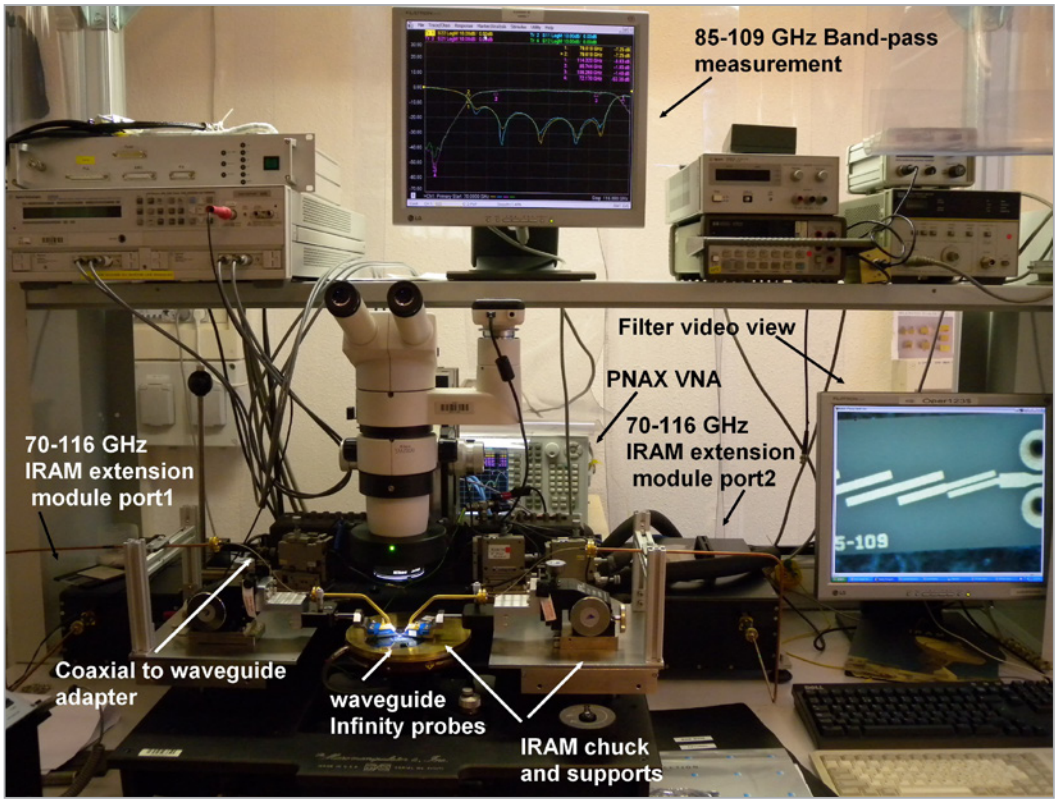

On-chip S-parameter measurement system for 70-116 GHz developed at IRAM.

ALMA BAND 7 CONTRACT

The IRAM Frontend group produced 73 ALMA Band 7 cold cartridges (275-373 GHz). The production ended in December 2012 with the delivery of the 73rd cartridge. One of the two cartridge test sets was shipped early 2013 to the ALMA Operation Science Facility (OSF), Chile, in preparation for a later on-site maintenance by the ALMA team.

In the course of 2013, five cartridges were returned to IRAM for repair, under guarantee. They were fixed and sent back to the OSF.

ALMA BAND 2+3

The IRAM Frontend Group is collaborating with other European institutes to carry out a 16-month feasibility study funded by ESO aiming at developing ALMA Band 2 and a combined Band 2 and 3 receiver system. During 2013, the IRAM contribution focused on the development of wideband feed-horns and orthomode transducers (OMTs) for the 67-116 GHz band (ALMA Band 2+3) as well as on the design of the vacuum window and IR filters. Some prototype units of OMTs and feed-horns were fabricated and tested and are within the ALMA Band 2+3 specifications.

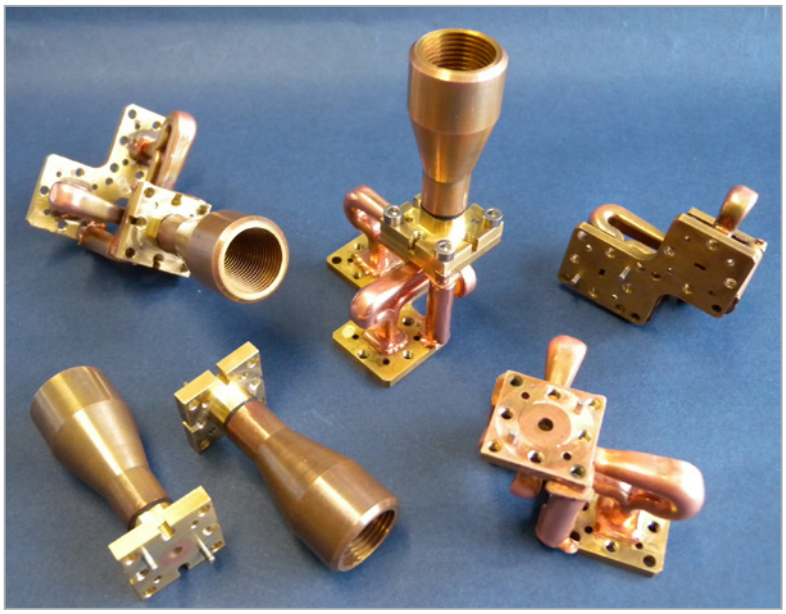

Prototypes of feed-horns and OMTs developed at IRAM for 67-116 GHz (ALMA Band 2+3).

AETHER ACTIVITIES

Within the framework of the three-year AETHER FP7 program, a collaborative effort of European research institutes, IRAM is involved in the two following tasks:

- Task 1: The development of a prototype pixel for a 67-116 GHz dual-polarization cryogenic module using methamorphic HEMT technology. Some mHEMT MMIC low noise amplifier chips were designed and fabricated at IAF (Fraunhofer Institut for Applied Solid State Physics, Freiburg, Germany) and delivered to IRAM, which was in charge for their packaging and tests. The mechanical packaging of the MMIC consists of a split-block design with WR10 waveguide accesses and broadband waveguide-to-microstrip transitions based on 80 µm thick quartz substrate fabricated by the IRAM SIS group. The mechanical packaging includes, besides the MMIC, a bias circuit based on commercial microelectronics components.
- Task 2: The development of advanced receiver pixels and LOs for large Focal Plane Arrays in the near mm-wave domain.

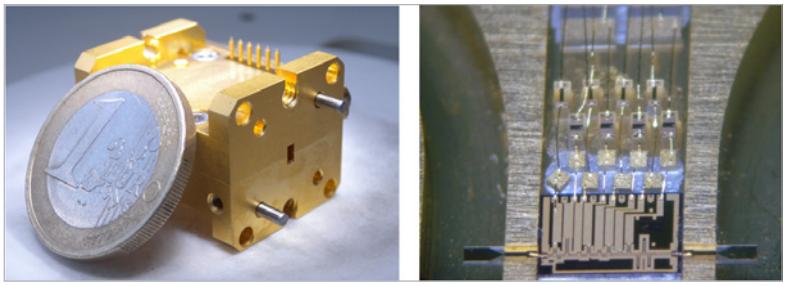

Left: W-band waveguide LNA with MMIC amplifier from IAF packaged at IRAM. Right: Detail of an IAF MMIC integrated between two waveguide probes. The microelectronics components of the bias circuit are also visible.

EXTERNAL PROJECTS

Eight IRAM 275-373 GHz 2SB SIS mixers were produced and delivered to MPIfR (Max Planck Institut für Radioastronomie), Bonn, Germany. The mixers will be part of the LASMA (Large Atacama SubMillimeter Array) focal plane array receiver to be installed on the APEX telescope, Chile.

Two EMIR E0-type 2SB mixers for the 3 mm band were produced and delivered to OSO (Onsala Space Observatory), Chalmers University of Technology, Sweden. The mixers will be part of the new dual band receiver to be installed on the Onsala 20-m radio telescope.

SIS Group

The activity of the IRAM SIS was mainly concentrated on two tasks during 2013. On one side, SIS junctions and passive IF hybrids were fabricated for the NOEMA project and the development of multibeam receivers. Careful parameter adjustment in design and device processing allowed to further extend the frequency coverage of the IRAM 3mm SIS mixers. At the same time the superconducting hybrids designed by the receiver group were an important factor of further performance improvements and mixer space reduction. Part of this work was supported by the EU FP-7 Radionet program AETHER.

On the other side, a rapidly growing number of developments were focussed on the new kinetic inductance technology (KIDs) as used for NIKA I and NIKA II. To support the NIKA II project, the 4 inch lithography was commissioned and explored together with the related structuring steps like dry and wet etching. In order to improve superconducting film homogeneity, the upgrade of a special planar sputter cathode from 4 to 6 inches with including a modified gas shower for reactive sputtering was prepared and will be ready for use in early 2014. TiN development was continued with a focus on physical and chemical film characterization. This work was supported by the French ANR Labex program FOCUS.

Deep silicon etching to create anti reflection layers for the KID detector arrays on Si wafers was successfully explored with promising results. Furthermore air bridge technology was continued to be improved in order to suppress undesired asymmetric modes in coplanar waveguide feed-lines as used in the KID arrays for frequency multiplexed readout.

Spare SIS mixer devices for ALMA band 7 were produced. Work on membrane based passive circuits was continued and OMT prototype circuits could be delivered to INAF within a common development program. The SIS group also produced auxiliary structures for waveguide MMIC transitions.

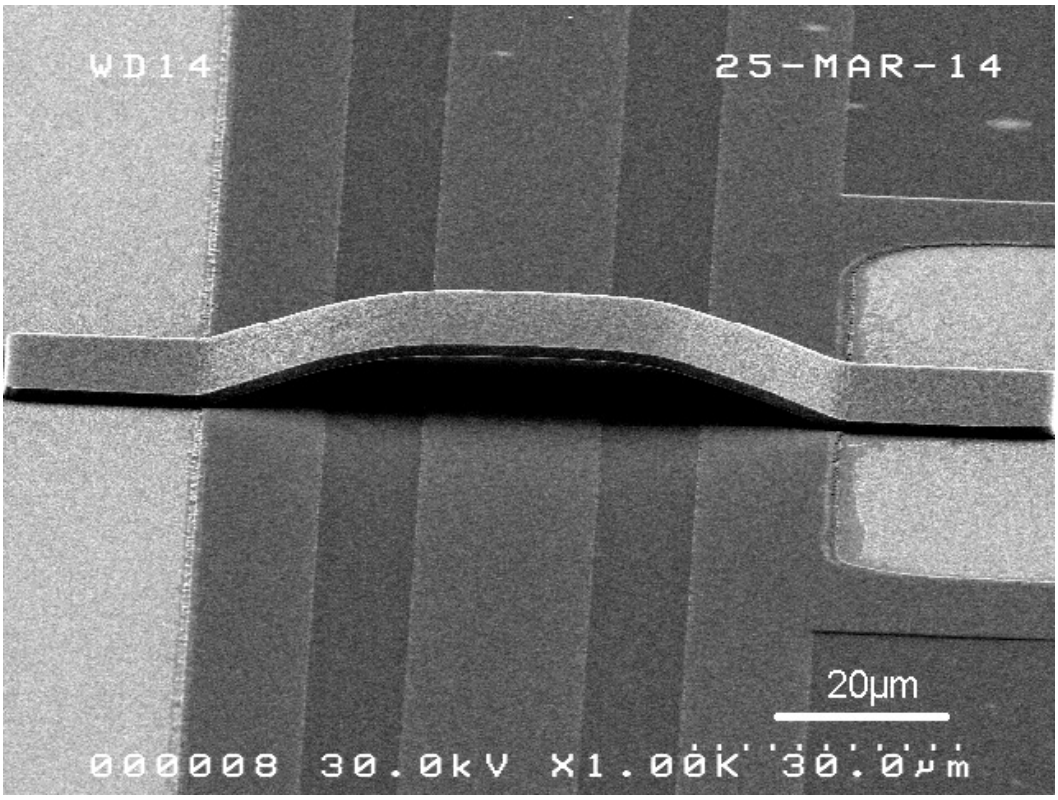

Aluminium air bridge for balancing of coplanar waveguide as used for KID frequency multiplexing readout line.

Backend Group

UPGRADE OF THE IF PROCESSOR: *LE STRAPONTIN* (JUMPSEAT)

The WideX digital correlator has been designed for eight antennas and installed in 2010. However, the IF processing for antennas 7 and 8 was not implemented, because this piece of equipment is far more simple and could be appended any time later. The beginning of the construction of antenna 7 has triggered the fabrication of a rack, dubbed "Le Strapontin" due to its temporary aspect. Actually it is a replication of what was built in 2006 for six antennas. Extra modules were built and stored at the time, which are now being revived and brought functional. The initial idea was to have fixed-phase LO2s for antenna 7, but it was found later that making them phase-steerable (like the six others) would greatly simplify the software, especially when sub-arrays will need to be formed. The additional hardware required being limited to an extra CAN interface so that it was decided to implement it that way. The equipment is scheduled to be installed on PdB June 2014, after a main computer change.

THE NEXT GENERATION CORRELATOR FOR NOEMA: POLYFIX

The number of antennas on the PdB interferometer has increased by discrete steps over the past 20 years. Each step has motivated a change in correlator technology. With a target of 12 antennas, NOEMA requires a giant leap in correlator design. A Polyphase filter bank, followed by an FX will supersede the traditional lag, XF processing.

ANALOG PROCESSING

A frequency plan that efficiently interleaves successive scans in order to cover very large segments of the mm-spectrum has been worked out in collaboration with the receiver and science groups. It uses a single downconversion scheme to minimize spurious line generation.

The IF signal travels to the building as modulated light and is later digitized in the correlator. Both forms do not degrade with distance. However, some operations like filtering and calibration noise injection need to be performed in an analog fashion.

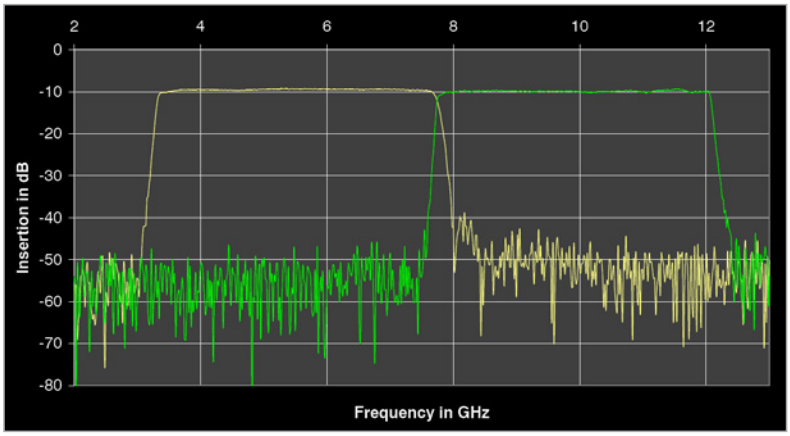

Response of the prototype IF processor. The exact crossover frequency of 7744 MHz yields an optimal stitching of the analyzed bands.

These functions have been implemented in a very compact design in order to minimize band flatness deterioration. Filters have been carefully selected and ordered. Low cost phase-locked oscillators have been designed and tested. A complete prototype chain has been built.

DIGITAL UNIT

The design has stabilized around a full-custom backplane capable of 192 connections running at 5.12 Gigabits/sec (Gsps). The samplers will operate at 5 bits, 8.192 Gsps and the bulk processing clock will be 128 MHz. All clocks can tolerate a +/-100ppm deviation in order to implement barycentric referencing in the future.

The chosen FPGA family is the Altera Arria-V. The correlation characteristics are defined by the configuration data which are loaded into the FPGAs. The hardware itself is better seen as a platform running 12 high speed digitizers and 66 cross-processors. By changing the FPGA configuration data, a different correlator can be created. This has been found an interesting feature. For this, on each board, a flash memory will be installed to store up to eight different mode programs that can be applied in a short time.

The baseline mode is an FX where every unit can cover ~4GHz of bandwidth, one quarter of which can be analyzed simultaneously at a higher resolution. There will be a total of 8 such units, giving an aggregated capacity of 32 GHz (4 IFs of 8 GHz each).

POSSIBLE LONG TERM IMPROVEMENTS

New mode programs will be devised after Polyfix delivery and baseline mode first light. Among these, several have already been identified:

- High resolution mode : narrower channels can be obtained at the sacrifice of a fraction of the continuum bandwidth.
- Survey mode : all the band is covered at an intermediate resolution. This mode nicely combines with the interleaved frequency plan to provide huge line surveys.
- Phased array mode: the signals from N (up to 12) antennas are summed up to a single output.

This is a non-exhaustive list. Other programs can be specifically tailored to match new observing needs that may show up in the future.

LO REFERENCE SYSTEM III

On the six existing antennas, two LO1s can be operated simultaneously at different frequencies. Bi-band observation is not currently practiced, though the LOs would allow for it. Having two different LO1 circuits has some operational benefits, however, like fast project switching, redundancy and eased troubleshooting. But for NOEMA, the sub-array feature makes it a requirement. A completely new hardware using the field-proven scheme of round-trip phase measurement has been built for twelve antennas, and installed on site this summer. It has been devised around 48-bit DDS synthesizer chips that give microhertz resolution and submicrosecond phase switching. It is linked to a dedicated real-time computer via an EtherCAT interface. A permanent cable health monitoring equipment is built-in. Together with the PLL-YIG reference oscillators that are operating in the antennas since 2010, this equipment provides the PdBI with a low phase noise, high accuracy Local Oscillator system for the years to come.

Low phase noise LO reference system for 12 antennas in operation on Plateau de Bure

Mechanical group

CONSTRUCTION OF THE MECHANICAL MOUNT FOR THE FIRST NOEMA ANTENNA

The assembly of the mechanical mount was started on April 10th, 2013. Several objectives had to be achieved during this first phase :

- Ensure the same high quality standards in manufacturing all components of the mechanical mount.
- Optimize some of the technical parts of the mechanical mount, such as the (azimuthal) cable drum.
- Ensure that the assembly of the mechanical mount follows the reference schedule used for Antenna 6 but with a completely new mechanical team.
- Verify all electrical studies of the antenna in order to improve its performance and reliability in compliance with new standards.

Phase 1: Production of the mechanical mount by our subcontracting partners

In order to ensure the best quality for all individual parts of the mechanical mount, the mechanical team guaranteed regular quality controls.

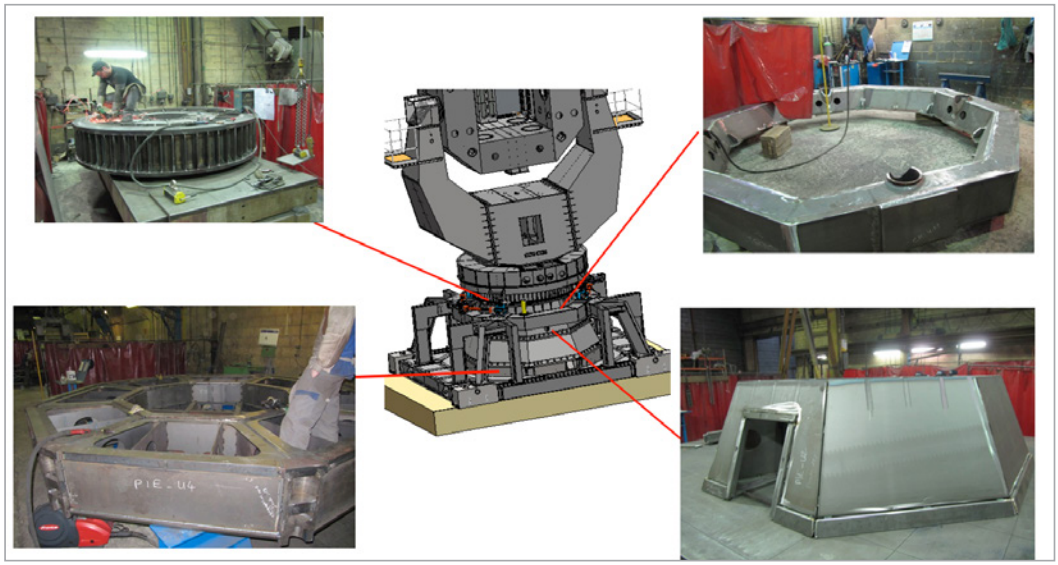

Some pictures of the production of the mechanical mount

Phase 2: Assembly of the mount on the Plateau de Bure

The assembly of the mechanical mount went without any major problem or delay in the schedule and is now completely finished. The next phase, i.e. the assembly of the reflector, is scheduled for early 2014.

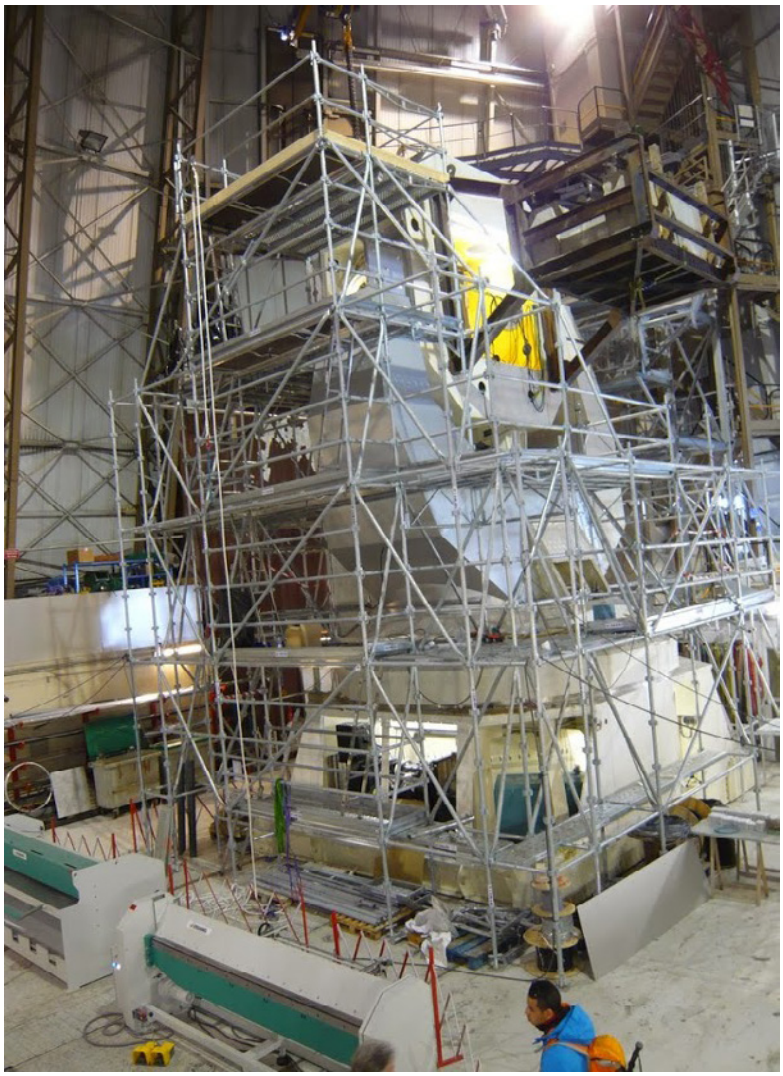

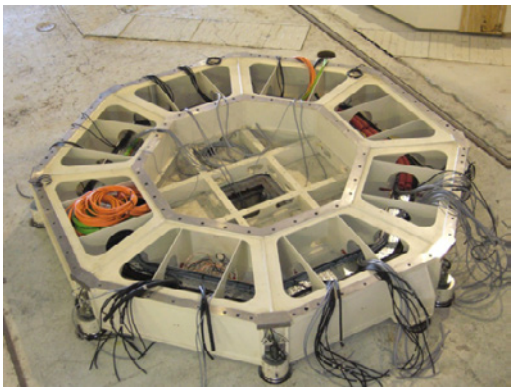

Computer group

UPGRADES OF CURRENT HARD- AND SOFTWARE

To support larger amount of data, the scientific file server has been extended up to 12 terabytes and most astronomer workstations have been upgraded. Thanks to both investments, IRAM astronomers and their external visitors can work in much improved conditions, especially with respect to disk space and computing speed. Following a past decision, new computers have been also delivered to the Frontend and Mechanical groups to run computing intensive applications like Solidworks. Finally, a total of 35 new computers have been bought in 2013.

The migration to newer operating systems has continued. At the end of 2013, the figures are: 66% completed for computers with Windows 7 as operating system and 80% for computers with Scientific Linux 6.4 as operating system.

Since 2008, the computer group has operated Linux virtual servers, but no virtual Windows servers yet because of the high license costs. The situation has changed in 2013 when the main vendors propose free editions of their virtualization products. Finally, Citrix XenServer 6.2 has been chosen, and 4 virtual Windows servers have been already configured.

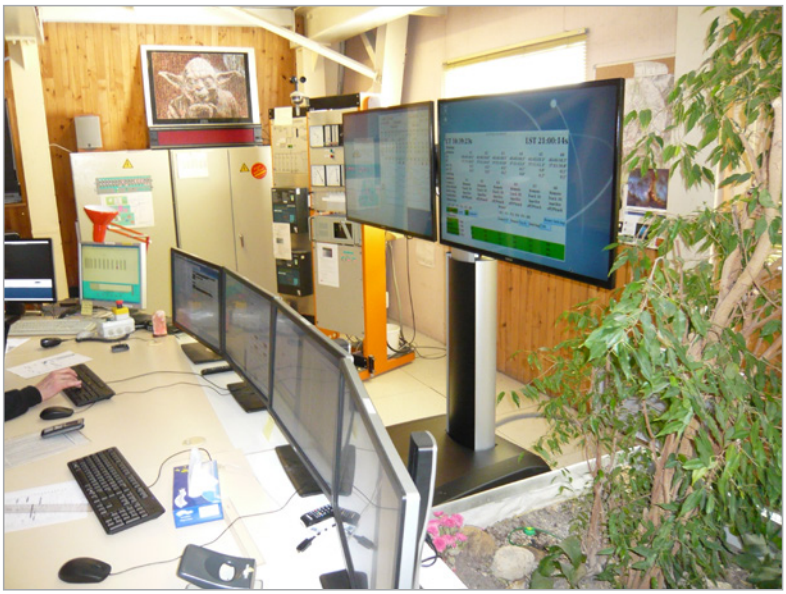

Picture of the control room showing the new large screens bought and installed in 2013.

NOEMA

In order to benefit from a high-speed network link to the observatory at Plateau de Bure, the computer group has continued to search for solutions by contacting and discussing with local authorities. The results from these discussions in 2013 are very promising, especially at the regional district level. Therefore, IRAM hopes to join AMPLIVIA, the regional high-speed network for high-school and universities, next year.

In 2013, the computer group has manufactured different kinds of NOEMA hardware like sun detectors, antenna display panels, and analog velocity loop boards. All these devices will be installed in the new antennas in the next years.

The group has also installed several NOEMA computing systems at Plateau de Bure like new computers for operators, phasers realtime computers, and head network switches for new antennas.

A new milestone was also achieved with the new antenna control software in August 2013, when the azimuth/elevation servo motion has been successfully tested on antenna 5, promising an efficient and good functioning of the final control software of antenna 7.

Science Software Activities

Overview

The main goal of the science software activities of the GILDAS group at IRAM is to support the preparation, the acquisition and the reduction of data both at the 30m and the Plateau de Bure Interferometer, including the NOEMA project. In 2013 these activities were encompassing the delivery of 1) software to the community for proposing and setting-up observations, 2) software to the IRAM staff for use in the online acquisition system, and 3) offline software to end-users for the final reduction of observational data. Specific efforts were also directed on the imaging and deconvolution of ALMA data inside GILDAS. Noteworthy, the GILDAS software suite is freely available to and used by a worldwide community of astronomers at other telescopes, like Herschel/HIFI, APEX, and SOFIA/GREAT.

The 30-meter telescope

At the 30m, much effort was invested to support the development and operation of GISMO and NIKA, the 2mm and 1mm continuum cameras. Several standard calibration modes were adapted and new observing modes, like the scanning of astronomical sources along Lissajou curves, were implemented. Moreover, NIKA is the prototype of the future dual band camera, which is scheduled for installation at the 30m in 2015. As such, dedicated work was done to pave the way towards a full integration of the future camera in the 30m control system. In particular, the 30m raw data format (IMBFITS) was upgraded to support NIKA's KIDS technology. On the spectroscopic side, work continued on MRTCAL, the new calibration software that was tailored to progressively replace MIRA in 2014. In addition to testing new calibration methods, this software was designed to ensure the most efficient processing as possible to prepare for the advent of the future 3mm and 1mm heterodyne multibeam receivers. The offline spectroscopic data reduction and analysis will continue to happen in CLASS. Several incremental improvements were also made to CLASS, including improving the software's readout performance. A better support of third-party telescopes was also implemented: 1) Fortran and Python data fillers, including the possibility to append instrument specific parameters, were coded and proposed to external developers that make use of the Class Data Format (e.g., APEX, Effelsberg, SOFIA). 2) In collaboration with the University of Cologne and the Herschel science center at ESAC, the double sideband deconvolution code was upgraded to handle Herschel/HIFI data. Finally, work started at the 30m to reinstate the possibility of processing holographic data by taking advantage of the 39.4 GHz beacon of the ESA Alphasat communication satellite launched in July 2013.

NOEMA

In the frame of the NOEMA project, two main routes were followed. The arrival of new antennas implied the need to first develop new software to interface to new hardware and to upgrade operating software and, second, to upgrade operating software and to compare behavior and performance of new with existing hardware. Among the upgrades, work was continued to validate the performance of an inclinometer from Applied Geomechanics/Jewell Instruments. In the former line of activities, a major effort was made to replace the local oscillator system of the observatory. The new system is designed to cope with all 12 antennas of NOEMA Phase 2. In particular, a slight adjustment of the 100 MHz reference signal implied a number of consistent changes in several software packages. Second, the NOEMA project will lead to an increase of the data rate by about two orders of magnitudes. This called for a review of the different limitations of the current raw data format used at the observatory. As the data formats in use at both the 30m and PdBI observatories share the same standards, it was decided in 2012 to create the CLASSIC library. The common library will help decrease software maintenance efforts and system downtimes. As part of this work, all known file size limitations were effectively removed in 2013. Software optimization and integration will take place in 2014.

Plateau de Bure Interferometer

Support for standard PdBI science operations continued. From the data acquisition viewpoint, work was carried out for a proper handling of coordinates and doppler tracking of fast moving bodies (e.g., comets). Many improvements were implemented in the calibration pipeline: 1) The flux and position of our main secondary flux calibrator, MWC349, were reviewed; 2) A new secondary flux calibrator, LkHa101, whose LST range nicely complements the one of MWC349, was introduced; 3) The monitoring tool to assess phase shifts, by which to compensate for changes in the electrical

cable length, was improved; 4) A new algorithm to correct for the atmospheric phase fluctuations measured via the 22GHz water vapor radiometers was tested; 5) The algorithm to detect and remove spurious signals in the bandpass calibration was made more sensitive to weak signals; 6) The level of polarization of quasars was taken into account to improve the amplitude calibration; and 7) The tool implemented in 2012 to assess whether a faint line is detected inside the receiver bandpass was further optimized. Further team efforts were directed to maintaining the pipeline and enforcing a high stability.

The tuning of the calibration algorithms is extremely instrument specific. It is thus recommended to reduce and calibrate data using the software developed by the instrument team. On the other hand, imaging and deconvolution of interferometric data is mostly independent of the acquisition instrument. Hence, the advent of broadband spectra (8 GHz per polarization) at high spectral resolution in ALMA triggered in 2013 a series of changes in MAPPING, the GILDAS imaging and deconvolution software. Efforts were directed to implementing the possibility to work on only a subset of a huge dataset, too large to fit in the main memory. This work, made in collaboration with the Observatoire de Bordeaux, lays out the path to the large bandwidth and high spectral resolution capabilities of the NOEMA project. Phase self-calibration was also tested on both ALMA and PdBI data and found to improve significantly the dynamic range of images obtained on compact sources with flux densities larger than 20 mJy.

Further activities

All these software developments are based on the common GILDAS services, a set of common low-level libraries, collectively named GILDAS kernel, which take care of the scripting and plotting capabilities of GILDAS. Among the many small improvements, which took place in 2013, a particular effort was made to comply with the newest standards, among which, the version 3.0 of the Python language. Extensive testing of recent versions of the GFORTRAN compiler was undertaken with the goal to make this open-source compiler the new default, in addition to using IFORT, the Intel Fortran Compiler. The use of Fortran interfaces was generalized in GILDAS, as they tend to produce more robust code. While essentially invisible to end-users, these time-consuming tasks are required for the long-term viability of GILDAS.

Finally, a major effort was invested on PMS, the IRAM Proposal Management System. The facility was designed to replace and extend the capabilities of the current proposal submission and processing system for the 30m and PdBI. The software was in part rewritten in 2013 to ensure a secure and efficient use of the IRAM servers at the time-critical proposal deadlines. IRAM astronomers extensively tested the functionality of the submission facility and a series of load tests was performed during autumn 2013. According to plans, PMS will be put into operation and be open for use for the astronomical community at the summer proposal deadline of 2014.

Members of the GILDAS developers group sharing a light moment after a successful workshop.

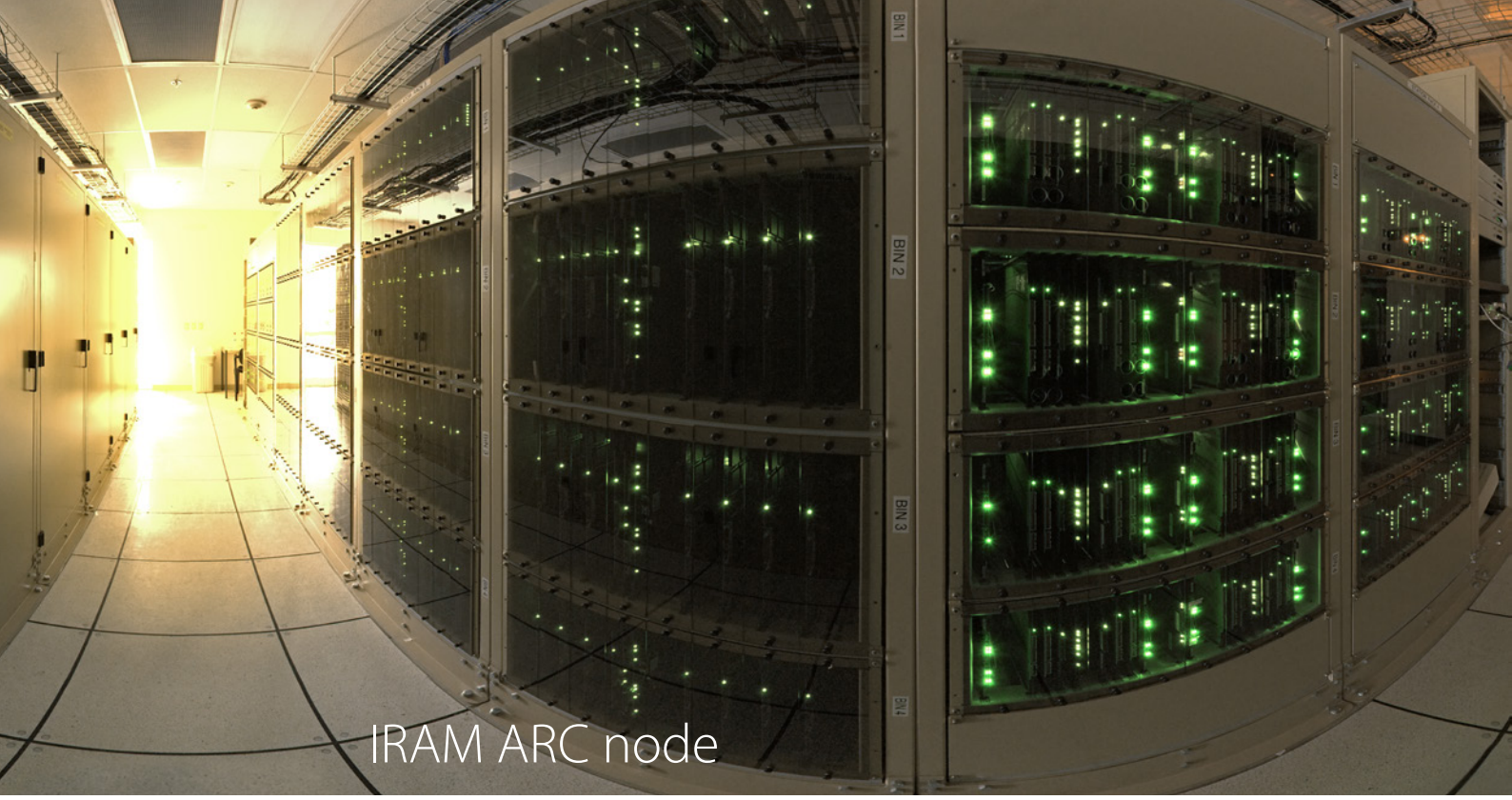

IRAM ARC node

The ALMA correlator is capable of performing up to 17 quadrillion operations per second.
Credit: ESO

IRAM is a node of the European ALMA Regional Center (ARC), the structure in charge of the ALMA science operations, including user support, in Europe. This is part of a long-term and more global involvement of IRAM in the design, construction, and operation of ALMA. One of the goals of the IRAM ARC node is to provide to the users a common support for the IRAM and ALMA facilities, hence maximizing the scientific synergies between the observatories.

ALMA USERS SUPPORT

The main tasks the IRAM ARC node was involved in were:

- Cycle 0 & Cycle 1 contact scientists: the ARC node staff acts as "Contact Scientists" for the accepted ALMA projects, providing expertise to check and validate the Scheduling Blocks that are created from the initial proposals. The IRAM ARC node supported more than 35% of all accepted+filler projects in Europe. Specific tools to display and possibly optimize the correlator setup in the ASTRO software were developed.
- Data quality assurance: within the European ARC network, IRAM is in charge of assessing the quality assurance of some of the datasets observed by ALMA. This implies calibration and imaging of the data, in order to check that the final data quality (in particular the noise rms) matches the initial requests from the proposal.
- Face-to-face support for data reduction: procedures similar to the Plateau de Bure rules are used to organize the visits of the PIs, including financial support for PIs affiliated to the IRAM funding agencies. Data fillers to transfer calibrated data from/to CASA to/from GILDAS were developed, allowing to image the data in both software environment.

TELESCOPE CALIBRATION SOFTWARE

IRAM is responsible for the development and maintenance of one of the key software for the real-time operations of ALMA, the Telescope Calibration (TelCal) software. TelCal is performing all real-time calibrations necessary to run the array: antenna pointing, focus, baseline measurements, atmospheric parameters, etc. 2013 was an important year for TelCal, as this year included the end of the Cycle 0 observations and the beginning of the Cycle 1, putting strong constraints on the performances and reliability of the real-time system. In parallel, the array commissioning continued, implying a continuous and important effort to correct, adapt, and further develop TelCal. A stand-alone version of TelCal, interfaced to the CASA off-line package, is also supported, to allow an off-line reprocessing of the real-time calibration. Finally, a specific version of CLIC, used for the ALMA holography processing, is also maintained in the TelCal package.

ADMINISTRATION

Exceptional transport arrangements at the Plateau de Bure Interferometer.

HIGHLIGHTS

The major event in 2013 concerning the administration was clearly the preparation and support of the prolongation of the partners' engagement for IRAM throughout 2024. This decision, taken during a general assembly in December 2013, underlines the confidence of the partner in IRAM's operation, developments and administration. The prolongation was connected to a relative complex process of preparation and adoption of new statutes which allows IRAM to pursue its tasks under well-defined conditions.

Apart from the regular activities within the IRAM administration the following special projects were pursued.

A dedicated reorganization of the running documentation and its classification was engaged. This reorganization followed two simultaneous objectives, on one side to improve the exchange of information within the administration group and on the other side to reduce overheads in the work of the individual group members.

Another project concerned a transversal activity to redefine and improve the application of procurement rules. This included the training of IRAM personnel as well as the redefinition of relations to some specific suppliers. In particular these activities allowed to better control costs related to external service and consulting.

FINANCIAL RESULTS

After the year 2012 with a negative balance, IRAM could re-establish financial balance for 2013. A dedicated and significant effort was required and while the institute's income increased by +1.7% from 2012 to 2013, the staff costs only increased by +0.5%.

The heavy activities in the new projects are also reflected by the capital value which increased by +12 MEu, basically due to the investments done in 2013 for the NOEMA project.

Tight cost control in particular for supplier contracts will remain essential to guarantee the success of the ambitious projects ahead.

IRAM STAFF LIST 2013

Group	NAME Surname	Position
IRAM Headquarter, Grenoble, France		
DIRECTION	SCHUSTER Karl-Friedrich	Director
	COX Pierre	Director until March 29, 2013
	GUETH Frédéric	Deputy Director
	DELLA BOSCA Paolo	
	GUELIN Michel	
	THIEVENT David	
	ZACHER Karin	
ADMINISTRATION FRANCE	DELAUNAY Isabelle	Head of Administration
	BACHET Claude	
	COHEN BOULAKIA Sandrine	
	DAMPNE Maryline	
	FERREIRA Dina	
	INDIGO Brigitte	
	LARDEMELLE Anne Carole	
	MAIRE Béatrice	
	MARCOUX Stéphane	
	PALARIC Laurent	
	SIMONE Jeannine	
	THIEVENT David	
MECHANICAL WORKSHOP AND DRAWING OFFICE	LEFRANC Bastien	Head Mechanical Group
	COPE Florence	
	COUTANSON Laurent	
	DANNEEL Jean-Marc	
	JUBARD Vincent	
	ORECCHIA Jean-Louis	
BACKEND GROUP	TORRES Marc	Head of Backend Group
	BALDINO Maryse	
	CHAVATTE Philippe	
	GARCIA GARCIA Roberto	
	GENTAZ Olivier	
	GEOFFROY Daniel	
	MAYVIAL Jean-Yves	
	MERRIEN Thierry	
COMPUTER GROUP	BLANCHET Sébastien	Head Computer Group
	AVRILLIER Xavier	
	CHALAIN Julien	
	DUMONTROTY Patrick	
	MOREL Francis	
	REYGAZA Mickaël	
FRONTEND GROUP	NAVARRINI Alessandro	Head Frontend Group
	ADANE Amar	
	BERTON Marylène	
	BORTOLOTTI Yves	
	BUTIN Gilles	
	CHENU Jean-Yves	
	COQ Fabrice	
	FONTANA Anne-Laure	
	GARNIER Olivier	
	LASLAZ Fabrice	
	LECLERCQ Samuel	
	MAHIEU Sylvain	
	MAIER Doris	
	MATTIOCCO François	
	MOUTOTE Quentin	
	PARIOLEAU Magali	
	PERRIN Guillaume	
	PISSARD Bruno	
	REVERDY Julien	
	SERRES Patrice	
SCIENCE SUPPORT GROUP	NERI Roberto	Head Science Support Group
	BARDEAU Sébastien	
	BERJAUD Catherine	
	BOISSIER Jérémie	
	BREMER Michael	
	BROGUIERE Dominique	
	CASTRO CARRIZO Aranzazu	
	CHANG Chin Chin	
	CHAPILLON Edwige	
	DOWNES Wilfriede	
	DUMAS Gaëlle	
	FERUGLIO Chiara	
	GRATIER Pierre	
	GUZMAN VELOSO Viviana	
	KRIPS Melanie	
	KÖNIG Sabine	
	MARTIN RUIZ Sergio	

Group	NAME Surname	Position
	PETY Jérôme	
	PIETU Vincent	
	REYNIER Emmanuel	
	ROCHE Jean-Christophe	
	VAN DER LAAN Tessel	
	WINTERS Jan-Martin	
	ZYLKA Robert	
SIS GROUP	SCHUSTER Karl-Friedrich	Interim Head SIS Group
	BARBIER Arnaud	
	BILLON-PIERRON Dominique	
	COIFFARD Grégoire	
	HALLEGUEN Sylvie	
	HAMELIN Catherine	
NOEMA Plateau de Bure, France		
NOEMA, PLATEAU DE BURE	GAUTIER Bertrand	Station Manager
	AZPEITIA Jean-Jacques	
	BARD Florentin	
	CASALI Julien	
	CAYOL Alain	
	CHAUDET Patrick	
	CONVERS Bruno	
	DAN Michel	
	DI LEONE SANTULLO Cécile	
	GROSZ Alain	
	LAPEYRE Laurent	
	LEONARDON Sophie	
	MASNADA Lilian	
	MOURIER Yvan	
	RAMBAUD André	
	SALGADO Emmanuel	
IRAM 30m TELESCOPE, Granada, Spain		
IRAM 30M TELESCOPE, GRANADA	KRAMER Carsten	Station Manager
	PENALVER Juan	Deputy Station Manager
	BILLOT Nicolas	
	BRUNSWIG Walter	
	DAMOUR Frederic	
	ESPANA Gloria	
	FRANZIN Esther	
	GALVEZ Gregorio	
	GARCIA José	
	GONZALES Manuel	
	HERMELO Israel	
	JOHN David	
	LARA Maria	
	LOBATO Enrique	
	LOBATO Javier	
	MELLADO Pablo	
	MENDEZ Isabel	
	MORENO Maria	
	MUNOZ GONZALEZ Miguel	
	NAVARRO Santiago	
	PAUBERT Gabriel	
	PEULA Victor	
	RUIZ Carmen	
	RUIZ Ignacio	
	RUIZ Manuel	
	SANCHEZ Salvador	
	SANCHEZ Rosa	
	SANTAREN Juan Luis	
	SANTIAGO Joaquin	
	SERRANO David	
	SIEVERS Albrecht	
	THUM Clemens	
	TREVINO Sandra	
	UNGERECHTS Hans	
	URBANO Paco	

Annex I – Telescope schedules

30-METER TELESCOPE

Ident.	Title	Authors
225-10	The complete CO(2-1) map of M33	Braine, Schuster, Kramer, Gonzalez, Sievers, Rodriguez, Gratier, Brouillet, Herpin, Bontemps, Israel, van der Werf, van der Tak, Tabatabaei, Henkel, Roellig, Combes, Wiedner
271-10	Physics of Gas and Star Formation in Galaxies at z=1.2	Combes, Tacconi, Genzel, Bolatto, Bournaud, Burkert, Cooper, Cox, Davis, Schreiber, García-Burillo, Gracia-Carpio, Lutz, Naab, Neri, Newman, Sternberg, Weiner
012-12	IRAM Chemical Survey of Sun-Like Star-Forming Regions	Bachiller, Lefloch, Cernicharo, Fuente, Tafalla, De Vicente, Alonso-Albi, Rodriguez, Ceccarelli, Kahane, Bacmann, Hily-Blant, Podio, Le Gall, López-Sepulcre, Faure, Wiesenfeld, Caux, Vastel, Bottinelli, Demyk, Marcelino, Codella, Vasta, Roueff, Gerin, Pineau Des Forets, Cabrit, Gomez-Ruiz, Viti, Caselli, Sakai, Yamamoto, Pety, Gonzalez
114-12	A Close-up Look at Comet PanSTARRS	Drahus
115-12	Molecular and isotopic survey of the Great comet PanSTARRS	Biver, Crovisier, Bockelée-Morvan, Colom, Moreno, Hartogh, Lis, Boissier, Paubert, Weaver, Russo, Vervack, Kawakita
116-12	Biological molecules in mass star forming regions	Favre, Jorgensen, Neill, Bergin, Crockett, Field, Brouillet, Despois, Baudry, Bisschop, Lykke
117-12	A search of the methoxy radical (CH_3O) in low-mass star forming regions	Marcelino, Cernicharo, Roueff, Gerin, Fuente, Muñoz Caro, Jiménez-Escobar
118-12	The role of PAH photodestruction in the carbon chemistry of PDRs (II).	Pilleri, Joblin, Berné, Gerin, Treviño-Morales, Montillaud, Fuente, Falgarone, Le Bourlot, Cernicharo, Pety, Kokkin, Goicoechea, González-García, Kramer, Cuadrado, Godard, Le Petit, Teyssier, Habart
119-12	A search for SH^+ in photon dominated regions	Agúndez, Goicoechea
121-12	Cosmic-ray induced chemistry in strongly irradiated molecular clouds	Ceccarelli, Vaupre, Hily-Blant, Montmerle, Lefloch, Dubus, Gabici
122-12	Chemistry in Disks: a survey of simple molecules bearing C,N,O and S	Reboussin, Guilloteau, Difolco, Piétu, Dutrey, Mokrane, Hersant, Wakelam, Semenov, Henning, Chapillon, Gueth, Launhardt, Schreyer
123-12	Confirmation of the Detection of Deuterated Ammonium Ion in Molecular Clouds	Cernicharo, Roueff, Marcelino, Tercero, Fuente, Gerin, Carrasco, Tanarro, Domenech, Herrero
124-12	Deuterated water in the solar-type protostar NGC 1333 IRAS 4B	Coutens, Vastel
126-12	The Search for Deuterated H_2O_2 - a Probe for Interstellar Water Formation	Herberth, Giesen, Parise, Schilke, Linnartz
127-12	Confirmation of D_3O^+ in L1544	Bizzocchi, Caselli, Dore, Ceccarelli, van der Tak, Angeloni, Leonardo
128-12	Deuterium fractionation in high-mass YSOs	Neill, Favre, Crockett, Bergin, Dishoeck, Lis
129-12	The role of surface chemistry in the deuteration of massive dense cores	Fontani, Caselli, Palau, Busquet, Sanchez-Monge, Tan, Audard
130-12	Completing the molecular survey towards the UCHII region Mon R2	Treviño-Morales, Fuente, Kramer, Gonzalez-Garcia, Pilleri, Cernicharo, Ginard, Berné, Joblin, Ossenkopf, Goicoechea, Garcia-Burillo, Roueff, Viti, Rizzo, Alonso-Albi
131-12	Chemical complexity in strongly UV-illuminated regions (cont.)	Goicoechea, Cuadrado, Cernicharo, Fuente, García-Burillo, Usero, Marcelino
132-12	Unbiased spectral survey of CygX-N63 a unique pre-hot core source	Bontemps, Fechtenbaum, Csengeri, Lefloch, Herpin, Duarte-Cabral, Hennemann, Schneider, Motte, Gursdorf, Wakelam
133-12	The link between filaments and star-formation in Cygnus X	Schneider, Bontemps, Csengeri, Hennemann, Motte, Simon, Klessen, Glover, Dale, Hennebelle
134-12	Flow-driven formation of Molecular Cloud Filaments: Widespread SiO in IRDCs	Jiménez-Serra, Henshaw, Caselli, Fontani, Tan, Hernandez, Butler
136-12	Is molecular gas formation triggered by the interaction between the HD34078 runaway star and the IC 405 nebula?	Gratier, Boissé, Cabrit, Gerin, Lesaffre, Pety, Pineau des Forêts
138-12	Probing cloud formation imprints and collapse dynamics with CO	Ragan, Beuther, Linz
139-12	The dynamic origin of CO in the high latitude sky	Falgarone, Hily-Blant, Aumont, Puget, Combet, Désert, Gorski, Radford, Phillips, Tauber, Martin
140-12	A study of the conditions favoring coreshine apparition	Pagani, Andersen, Bacmann, Steinacker
141-12	Diffuse and Dense molecular gas in M17 SW	Pérez-Beaupuits, Stutzki, Güsten, Wiesemeyer, Spaans, Ossenkopf
142-12	Core Chains in Taurus: New Clues to Core Formation	Tafalla, Hacar
146-12	On the characterization of far-IR-variable Class 0 protostars	Billot, Lefloch, Ceccarelli, Megeath, Fisher, Puravankara
156-12	A Search for Water in Protoplanetary disks	Cernicharo, Fuente, Neri
157-12	Evolution of dusty debris around young Solar analogues	Greaves, Hales, Wyatt, Panic
158-12	Constraining the coupling of gas and magnetic field in the pipe cores	Frau, Girart, Beltrán, Alves, Morata, Franco

Ident.	Title	Authors
160-12	Non-Zeeman Circular Polarization of Molecular Rotational Spectral Lines	Houde, Falgarone, Hezareh, Jones
161-12	Searching for CO Gas Among the Dustiest Nearby Stars	Forveille, Zuckerman, Vican
162-12	A Line Survey of the Supergiant O-rich star VY CMa. II	Quintana-Lacaci, Cernicharo, Sánchez Contreras, Velilla, Bujarrabal, Marcelino, Alcolea, Santander, Pearson, Teyssier
163-12	Unveiling the rich chemistry of yellow hypergiant stars: IRC+10420	Quintana-Lacaci, Cernicharo, Bujarrabal, Castro-Carrizo, Sánchez Contreras, Alcolea
164-12	Nucleosynthesis in AGB stars traced by isotopic ratios	Decin, Daza, Ramstedt, Olofsson, Milam
165-12	Molecular complexity in O-rich evolved stars: OH231.8+4.2 and IK Tau	Sanchez Contreras, Velilla, Alcolea, Cernicharo, Bujarrabal, Agundez, Quintana-Lacaci, Herpin, Pardo, Menten, Wyrowsky
166-12	Mm-wave observations of circumstellar envelopes well studied with Herschel/HIFI	Teyssier, Cerrigone, Cernicharo, Bujarrabal, Alcolea, Castro-Carrizo, Olofsson, Justtanont, Danilovitch
167-12	Further observations of Keplerian disks around post-AGB stars	Bujarrabal, Alcolea, Van Winckel, Santander-García, Castro-Carrizo
168-12	Mass loss in mid- to far-IR selected circumstellar envelopes	Flagey, Billot, Noriega-Crespo, Carey, Umana
170-12	GISMO mapping of SNR W49B to constrain the origin of cosmic rays	Hewitt, Decesar, Brandt
171-12	Probing Particle Injection and Diffusion in Pulsar Wind Nebulae	Decesar, Hewitt, Brandt
172-12	Total molecular gas mass of clouds in the southern spiral arm of M33	Kramer, Buchbender, González-García, Gratier, Braine, Garcia-Burillo, Israel, Mookerjea, Nikola, Glück, Röllig, Combes, Henkel
173-12	Molecular gas in luminous M33 HII region complexes	Israel, Buchbender, Heiner, Braine
174-12	EMIR ^{12}CO and ^{13}CO maps of the M83 central bar	Kramer, García-Burillo, Israel, Lord
175-12	The molecular gas mass in the dwarf elliptical NGC 205	Israel, Buchbender, Loenen
176-12	Tracing molecular gas in the outer parts of XUV disk galaxies	Verdugo, Combes, Dessauges
177-12	Star formation laws and efficiency from the centre to the outer edge of the XUV disk of the isolated galaxy CIG 96	Verdes-Montenegro, Leon, Moreta, Scott, Gil De Paz, Dobbs, Usero, García-Burillo, Aladro
178-12	Tidal versus ram pressure gas compression - the molecular view	Vollmer, Nehlig, Braine
180-12	Mapping the Molecular Gas in Luminous Infrared Galaxies	Sliwa, Wilson, Krips
181-12	The gas content of local high sSFR galaxies: implications for distant galaxies	Lehnert, Driel
182-12	An IRAM study of dusty spheroids: probing the minor merger process	Davis, Kaviraj, Rowlands, Combes, Cava, Lintott, Bourne, Michalowski, Temi, Coppin, Clements, Baes, Bussman, Serjeant, Cooray, Baker, Vlahakis, Leeuw, Dunne
185-12	Searching for evidence of cooling in group-dominant ellipticals.	O'sullivan, Combes, Salomé, Babul, Raychaudhury
188-12	Star formation efficiencies and XCO in intermediate mass galaxies	Saintonge, Tacconi, Kramer, Schiminovich, Buchbender, Catinella, Cortese, Genzel, Gracia-Carpio, Giovanelli, Haynes, Heckman, Lutz, Moran, Schuster, Sternberg, Wang
189-12	Water in Arp220	Cernicharo, Fuente, Garcia-Burillo
190-12	Searching for molecular oxygen in nearby (U)LIRGs	Wang, Li, Zhang
192-12	Molecular Line Anchors for Maser Proper Motions in the Andromeda Galaxy	Amiri, Darling, Brunthaler
193-12	Mapping at 1.2mm the outflow of M 82: evidences for Chemical differentiation	González-García, García-Burillo, Fuente, Usero, Aladro, Abreu, Pilleri, Berné, Bayet
194-12	Short-spacing observations of HCO^+ towards GMC no3 in M33	Buchbender, Kramer, Gonzalez-Garcia, Gratier
195-12	Mapping 2 mm emission of NGC 604/M33 - a pilot study	Kramer, Buchbender, Garcia-Burillo, Rosolowsky, Albrecht, Bertoldi, Braine, Israel, Kovács, Relano, Staguhn, Quintana-Lacaci
196-12	Determining the Resolved Star Formation Rate in Messier 51	Eufrasio, Staguhn, Arendt, Dwek
197-12	Cartography of the dust excess in nearby galaxies: GISMO imaging of NGC4631	Albrecht, Galametz, Bertoldi
198-12	A pilot study of polar ring/dust lane mergers in the continuum	König, Aalto, Muller, Jütte, Beswick, Gallagher
199-12	Formaldehyde as a thermometer of the molecular gas in nearby active galaxies	Rodríguez, Mühle, Aalto, Odriozola, Pérez Torres
200-12	Molecular Tracers of Galaxy Evolution II: Chemistry or Excitation?	Costagliola, Aalto, Spoon, van der Werf, Muller, Jütte, Lahuis, Martín, Rodriguez, Perez-Torres, Alberdi
201-12	Measuring the ISM Content of Optically Luminous Type 2 QSOs	Petric, Ho, Flagey, Lacy, Omont, Billot
202-12	The molecular gas content of six ULIRG type 2 quasars at z~0.3.	Villar Martín, Colina, García-Burillo, Pérez-Torres, Rodríguez, De Breuck, Emonts, Drouart, Humphrey
203-12	Radio cores shedding light on molecular outflows - II	Dasyra, Combes
204-12	Understanding AGN feedback with gas chemistry in NGC 1266	Davis, Bayet, Martín, Meier, Young, Alatalo, Crocker, Bureau, Blitz

Ident.	Title	Authors
205-12	Testing the link between star formation and AGN	Dicken, Nesvadba, Boulanger, Lehnert, Combes, Tadhunter, Rose
206-12	Searching for SiO mega-maser in type II AGN with strong water maser	Wang, Zhang
207-12	MAPI: Monitoring AGN with Polarimetry at the IRAM-30 m	Agudo, Thum, Gómez, Casadio, Molina, Marscher, Jorstad, Wiesemeyer
209-12	The variability of the intrinsic radio power of AGN in cluster cores with GISMO	Edge, Hogan, Wilman, Kovács, Benford, Hlavacek-Larrondo, Fabian, Salomé, Grainge, Rumsey, Russell, Mcnamara
212-12	Coordinated cm to mm monitoring of variability and spectral evolution of a selected it Fermi blazar sample	Fuhrmann, Zensus, Nestoras, Karamanavis, Krichbaum, Angelakis, Myserlis, Ungerechts, Sievers, Readhead
213-12	Resolving the Pressure Structure in Galaxy Clusters: Shock Fronts and Cool Cores	Wollack, Markevich, Chuss, Bulbul, Staguhn, Su, Rostem
214-12	Molecular gas in dusty Lyman break galaxies at $0.6 \leq z \leq 0.7$	Oteo, Bongiovanni, Pérez García, Cepa
215-12	Detection of extreme molecular outflows in intermediate redshift ULIRGs	Sethuram, Lattanzi, Petitjean, Noterdame, Srianand
217-12	Detection of high-redshift methanol in the lensed galaxy B0218+357	Ubachs, Bagdonaite, Dapra, Henkel, Menten
218-12	A search for HeH^+ at high redshifts	Zinchenko, Dubrovich, Henkel
219-12	CO(8-7) in the *z*=5.24 Submillimeter Galaxy	Boone, Combes, Richard, Egami, Rex, Rawle, Smail, Ivison, Omont, Dessauges-Zavadsky, Schaerer, Kneib, Zamojski, van der Werf, Pham, Pello
220-12	CO Redshift Search for Exceptionally Bright Lensed Herschel Sources	Kneib, Dessauges-Zavadsky, Boone, Combes, Omont, Egami, Rex, Rawle, Swinbank, Schaerer, Smail, van der Werf, Coppin
221-12	GISMO photometry of the most distant lensed galaxies behind clusters	Edge, Egami, Rawle, Rex, Geach, Schaerer, Dessauges, Zamojski, Simpson, Swinbank, Smail, Karim, Ebeling, Finoguenov, Boone, van der Werf
222-12	Confirming $z \geq 2$ cluster candidates observed by Planck and Herschel	Dole, Nesvadba, König, Krips, Beelen, Chary, Flores-Cacho, Frye, Giard, Guery, Kneissl, Lagache, Le Floc'h, Montier, Omont, Pointecouteau, Puget, Scott, Welikala, Yan
223-12	A systematic search for absorption lines in z~2 radio galaxies	Nesvadba, Combes, García-Burillo, Collet, Boulanger, Lehnert
225-12	Dust and Star formation in and around High Redshift Radio Galaxies	Kovács, Lehnert, De Breuck, Seymour, Nesvadba, Rocca-Volmerange, Drouart, Greve, Wylezalek, Vernet, Röttgering, Staguhn, Benford
226-12	Disentagling SZ Clusters and Dusty Galaxies.	Kovács, Staguhn, Benford
227-12	COSMO Part II: The synergetic GISMO survey in the COSMOS field	Staguhn, Karim, Schinnerer, Smolvcic, Bertoldi, Aravena, Smail, Benford, Kovács, Swinbank, Dwek, Su
228-12	Studying the Origin of Jets in bright nearby Galaxies with 1.3 mm VLBI	Krichbaum, Alef, Roy, Wagner, Rottmann, Zensus, Bremer, Sanchez, Cox, Güsten, Muders, Menten, Lindqvist, Conway, Ziurys, Strittmatter, Freund, Marone, Doeleman, Fish, Lu, Plambeck, Wright, Bower, Young, Weintroub, Zhao, Blundell
232-12	First high resolution mapping of C_3H^+ in the ISM	Pety, Guzmán, Gratier, Goicoechea, Gerin
D04-12	Physico-Chimie des Chocs Protostellaires	Lefloch, Hily-Blant, Kahane
D05-12	Confirming the redshift of the second Eyelash	Nesvadba, Dole, Boone, Koenig, Krips, Lehnert, Mackenzie, Omont, Scott, Beelen, Boulanger, De Breuck, Dicken, Flores-Cacho, Frye, Guery, Lagache, Le Floc'h, Montier, Puget, Pointecouteau, Soucail, Welikala
D06-12	Paris M2 AAIS survey of M82	Le Bourlot, Lefevre
D07-12	GISMO Observations of the Double Helix Nebula	Morris, Staguhn, Enokiya, Torii, Fukui
D08-12	Confirmation of the first O-type `swollen star' candidate	Palau, Sánchez Contreras, Sánchez-Monge, Sahai
D09-12	Spectroscopic redshifts of the brightest submm lenses on the sky	Nesvadba, Dole, Boone, Beelen, Dicken, Flores-Cacho, Frye, Guery, Le Floc'h, Mackenzie, Montier, Omont, Scott, Welikala
D10-12	ToO observations of BL Lacertae to follow the ongoing historic outburst	Rani, Hodgson, Krichbaum, Fuhrmann, Zensus, Marscher, Jorstad
D11-12	Request for Directors Time: Comet PanSTARRS in the millimeter continuum	Altenhoff, Menten, Sievers, Schmidt, Thum
D12-12	Uncovering the Origin of Anomalous Microwave Emission in External Galaxies	Murphy, Staguhn, Hensley
D13-12	The GISMO 2 mm GDF: Pushing the Deepest (Sub-)Millimeter Field To the Confusion Limit	Staguhn, Walter, Kovacs, Benford, Decarli, Da Cunha
D15-12	Phase transitions in the neutral ISM: probing GMC complexes in Nearby Galaxies	Cormier, Usero, Bigiel
188-12	Star formation efficiencies and X_{CO} in intermediate mass galaxies	Saintonge, Tacconi, Kramer, Schiminovich, Buchbender, Catinella, Cortese, Genzel, Gracia-Carpio, Giovanelli, Haynes, Heckman, Lutz, Moran, Schuster, Sternberg, Wang
001-13	Great Comet ISON and the Origin and Lifetime of Comets	Drahus, Lis, Treviño-Morales, Hermelo, Giesen, Herberth
002-13	Fire and Ice in comet C/2012 S1 (ISON)	Biver, Bockelée-Morvan, Moreno, Debout, Colom, Crovisier, Lis, Boissier, Paubert, Weaver, Russo, Vervack, Kawakita
003-13	Searching for phosphine in the coma of comet C/2012 S1 (ISON)	Agúndez, Santos-Sanz, Bockelée-Morvan, Biver, Moreno
004-13	A search of the methoxy radical (CH_3O) in low-mass star forming regions	Marcelino, Cernicharo, Roueff, Gerin, Fuente, Muñoz Caro, Jiménez-Escobar
006-13	Complex Molecules toward Low-mass Protostellar Ice Sources	Lauck, Öberg, Garrod

Ident.	Title	Authors
007-13	Mapping complex organic molecules in pre-stellar cores	Bacmann, Taquet, Faure, Dislaire
008-13	Nitrogen chemistry in dark clouds: the HCN:HNC abundance ratio	Le Gal, Hily-Blant, Faure, Pineau des Forêts
009-13	Using chemistry to constrain the evolutionary state of prestellar cores	Maret, Tafalla, Bergin, Hily-Blant
010-13	Non-equilibrium chemistry in AGB S-stars - The importance of SiS	Ramstedt, Gobrecht, Cherchneff, Olofsson
013-13	Mapping of singly and doubly deuterated cyclopropenylidene in L1544	Spezzano, Bizzocchi, Caselli, Brünken, Schlemmer
014-13	The Origin of the Depolarization Effect in Molecular Clouds	Jones, Houde, Falgarone, Hezareh, Wiesemeyer, Paubert
015-13	Monitoring the Encounter of a Gas Cloud with Sgr A*	Agudo, Thum, Wiesemeyer, Sievers, Gómez, Casadio, Molina
017-13	Is interstellar grain alignment destroyed by gas-grain collisions?	Andersson, Weaver, Vaillancourt, Lazarian
018-13	A study of the conditions favoring coreshine apparition	Pagani, Andersen, Bacmann, Steinacker
019-13	A synoptic spectro-imagery view of the Horsehead pillar	Pety, Gratier, Guzman, Goicoechea, Gerin, Tremblin, Bardeau, Sievers
020-13	A Thick Diffuse Molecular Disk in the Galaxy?	Lucas, Pety, Liszt
021-13	Converging flows in the Infrared Dark Cloud G14.225-0.506	Busquet, Palau, Zhang, Estalella, de Gregorio-Monsalvo, Girart, Ho, Liu, Pillai, Sánchez-Monge, Wyrowski, Franco, Santos
022-13	Probing cloud formation imprints and collapse dynamics with CO	Ragan, Beuther, Linz, Henning
023-13	Understanding the link between cloud morphology and massive core formation	Peretto, Fuller, Duarte Cabral
024-13	Understanding the formation of a massive filamentary IRDC	Peretto, Falgarone, Fuller, Hily-Blant, André
025-13	Dynamics of massive dense cold filaments	Guzman, Sanhueza, Smith
026-13	Probing converging flows with SiO emission: the W43-MM1 ridge	Louvet, Gusdorf, Lesaffre, Schilke, Carlhoff, Motte, Nguyen-Luong
027-13	Flow-driven formation of Molecular Cloud Filaments: Widespread SiO in IRDCs	Jiménez-Serra, Henshaw, Caselli, Wang, Fontani, Tan, Hernandez
028-13	Tracing a dense filamentary region interacting with the W51E region	Vastel, Mookerjea, Gérin
029-13	Probing the growth of the Serpens-South ridge by filamentary accretion	Könyves, André, Arzoumanian, Maury, Peretto, Ntormousi, Palmeirim, Roy, Hennebelle
030-13	Filaments seen as a multi-arm spiral structure in Orion B - accretion and rotation?	Palmeirim, Könyves, André, Peretto, Arzoumanian, Didelon, Ntormousi, Roy
032-13	Understanding the internal structure of massive filaments	Hacar, Tafalla, Goicoechea, Frau
033-13	Triggered star formation in the filament G110-13	Montillaud, Juvela, Ristorcelli, Pilleri, Miettinen, Toth, Pelkonen, Malinen
034-13	Confirming the existence of a failed core: the star that never was	Frau, Girart, Beltrán, Tafalla
037-13	Building a chemical sequence of core evolution II: the Taurus cloud	Frau, Girart, Beltrán, Tafalla, Alves, Franco
038-13	A turbulent shock origin for the pre-brown dwarf core Oph B-11 ?	André, Greaves, Ward-Thompson, Könyves, Palmeirim, Lesaffre
041-13	An IRAM legacy: The IRAM 30-m line survey of Orion KL	Tercero, Cernicharo, López, Bañó, Carvajal, Margulès, Haykal, Kleiner, Coudert, Guillemin, Motiyenko, Huet, Alonso, Cabezas, Kolesniková, Marcelino, Bell, Palau
043-13	Triggered Star Formation At The End of the Galactic Bar?	Gong, Henkel, Urquhart, Wang, Zhang, Mao, Wyrowski
044-13	Close encounters of the protostellar kind in IC 1396N	Beltrán, Massi, Codella, Fontani, Neri, López
045-13	Chemical study of the flat disk around the B0 star R Mon	Fuente, Treviño-Morales, González-García, Bachiller, Cernicharo, Lefloch
047-13	MAYS: Mass (and ages) of Young Stars - a CN survey in rho Oph	Guilloteau, Difolco, Simon, Piétu, Dutrey, Hersant, Wakelam, Ducourant, Grosso, Guillout, Schaefer, White, Teixera, Palla
048-13	The puzzle of BN-type massive young stellar objects - IRAM and SMA in concert	Linz, Beuther, Henning, Stecklum, Keto
050-13	Observation of high-order radio-recombination lines toward MWC349A	Báez-Rubio, Martín-Pintado
052-13	A pilot molecular inventory of AGB stars	Maercker, De Beck, Stancliffe, Pérez-Sánchez, Leal-Ferreira, Keller, Ramstedt, Justtanont, Olofsson, Vlemmings, Danilovich, Decin, Lombaert, Homan, Daza, Khouri Silva
055-13	X-ray induced chemistry: the case of BD+30.3639	Santander-García, Alcolea, Bujarrabal, Kastner, Montez, Castro-Carrizo, Agúndez, Balick
057-13	Molecular complexity in O-rich evolved stars: OH231.8+4.2 and IK Tau	Sánchez Contreras, Velilla, Alcolea, Cernicharo, Bujarrabal, Agúndez, Quintana-Lacaci, Herpin, Pardo, Menten, Wyrowski
058-13	The unbiased spectral survey of IC443	Riquelme, Pérez-Beaupuits, Güsten, Gusdorf
059-13	Is Type Ia SNR Tycho "naked" or associated with a molecular cloud?	Zhou, Chen, Safi-Harb, Zhang, Zhou

Ident.	Title	Authors
060-13	Searching for cool CO emission within the Cas A remnant	Wallström, Muller, Black, Biscaro, Cherchneff, Rho, Tielens
063-13	Determining the origin of the ISM in Coma Cluster ETGs with IRAM & Herschel	Davis, Rowlands, Amblard, Baes, Bourne, Boselli, Cooray, Cortese, Dunne, Eales, Fuller, Gomez, Ibar, Kaviraj, Michalowski, Smith, Temi, Vlahakis, De Zotti
064-13	Census of Molecular Gas Reservoirs in CALIFA Galaxies: I. Search of CO	Dannerbauer, Ziegler, Puschnig, Perez-Torres, Van De Ven, Alves, Krips, Sanchez, Walcher, Wild
065-13	The gas content of local high sSFR galaxies: implications for distant galaxies	Lehnert, Driel
066-13	Searching for evidence of cooling in group-dominant ellipticals.	O'sullivan, Combes, Salomé, Babul, Raychaudhury
068-13	The ISM properties under ICM pressure in the cluster environment	Lee, Chung, Meier
069-13	Compressed molecular gas bridges in galaxy head-on collisions	Vollmer, Nehlig, Braine
070-13	The Behaviour of Cold Gas in Damp-Mergers	Brassington, Duc, Lisenfeld, Brinks, Belles, Mundell, Zezas
071-13	Sulphur-bearing species in galaxy mergers	Bañó, Cernicharo, Goicoechea, Bell
072-13	Evaluating the star formation and cosmic ray chemistry in active galaxies through H218O, C_2H and N_2H^+ emission	Krips, Aladro, Dumas, Feruglio, König, Van Der Laan, Martín Ruiz, Neri
075-13	Origin of the deviation from the L_{FIR}-L_{HCN} correlation in the most isolated galaxies	Ocaña Flaquer, Scott, Leon, Martín Ruiz, Verdes-Montenegro
076-13	Mapping at 1.2mm the outflow of M 82: evidences for Chemical differentiation	González-García, García-Burillo, Fuente, Usero, Aladro, Abreu, Pilleri, Berné, Bayet
077-13	Mapping 2 mm emission in the nearby galaxy M 33 with GISMO - a pilot study	Kramer, Hermelo, Relano, Verley, Albrecht, Israel, Rosolowsky, Boquien, Kovács, Staguhn, Xilouris
078-13	Mapping NGC4449 and NGC1569 with GISMO	Hermelo
079-13	Cartography of the dust excess in nearby galaxies: GISMO imaging of NGC4631	Albrecht, Galametz, Bertoldi
081-13	TANGO: Molecular gas content in radio galaxies at medium redshift	Ocaña Flaquer, Leon
082-13	CO Study for Dust-Rich Broad-Emission-Line Quasars at Intermediate Redshifts	Dai, Bergeron, Omont, Huang, Hatziminaoglou, Perez-Fournon, Elvis, Fazio
083-13	Molecular gas in low-*z* obscured quasars: testing models of AGN feedback	Harrison, Alexander, Danielson, Moro, Mullaney, Rovilos, Swinbank
084-13	Coordinated cm to mm monitoring of variability and spectral evolution of a selected it Fermi blazar sample	Fuhrmann, Zensus, Nestoras, Karamanavis, Krichbaum, Angelakis, Myserlis, Ungerechts, Sievers, Readhead
085-13	MAPI: Monitoring AGN with Polarimetry at the IRAM-30 m	Agudo, Thum, Gómez, Casadio, Molina, Marscher, Jorstad, Wiesemeyer
086-13	Cold and Warm Molecular Gas in Active Galaxies	Pereira Santaella, Busquet, Spinoglio
087-13	Toward the first sample of overly massive black holes in massive halos	Scharwächter, Bogdán, Combes, Forman, Salomé, Forman
088-13	Ultra-massive black holes in cluster-embedded small X-ray coronae	Scharwächter, Sun, Combes, Salomé
090-13	An remarkable group of 3.6micron galaxies with very bright, extended far-IR emission	Yan, Combes, Blain, Benford, Eisenhardt, Wu, Tsai, Stern, Assef
091-13	The Mass Budget of a Milky Way-like Lens Galaxy	Dutton, Auger, Treu, Barnabe, Brewer, Marshall, Williams
092-13	Ident.ifying a serendipitous (possibly lensed) source at high z	Magrini, Casasola, Combes, Mignano, Fontani, Paladino, Sani
093-13	CO Redshift Search for Exceptionally Bright Lensed Herschel Sources	Kneib, Dessauges-Zavadsky, Boone, Combes, Omont, Rawle, Smail, Swinbank, van der Werf, Schaerer, Jauzac, Egami, Coppin
094-13	Spectroscopic confirmation of the brightest submm lenses on the sky	Nesvadba, Boone, Boulanger, Beelen, Dicken, Dole, Flores-Cacho, Frye, Guery, Guillard, König, Krips, Le Floc'h, Lehnert, Mackenzie, Malhotra, Montier, Omont, Rhoads, Scott, Welikala
095-13	ISM physical conditions in *z*=2 lensed galaxies: [CI] observations of galaxies from the Herschel Extreme Lensing Line Observations (HELLO) Survey	Guillard, Combes, Frye, Gerin, Malhotra, Nesvadba, Papovich, Rhoads, Spaans, Strauss
097-13	GISMO photometry of the most distant lensed galaxies behind clusters	Edge, Egami, Rawle, Rex, Geach, Schaerer, Dessauges, Zamojski, Simpson, Swinbank, Smail, Karim, Ebeling, Finoguenov, Boone, van der Werf
098-13	Unveiling the most distant star forming galaxies behind clusters with GISMO	Aravena, Gonzalez, Staguhn, Anguita, Infante, Postman, Bauer
099-13	Dust and Star formation in High Redshift Radio Galaxies	Kovács, Lehnert, De Breuck, Greve, Wylezalek, Seymour, Rocca-Volmerange, Drouart, Nesvadba, Vernet, Röttgering, Staguhn, Benford
100-13	Confirming $z \geq 2$ cluster candidates observed by Planck and Herschel	Dole, Beelen, Chary, Dicken, Flores-Cacho, Frye, Giard, Guery, Kneissl, König, Krips, Lagache, Le Floc'h, Mckenzie, Montier, Nesvadba, Omont, Pointecouteau, Puget, Scott, Welikala, Yan
101-13	GISMO snapshots: Obtaining the flux at 2 mm of Ultra-Red Herschel Galaxies	Pérez-Fournon, Dannerbauer, Bertoldi, Omont, Riechers, Clements, Conley, Cox, Ivison, Michalowski
102-13	SEARCH FOR DUST IN THE Z=9.6 GALAXY MACS1149-JD	Dwek, Su, Staguhn
103-13	The GISMO 2 mm GDF: Pushing the Deepest (Sub-)Millimeter Field To the Confusion Limit	Staguhn, Walter, Kovács, Benford, Decarli, Da Cunha

PLATEAU DE BURE INTERFEROMETER

Ident.	Title of Investigation	Authors
T0CC	IRAM Lensing Survey: Probing Galaxy Formation in the Early Universe	Kneib, Clément, Cuby, Peroux, Ilbert, Jablonka, Boone, Combes, Neri, Krips, Lagache, Beelen, Pello, Courbin, Meylan, Schaerer, Dessauges, Knudsen, Van Der Werf, Richard, Smail, Swinbank, Chapman, Ivison, Egami, Altieri, Valtchanov
U052	Class 0 protostars with PdBI: Solving the angular momentum problem?	André, Maury, Testi, Launhardt, Codella, Cabrit, Gueth, Lefloch, Maret, Bottinelli, Bacmann, Belloche, Bontemps, Hennebelle, Klessen, Dullemond
U06D	Are faint protoplanetary disks just smaller rather than more tenuous?	Piétu, Guilloteau, Dutrey, Boehler
V04A	An efficient Program for Finding Lensed Galaxies at z>4 - II	Krips, Cox, Dannerbauer, Eales, Omont, Beelen, Bertoldi, Dunne, Aretxaga, Hughes, Ivison, Cooray, Dye, Frayer, Negrello, Smail
W--6	Confirmation of a strongly-lensed sub-millimeter galaxy	Leipski, Barthel, Wilkes, Willner
W--8	The second Eyelash! Confirming the redshift and exceptional nature of the first Planck/Scuba-2 high-*z* lens	Nesvadba, Dole, Boone, Koenig, Krips, Mackenzie, Omont, Scott, Beelen, Boulanger, Dicken, Flores-Cacho, Frye, Guery, Le Floc'h, Lehnert, Montier, Puget, Welikala
W--9	Gas-rich major merger at z=2.3	Feruglio, Omont, Cox, Neri, Gavazzi, Ivison
W--A	Small-scale structure of molecular gas at z=5.243 (continued)	Boone, Combes, Richard, Egami, Rex, Rawle, Smail, Ivison, Omont, Dessauges-Zavadsky, Schaerer, Kneib, Zamojski, van der Werf, Pham, Pello
W--B	First CO detection in the Crab Nebula	Salomé, Castro-Carrizo, Combes, Baldwin, Ferland, Loh, Fabian
W--C	Redshift measurement of a blind, high-*z* (z=2.071?) CO detection in the HDF-N	Decarli, Walter, Riechers, Carilli, Neri, Cox
W018	Structure and excitation in the CSEs around C-stars with high expansion velocity	Quintana-Lacaci, Castro-Carrizo, Bujarrabal, Alcolea
W037	Galaxy Evolution and Star Formation Efficiency at 0.6 < z < 1	Combes, García-Burillo, Braine, Schinnerer, Walter, Colina
W03A	Feedback & Mergers in Luminous AGN at z=1.3	Rosario, Lutz, Genzel, Tacconi, Combes, Saintonge
W04D	Exploring the Cores of Lensed Herschel Galaxies Using H_2O Lines	Omont, van der Werf, Yang, Neri, Beelen, Krips, Ivison, Cox, Riechers, Harris, Weiss, Gavazzi, Baker, Bertoldi, Bussmann, Cooray, Dannerbauer, Eales, Gao, Fu, Guélin, Lehnert, Lupu, Menten, Negrello
W056	Exploring the Unusual CO and H_2O Excitation of z~6 Quasars	Riechers, Neri, Walter, Carilli, Wang, Cox, Weiss, Bertoldi, Omont, van der Werf, Fan, Maiolino
W059	Mapping a quasar-driven massive outflow in the early Universe	Maiolino, Gallerani, Neri, Cicone, Ferrara, Genzel, Lutz, Sturm, Tacconi, Walter, Feruglio, Fiore, Pinconcelli
W05A	Blind redshifts for ultra-red Herschel galaxies	Krips, Ivison, Bertoldi, Omont, Cox, Neri, Koenig, van der Werf, Dannerbauer, Eales, Valiante, Clements, Swinbank
W05F	The nucleus and inner coma of comet C/2011 L4 (PanSTARRs)	Boissier, Bockelée-Morvan, Groussin, Biver, Crovisier, Moreno, Colom, Jorda, Lamy
W060	Mapping CH_3CCH and dynamics of Titan's atmosphere	Moreno, Lellouch, Vinatier
W061	First high resolution mapping of C_3H^+ in the ISM	Guzmán, Pety, Gratier, Goicoechea, Gerin
W068	The origin of deuterated formaldehyde in the protostellar shock L1157-B1	Fontani, Codella, Ceccarelli, Lefloch, Taquet
W069	Imaging the spectral signature of a protostellar J-shock	Codella, Gueth, Benedettini, Busquet, Cabrit, Ceccarelli, Lefloch, Nisini, Gómez-Ruiz
W06A	A first direct measure of the SiO abundance in the HH211 jet	Gueth, Cabrit, Codella, Yvart
W06E	Small-scale fragmentation of genuine high-mass starless cores (HMSCs)	Beuther, Feng, Ragan, Linz, Tackenberg, Smith, Bihr, Henning, Sakai
W06A	A first direct measure of the SiO abundance in the HH211 jet	Gueth, Cabrit, Codella, Yvart
W06E	Small-scale fragmentation of genuine high-mass starless cores (HMSCs)	Beuther, Feng, Ragan, Linz, Tackenberg, Smith, Bihr, Henning, Sakai
W071	Hot water in the inner envelope of massive proto-stars/clusters	Wyrowski, van der Tak, Herpin, Leurini
W074	Rotationally Supported Disks in the Embedded Stage of Star Formation	van Dishoeck, Harsono, Jørgensen, Hogerheijde, Persson
W075	How much water in the protoplanetary disk of DG Tau?	Podio, Codella, Cabrit, Kamp, Nisini, Dougados, Gueth, Bacciotti
W07A	Inner structure of the protoplanetary disks MWC 758	Chapillon, Tang, Guilloteau, Dutrey, Ohashi, Piétu, Fukagawa, Momose, Muto, Di Folco, Tamura, Hashimoto
W07D	Keplerian disks and expanding bipolar flows in post-AGB stars	Bujarrabal, Castro-Carrizo, Winckel, Alcolea, Santander-García
W07E	Chemistry and environment of M 82 and IC 342: a mapping survey	Henkel, Mauersberger, Martin, Aladro, Bayet, Viti, Wiklind, Peck, Vila-Vilaro, Sawada, Matsushita, Krips, Papadopoulos
W084	Morphological study of the massive outflow in Mrk231	Feruglio, Cicone, Fiore, Maiolino, Carpio, Sturm, Piconcelli, Veilleux
W085	On edge? - disentangling the structure of the dense, nuclear wind of Mrk231	Aalto, Muller, Costagliola, Garcia-Burillo, van der Werf, Winters, Henkel, Gonzalez-Alfonso, Neri
W086	The exceptional outflow of OQ208: cornerstone observations for studying the molecular gas properties in an AGN-driven outflow	Dasyra, Combes, Salomé
W088	High-resolution observations of massive molecular outflows in active galaxies	Sturm, Graciá-Carpio, Maiolino, González-Alfonso, Hailey-Dunsheath, Davies, Veilleux, Fischer, Feruglio, Piconcelli, Fiore, Garcia-Burillo, Aalto, Cicone, Rupke

Ident.	Title of Investigation	Authors
W089	Resolving the molecular outflow in the advanced merger NGC 1614	García-Burillo, Usero, Casznadas, Colina, Aalto, Alonso-Herrero, Combes, Hunt, Tacconi, Graciá-Carpio, Neri, Planesas, Arribas
W08E	Detecting in CO(1-0) the most powerful molecular outflow discovered by Herschel	Spoon, Farrah, Fischer, González-Alfonso, Graciá-Carpio, Maiolino, Sturm, Veilleux, Afonso, Bernard-Salas, Clements, Lebouteiller, Rigopoulou, Smith
W097	Tests of the transformation of lenticular galaxies	Smail, Koyama, Swinbank, Simpson, Kodama, Geach
W098	High resolution mapping of the cold gas in an intermediate redshift cluster galaxy	Jablonka, Combes, Kneib, Jauzac, Egami, Haines, Pereira
W09A	The highest density starbursts in the Universe	Hickox, Geach, Diamond-Stanic, Coil, Moustakas, Robania, Rudnick, Tremonti, Sell
W09B	CO maps of starburst galaxies at 0.6 < z < 1	Combes, García-Burillo, Braine, Schinnerer, Walter, Colina
W09C	The nature of the unique source SWIFT J1644+57	Agudo, Castro-Tirado, Guziy, Bremer, Winters, Gorosabel, Gómez, Sánchez-Ramirez, Tello
W0A0	The Resolved Star Formation - Gas (K-S) Relation at z~1	Tacconi, Genzel, Combes, Neri, Bolatto, Cooper, Cox, Schreiber, Garcia-Burillo, Lutz, Bournaud, Burkert, Gracia-Carpio, Naab, Newman, Saintonge, Sternberg, Weiner, Wuyts
W0A6	Physical properties of resolved star-forming clumps in a strongly lensed z~ 1.6 galaxy	Dessauges-Zavadsky, Combes, Boone, Kneib, Omont, Schaerer, Zamojski, Richard, Egami, Rawle, van der Werf, Coppin
W0A9	Herschel Extreme Starbursts at Redshift ~ 2	Rodighiero, Lutz, Tacconi, Genzel, Förster Schreiber, Wuyts, Popesso, Berta, Renzini, Cimatti, Gruppioni, Zamorani, Andreani, Daddi, Carollo, Lilly, Onodera, Bschorr, Franceschini, Baronchelli, Lofaro, Silverman
W0AA	Testing the evolutionary link between QSOs and submm galaxies	Simpson, Swinbank, Smail, Cox, Danielson, Bonfield, van der Werf, Jarvis, Coppin, Ivison, Hughes, Vaccari, Dunlop, Verma, Clements, Leeuw, Smith, Benford, Owski, Omont
W0AB	Understanding the Nature of Herschel-Selected Submillimeter Galaxies	Riechers, Omont, Perez-Fournon, Neri, Cox, Cooray, Wardlow, Clements, Ivison, Magdis, Bock, Oliver
W0AD	Resolving the morphology of the first WISE-identified ULIRG	Blain, Benford, Bridge, Eisenhardt, Jones, Yan, Tsai, Wu
W0AE	The quest for counterparts of SMGs in the COSMOS field: The first statistically significant and complete mm-selected sample	Smolčić, Aravena, Navarrete, Bertoldi, Schinnerer, Karim, Riechers, Sheth, Capak
W0B1	Do SMGs really concentrate into a proto-cluster core?	Umehata, Tamura, Kohno, Suzuki, Ikarashi, Takata, Matsuda, Iono, Nakanishi, Yamada, Hatsukade, Wilson, Yun, Hughes
W0B2	Submillimetre-selected protoclusters at *z*=3-4	Ivison
W0B3	Exploring the dense molecular gas in two lensed Herschel galaxies at z~3.6	Yang, Omont, Lupu, Gao, Beelen, Bussmann, Coppin, Cox, Dannerbauer, Gavazzi, Guélin, Ivison, Krips, Michalowski, Neri, Riechers, Temi, van der Werf
W0B4	Probing the Excitation of H_2O in Lensed Herschel Galaxies	Omont, van der Werf, Yang, Neri, Beelen, Krips, Ivison, Cox, Riechers, Harris, Weiss, Gavazzi, Spaans, Baker, Bertoldi, Bussmann, Dannerbauer, Downes, Eales, Gao, Fu, Guélin, Lehnert, Lupu, Menten, Michalowski, Negrello, Temi, Valiante
W0B6	An IRAM Pilot Project for a 1000-Lens Survey	Eales, Krips, Cox, Neri, Beelen, Bertoldi, Omont, Ivison, Dannerbauer, Dye, Gonzalez-Nuevo, Lapi, Negrello, Swinbank
W0B7	Ionized Nitrogen ([NII]) at high redshift	Decarli, Walter, Maiolino, Carilli, Riechers, Bertoldi, Weiss, Cox, Neri
W0B8	Are CO lines detectable in Lyman Break Galaxy at z~4 ?	Tan, Daddi, Sargent, Magdis, Hodge, Dickinson, Walter, Carilli, Gao
W0BD	Identification of the highest redshift H-ATLAS and HerMES galaxies	Bertoldi, Perez Fournon, Omont, Dannerbauer, Lagache, Bethermin, Michalowski, Ivison, Clements, Negrello, White, Benford, Temi, Vaccari, Riechers, Bock, Vieira, Cooray, Wardlow, Coppin, Frayer, De Zotti, Massardi, Cava, Smail, Swinbank, Bremer, Verma, Rigopoulou, Aretxaga, Hughes, Marrone, van Kampen, Eales, van der Werf, Bussmann, Conley, Oliver, Valiante
W0BE	Small-scale structure of molecular gas at *z*=5.243	Boone, Combes, Richard, Egami, Rex, Rawle, Smail, Ivison, Omont, Dessauges-Zavadsky, Schaerer, Kneib, Zamojski, van der Werf, Pham, Pello
W0C3	A Quasar-Starburst Merger System at the Epoch of Reionization ?	Wang, Carilli, Neri, Walter, Riechers, Fan, Willott, Cox, Bertoldi, Omont, Menten, Strauss, Wagg
W0C4	A Detailed Investigation of the ISM in the Most Distant Starburst Galaxy	Riechers, Perez-Fournon, Omont, Neri, Cox, Bradford, Clements, Cooray, Wardlow, Krips, Dowell, Ivison, Kamenetzky, Conley, Vieira, Bock, Oliver
W0C5	A Direct Probe of Molecular Outflows at z>6	Riechers, Walter, Neri, Cox, Carilli, Wang
W0C6	Chasing dust in strongly lensed z>6 star-forming galaxies	Schaerer, Staguhn, Dessauges, Boone, Combes, Kneib, Richard, Zamojski
W0C9	Star formation efficiency in the host galaxy of the dark GRB 080207	Le Floc'h, Basa, Bournaud, Charmandaris, Daddi, Dannerbauer, Duc, Elbaz, Feruglio
W0CA	Unveiling the population of highly obscured and high-*z* gamma-ray bursts (ToO)	Castro-Tirado, Bremer, Winters, Gorosabel, Guziy, Pérez-Ramírez, Castro Cerón, Tello, Sánchez-Ramírez
X--1	Circumbinary and Circumstellar disks in the multiple system HV Tau	Guilloteau, Di Folco, Simon, Piétu, Dutrey, Chapillon, Prato, Schaefer
X--2	Pinpointing a potential z ~ 10 gamma-ray burst (DDT)	Castro-Tirado, Bremer, Winters
X001	Can CF^+ be used as a proxy for C^+ in the diffuse medium? A search for CF^+ absorption in diffuse clouds along the sight-line to W49N	Guzmán, Pety, Gerin, Liszt, Neufeld, Gratier
X002	Understanding small and bright CO clumps exposed to far-UV illumination from the runaway O star HD34078	Gratier, Boissé, Cabrit, Gerin, Lesaffre, Pety, Pineau des Forêts
X003	The reservoir of nitrogen in the inner parts of starless cores	Hily-Blant, Dumas, Le Gal, Pineau des Forêts, Faure
X004	Imaging spatial variations of the N-isotopic composition in a nascent solar system	Wampfler, Jørgensen, Bisschop, Bizzarro
X008	Probing the birth of low mass stars: the Barnard 1b core	Cernicharo, Marcelino, Pety, Gerin, Fuente, Roueff, Lis, Levrier, Commerçon

Ident.	Title of Investigation	Authors
X009	Warm $H_2{}^{18}O$ immediately surrounding the massive proto-star in DR21(OH)	Braine, Herpin, Bontemps, Wyrowski, van der Tak, Chavarría, Jacq, Baudry, Schneider
X00A	HH114-MMS: a new chemically active outflow	Tafalla, Hacar, Frau
X00C	Filament fragmentation in high-mass star formation	Beuther, Tackenberg, Johnston, Ragan, Henning
X015	PdBI Observations of the Extreme Debris Disk around HD 15407A	Fujiwara, Marshall, Eiroa, White, Krivov, Ishihara, Takita, Ohashi, Onaka
X016	Testing the anion chemistry in IRC+10216: Where is C_4H^-?	Guélin, Cernicharo, Agundez, Winters, Thaddeus, Gottlieb
X019	Dense Gas in Giant Molecular Clouds in Andromeda	Schruba, Dishoeck, Tacconi, Walter, Sandstrom, Usero, Leroy, Dalcanton
X01A	The Anatomy of a Spiral Arm: From Molecular Gas to Stellar Clusters	Schinnerer, Meier, Meidt, Garcia-Burillo, Bigiel, Usero, Pety, Dumas, Hughes
X01E	Dense gas vs. intense star formation in the circumnuclear ring of NGC 4736	van der Laan, Armus, Beirão, Sandstrom, Groves, Schinnerer
X020	Molecular gas to probe dark matter in polar rings	Moiseev, Combes, Reshetnikov
X029	The Interplay Between Feedback and Gas Supply at Intermediate Redshift	Rubin, Decarli, Cucchiara, Walter, Hennawi, Prochaska, Fumagalli
X02C	The Fate of Cold Gas in Local Turbulent Disk Galaxies	Obreschkow, Fisher, Glazebrook, Poole, Bassett, Cooper, Popping, Wisnioski, Abraham, Damjanov, Green, McGregor, Sharp, Satterthwaite
X02D	LoCuSS: the fate of cold gas in cluster galaxies at intermediate redshift	Jablonka, Combes, Kneib, Jauzac, Egami, Haines, Pereira
X02F	The nature of the unique source SWIFT J1644+57	Agudo, Castro-Tirado, Guziy, Bremer, Winters, Gorosabel, Gómez, Sánchez-Ramirez, Tello
X031	J0927+2943: A massive black hole binary?	Decarli, Dotti, Volonteri, Walter
X033	The Molecular Gas in High-*z* Star-Forming Galaxies from HiZELS	Swinbank, Smail, Simpson, Sobral, Best, Geach, van der Werf
X036	Lensed Galaxies Extend CO Studies to Lower Stellar Masses	Wuyts, Saintonge, Tacconi, Lutz, Gladders, Rigby, Sharon
X037	Uncovering the ISM in a highly lensed dwarf galaxy at *z*~2	Aravena, Brammer, Walter, Da Cunha, van der Wel
X039	A study of the ISM properties of `normal' star-forming galaxies at *z*=2	Aravena, Riechers, Walter, Wagg, Carilli, Hodge, Daddi
X03D	Molecular gas in the most luminous quasars at *z*=2.5	Feruglio, Krips, Piconcelli, Brusa, Fiore, Maiolino, Santini, Bongiorno, Daddi, Sargent
X03E	Search for molecular gas in a $M_* \sim 10^9$ M LIRG at *z*=2.6	Richard, Knudsen, Kneib, Lindroos, Altieri, Stark, Clement, Smail
X03F	Molecular Gas from Host Galaxies of Weak Line Quasars at z>2	Wang, Fan, Carilli, Plotkin, Shemmer, Walter, Neri, Wagg, Omont, Strauss, Cox, Bertoldi, Menten, Diamond-Stanic
X041	The faint siblings of High-Redshift Radio Galaxies	Herzog, Middelberg
X042	Milky-Way Like CO Excitation in Lyman α Blobs?	Yang, Walter, Decarli, Bertoldi, Weiss, Badescu
X043	Zooming in onto the brightest sub-mm lenses on the sky	Nesvadba, Boone, Boulanger, Beelen, Dicken, Dole, Flores-Cacho, Frye, Guery, Guillard, Koenig, Krips, Le Floc'h, Lehnert, MacKenzie, Malhotra, Montier, Omont, Rhoads, Scott, Welikala
X045	Understanding the Nature of Herschel-Selected Submillimeter Galaxies	Riechers, Omont, Perez-Fournon, Neri, Cox, Cooray, Wardlow, Clements, Ivison, Magdis, Bock, Oliver
X046	Mapping of a Strongly Lensed Infrared-Luminous Arc at *z*=3.6	Zamojski, Dessauges-Zavadsky, Egami, Combes, Rawle, Boone, Schaerer, Richard, Kneib, Cément, Walth
X04A	Cold Dust in Two Massive ULIRGs at z~5	Caputi, Michalowski, Ashby, Huang, Fazio, Almaini, Castellano, Dunlop, Fontana, Koekemoer, Kohno, Pöpping, Spaans, Trager
X04B	Identification of the highest redshift H-ATLAS and HerMES galaxies	Bertoldi, Perez Fournon, Omont, Dannerbauer, Michalowski, Ivison, Clements, Negrello, White, Benford, Temi, Vaccari, Riechers, Bock, Vieira, Cooray, Wardlow, Coppin, Frayer, De Zotti, Eales, Valiante
X04C	Tracing ion chemistry and outflows in a high-*z* ULIRG	Omont, Boone, Combes, Yang, Neri, Cox, Richard, Egami, Rex, Smail, Ivison, Dessauges-Zavadsky, Schaerer, Kneib, van der Werf, Rawle, Zamojski, Pham, Pello
X04D	A census of [CI] in high-*z* galaxies with available [CII] observations	Decarli, Walter, Riechers, Weiss, Bertoldi, Carilli, Ferkinhoff, Groves, Neri
X04F	CO emission in a flux limited sample of *z*=6 UKIDSS quasars	Venemans, Walter, Decarli, Banados, Cox, Neri
X050	Accurate positions for 2 mm GISMO deep field detected sources with no counterparts	Staguhn, Walter, Kovacs, Decarli
X052	Unveiling the population of highly obscured and high-*z* gamma-ray bursts (ToO)	Castro-Tirado, Bremer, Winters, Gorosabel, Guziy, Pérez-Ramírez, Castro Cerón, Pandey, Tello, Sánchez-Ramírez
X053	PHIBSS2: molecular gas at the peak epoch of galaxy formation	Combes, García-Burillo, Neri, Tacconi, Genzel, Contini, Bolatto, Lilly, Boone, Bouché, Bournaud, Burkert, Carollo, Colina, Cooper, Cox, Feruglio, Freundlich, Schreiber, Juneau, Kovac, Lippa, Lutz, Naab, Omont, Renzini, Saintonge, Salomé, Sternberg, Walter, Weiner, Weiss, Wuyts
X056	Comet ISON after its passage at 1.7 solar radii from the Sun	Boissier, Bockelée-Morvan, Biver, Crovisier, Moreno, Colom, Groussin, Lamy, Jorda
X058	SO^+ as a probe of the dissociative shock in L1157-B1	Podio, Lefloch, Codella, Fontani, Ceccarelli, Bachiller, Cernicharo, Gusdorf, Benedettini
X060	Probing the heavy water content in a star-forming region	Coutens, Persson, Jørgensen, Vastel, Dishoeck, Taquet

Ident.	Title of Investigation	Authors
X06B	Deuteration as a Tool to investigate the physics of protoplanetary disk midplanes: the GG Tau case	Dutrey, Di Folco, Guilloteau, Hersant, Wakelam, Vastel, Piétu, Gueth, Chapillon, Beck, Bary, Simon, Boehler, Tang
X07F	Mapping the molecular gas conditions in nearby starburst galaxies	Rodríguez, Mühle, Aalto, Costagliola, Alberdi, Pérez-Torres
X087	Mapping the ionisation of NGC1068: what feedback where?	Ceccarelli, Fiore, Feruglio, Neri, Antonucci, Hily-Blant, Krips, Piconcelli, Vaupré
X09C	Confirming a 1000 km/s molecular outflow in an Eddington-limited starburst	Geach, Hickox, Krips, Diamond-Stanic, Moustakas, Rudnick, Tremonti, Coil
X0B3	First Systematic Survey for CO and Dust in Lyman α Blobs	Yang, Walter, Decarli, Bertoldi, Weiss, Adescu
X0BA	The Extreme Dense Gas Excitation in the z=4 Galaxy APM 08279+5255	Riechers, Neri, Weiss, Walter, Downes, Cox, Wagg
X0BC	Resolving the star formation in a z=4 starburst	Hodge, Decarli, Walter, Riechers, Carilli
X0C8	Small-scale structure of molecular gas at z=5.243 (continued)	Boone, Combes, Krips, Richard, Egami, Rawle, Smail, Ivison, Omont, Dessauges-Zavadsky, Schaerer, Kneib, Zamojski, van der Werf, Pham, Pello
X0CC	A Detailed Investigation of the ISM in the Most Distant Starburst Galaxy	Riechers, Perez-Fournon, Omont, Neri, Bradford, Clements, Cooray, Wardlow, Cox, Krips, Dowell, Ivison, Kamenetzky, Conley, Vieira, Bock, Oliver
X0CD	Chasing dust and [CII] in a spectroscopically confirmed bright z=7.51 galaxy	Schaerer, Boone, Finkelstein

Annex II – Publications in 2013

The list of refereed publications, conferences and workshop papers as well as thesis based upon data obtained using the IRAM instruments are provided in the following two tables : the first table gives the publications with the IRAM staff members as co-author (including technical publications by the IRAM staff), and the second table those with results from the user's community.

The running number is the cumulative number since the first annual report was published for the year 1987.

2013 PUBLICATION LIST: IRAM COMMUNITY:

1781	Initial phases of massive star formation in high infrared extinction clouds. II. Infall and onset of star formation	Rygl K. L. J., Wyrowski F., Schuller F., Menten K. M.	2013, A&A 549, A5
1782	A cold-gas reservoir to fuel the M 31 nuclear black hole and stellar cluster	Melchior A.-L., Combes F.	2013, A&A 549, A27
1783	The dust SED of dwarf galaxies. I. The case of NGC 4214	Hermelo I., Lisenfeld U., Relaño M., Tuffs R. J., Popescu C. C., Groves B.	2013, A&A 549, A70
1784	Gas fraction and star formation efficiency at $z < 1.0$	Combes F., García-Burillo S., Braine J., Schinnerer E., Walter F., Colina L.	2013, A&A 550, A41
1785	CH_3OCH_3 in Orion-KL: a striking similarity with $HCOOCH_3$	Brouillet N., Despois D., Baudry A., Peng T.-C., Favre C., Wootten A., Remijan A. J., Wilson T. L., Combes F., Wlodarczak G.	2013, A&A 550, A46
1786	The abundance of HCN in circumstellar envelopes of AGB stars of different chemical type	Schöier F. L., Ramstedt S., Olofsson H., Lindqvist M., Bieging J. H., Marvel K. B.	2013, A&A 550, A78
1787	Triggered/sequential star formation? A multi-phase ISM study around the prominent IRDC G18.93-0.03	Tackenberg J., Beuther H., Plume R., Henning T., Stil J., Walmsley M., Schuller F., Schmiedeke A.	2013, A&A 550, A116
1788	The Earliest Phases of Star Formation (EPoS): a Herschel key project. The thermal structure of low-mass molecular cloud cores	Launhardt R., Stutz A. M., Schmiedeke A., Henning T., Krause O., Balog Z., Beuther H., Birkmann S., Hennemann M., Kainulainen J., Khanzadyan T., Linz H., Lippok N., Nielbock M., Pitann J., Ragan S., Risacher C., Schmalzl M., Shirley Y. L., Stecklum B., Steinacker J., Tackenberg J.	2013, A&A 551, A98
1789	A molecular outflow driven by the brown dwarf binary FU Tauri	Monin J.-L., Whelan E. T., Lefloch B., Dougados C., Alves de Oliveira C.	2013, A&A 551, L1
1790	The Canada-France High-*z* Quasar Survey: 1.2 mm observations	Omont A., Willott C. J., Beelen A., Bergeron J., Orellana G., Delorme P.	2013, A&A 552, A43
1791	Warm gas in the rotating disk of the Red Rectangle: accurate models of molecular line emission	Bujarrabal V., Alcolea J.	2013, A&A 552, A116
1792	Mono-deuterated dimethyl ether: laboratory spectrum up to 1 THz. Torsion-rotational spectrum within the vibrational ground-state for the symmetric and asymmetric conformers and first detection in IRAS 16293-2422	Richard C., Margulès L., Caux E., Kahane C., Ceccarelli C., Guillemin J.-C., Motiyenko R. A., Vastel C., Groner P.	2013, A&A 552, A117
1793	HH 114 MMS: a new chemically active outflow	Tafalla M., Hacar A.	2013, A&A 552, L9
1794	Resolving the molecular gas around the lensed quasar RXJ0911.4+0551	Anh P. T., Boone F., Hoai D. T., Nhung P. T., Weiß A., Kneib J.-P., Beelen A., Salomé P.	2013, A&A 552, L12
1795	The HIFI spectral survey of AFGL 2591 (CHESS). I. Highly excited linear rotor molecules in the high-mass protostellar envelope	van der Wiel M. H. D., Pagani L., van der Tak F. F. S., Kaźmierczak M., Ceccarelli C.	2013, A&A 553, A11
1796	Vertical settling and radial segregation of large dust grains in the circumstellar disk of the Butterfly Star	Gräfe C., Wolf S., Guilloteau S., Dutrey A., Stapelfeldt K. R., Pontoppidan K. M., Sauter J.	2013, A&A 553, A69
1797	Long-term variability of extragalactic radio sources in the Planck Early Release Compact Source Catalogue	Chen X., Rachen J. P., López-Caniego M., Dickinson C., Pearson T. J., Fuhrmann L., Krichbaum T. P., Partridge B.	2013, A&A 553, A107
1798	Fragmentation and dynamical collapse of the starless high-mass star-forming region IRDC 18310-4	Beuther H., Linz H., Tackenberg J., Henning T., Krause O., Ragan S., Nielbock M., Launhardt R., Bihr S., Schmiedeke A., Smith R., Sakai T.	2013, A&A 553, A115
1799	Formation and evolution of interstellar filaments. Hints from velocity dispersion measurements	Arzoumanian D., André P., Peretto N., Könyves V.	2013, A&A 553, A119
1800	Molecular content of polar-ring galaxies	Combes F., Moiseev A., Reshetnikov V.	2013, A&A 554, A11
1801	Towards understanding the relation between the gas and the attenuation in galaxies at kpc scales	Boquien M., Boselli A., Buat V., Baes M., Bendo G., Boissier S., Ciesla L., Cooray A., Cortese L., Eales S., Koda J., Lebouteiller V., de Looze I., Smith M. W. L., Spinoglio L., Wilson C. D.	2013, A&A 554, A14
1802	Cores, filaments, and bundles: hierarchical core formation in the L1495/B213 Taurus region	Hacar A., Tafalla M., Kauffmann J., Kovács A.	2013, A&A 554, A55
1803	Acetone in Orion BN/KL. High-resolution maps of a special oxygen-bearing molecule	Peng T.-C., Despois D., Brouillet N., Baudry A., Favre C., Remijan A., Wootten A., Wilson T. L., Combes F., Wlodarczak G.	2013, A&A 554, A78
1804	Detection of $^{15}NNH^+$ in L1544: non-LTE modelling of dyazenilium hyperfine line emission and accurate $^{14}N/^{15}N$ values	Bizzocchi L., Caselli P., Leonardo E., Dore L.	2013, A&A 555, A109
1805	Long-term multiwavelength studies of high-redshift blazar 0836+710	Akyuz A., Thompson D. J., Donato D., Perkins J. S., Fuhrmann L., Angelakis E., Zensus J. A., Larsson S., Sokolovsky K., Kurtanidze O.	2013, A&A 556, A71
1806	Search for cold and hot gas in the ram pressure stripped Virgo dwarf galaxy IC 3418	Jáchym P., Kenney J. D. P., Ržuička A., Sun M., Combes F., Palouš J.	2013, A&A 556, A99

1807	OH/IR stars and their superwinds as observed by the Herschel Space Observatory	Justtanont K., Teyssier D., Barlow M. J., Matsuura M., Swinyard B., Waters L. B. F. M., Yates J.	2013, A&A 556, A101
1808	A line confusion-limited millimeter survey of Orion KL. III. Sulfur oxide species	Esplugues G. B., Tercero B., Cernicharo J., Goicoechea J. R., Palau A., Marcelino N., Bell T. A.	2013, A&A 556, A143
1809	The CN/^{15}CN isotopic ratio towards dark clouds	Hily-Blant P., Pineau des Forêts G., Faure A., Le Gal R., Padovani M.	2013, A&A 557, A65
1810	Evolution and excitation conditions of outflows in high-mass star-forming regions	Sánchez-Monge Á., López-Sepulcre A., Cesaroni R., Walmsley C. M., Codella C., Beltrán M. T., Pestalozzi M., Molinari S.	2013, A&A 557, A94
1811	Cold gas in the inner regions of intermediate redshift clusters	Jablonka P., Combes F., Rines K., Finn R., Welch T.	2013, A&A 557, A103
1812	Nature of the gas and dust around 51 Ophiuchi. Modelling continuum and Herschel line observations	Thi W. F., Ménard F., Meeus G., Carmona A., Riviere-Marichalar P., Augereau J.-C., Kamp I., Woitke P., Pinte C., Mendigutía I., Eiroa C., Montesinos B., Britain S., Dent W.	2013, A&A 557, A111
1813	Non-Zeeman circular polarization of CO rotational lines in SNR IC 443	Hezareh T., Wiesemeyer H., Houde M., Gusdorf A., Siringo G.	2013, A&A 558, A45
1814	Deep observations of O_2 toward a low-mass protostar with Herschel-HIFI	Yıldız U. A., Acharyya K., Goldsmith P. F., van Dishoeck E. F., Melnick G., Snell R., Liseau R., Chen J.-H., Pagani L., Bergin E., Caselli P., Herbst E., Kristensen L. E., Visser R., Lis D. C., Gerin M.	2013, A&A 558, A58
1815	A gas-rich AGN near the centre of a galaxy cluster at z ~ 1.4	Casasola V., Magrini L., Combes F., Mignano A., Sani E., Paladino R., Fontani F.	2013, A&A 558, A60
1816	Fragmentation, infall, and outflow around the showcase massive protostar NGC 7538 IRS1 at 500 AU resolution	Beuther H., Linz H., Henning T.	2013, A&A 558, A81
1817	CO outflows from high-mass Class 0 protostars in Cygnus-X	Duarte-Cabral A., Bontemps S., Motte F., Hennemann M., Schneider N., André P.	2013, A&A 558, A125
1818	PO and PN in the wind of the oxygen-rich AGB star IK Tauri	De Beck E., Kamiński T., Patel N. A., Young K. H., Gottlieb C. A., Menten K. M., Decin L.	2013, A&A 558, A132
1819	Complex organic molecules in the interstellar medium: IRAM 30 m line survey of Sagittarius B2(N) and (M)	Belloche A., Müller H. S. P., Menten K. M., Schilke P., Comito C.	2013, A&A 559, A47
1820	Combined IRAM and Herschel/HIFI study of cyano(di) acetylene in Orion KL: tentative detection of DC_3N	Esplugues G. B., Cernicharo J., Viti S., Goicoechea J. R., Tercero B., Marcelino N., Palau A., Bell T. A., Bergin E. A., Crockett N. R., Wang S.	2013, A&A 559, A51
1821	Chemical modeling of the L1498 and L1517B prestellar cores: CO and HCO^+ depletion	Maret S., Bergin E. A., Tafalla M.	2013, A&A 559, A53
1822	HIFISTARS Herschel/HIFI observations of VY Canis Majoris. Molecular-line inventory of the envelope around the largest known star	Alcolea J., Bujarrabal V., Planesas P., Teyssier D., Cernicharo J., De Beck E., Decin L., Dominik C., Justtanont K., de Koter A., Marston A. P., Melnick G., Menten K. M., Neufeld D. A., Olofsson H., Schmidt M., Schöier, F. L., Szczerba R., Waters L. B. F. M.	2013, A&A 559, A93
1823	Nitrogen isotopic ratios in Barnard 1: a consistent study of the N_2H^+, NH_3, CN, HCN, and HNC isotopologues	Daniel F., Gérin M., Roueff E., Cernicharo J., Marcelino N., Lique F., Lis D. C., Teyssier D., Biver N., Bockelée-Morvan D.	2013, A&A 560, A3
1824	Deuterated water in the solar-type protostars NGC 1333 IRAS 4A and IRAS 4B	Coutens A., Vastel C., Cabrit S., Codella C., Kristensen L. E., Ceccarelli C., van Dishoeck E. F., Boogert A. C. A., Bottinelli S., Castets A., Caux E., Comito C., Demyk K., Herpin F., Lefloch B., McCoey C., Mottram J. C., Parise B., Taquet V., van der Tak F. F. S., Visser R., Yıldız U. A.	2013, A&A 560, A39
1825	Gas-phase CO depletion and N2H abundances in starless cores	Lippok N., Launhardt R., Semenov D., Stutz A. M., Balog Z., Henning T., Krause O., Linz H., Nielbock M., Pavlyuchenkov Y. N., Schmalzl M., Schmiedeke A., Bieging J. H.	2013, A&A 560, A41
1826	Sensitive CO and ^{13}CO survey of water fountain stars. Detections towards IRAS 18460-0151 and IRAS 18596+0315	Rizzo J. R., Gómez J. F., Miranda L. F., Osorio M., Suárez O., Durán-Rojas M. C.	2013, A&A 560, A82
1827	Herschel and IRAM-30 m observations of comet C/2012 S1 (ISON) at 4.5 AU from the Sun	O'Rourke L., Bockelée-Morvan D., Biver N., Altieri B., Teyssier D., Jorda L., Debout V., Snodgrass C., Küppers M., A'Hearn M., Müller T. G., Farnham T.	2013, A&A 560, A101
1828	Early Stages of Cluster Formation: Fragmentation of Massive Dense Cores down to <~ 1000 AU	Palau A., Fuente A., Girart J. M., Estalella R., Ho P. T. P., Sánchez-Monge Á., Fontani F., Busquet G., Commerçon B., Hennebelle P., Boissier J., Zhang Q., Cesaroni R., Zapata L. A.	2013, ApJ 762, 120
1829	Detection of Formamide, the Simplest but Crucial Amide, in a Solar-type Protostar	Kahane C., Ceccarelli C., Faure A., Caux E.	2013, ApJ 763, L38
1830	The VIRUS-P Exploration of Nearby Galaxies (VENGA): The X_{CO} Gradient in NGC 628	Blanc G. A., Schruba A., Evans N. J., II, Jogee S., Bolatto A., Leroy A. K., Song M., van den Bosch R. C. E., Drory N., Fabricius M., Fisher D., Gebhardt K., Heiderman A., Marinova I., Vogel S., Weinzirl T.	2013, ApJ 764, 117
1831	The Molecular Gas Density in Galaxy Centers and how it Connects to Bulges	Fisher D. B., Bolatto A., Drory N., Combes F., Blitz L., Wong T.	2013, ApJ 764, 174
1832	Resolved Depletion Zones and Spatial Differentiation of N_2H^+ and N_2D^+	Tobin J. J., Bergin E. A., Hartmann L., Lee J.-E., Maret S., Myers P. C., Looney L. W., Chiang H.-F., Friesen R.	2013, ApJ 765, 18
1833	G048.66-0.29: Physical State of an Isolated Site of Massive Star Formation	Pitann J., Linz H., Ragan S., Stutz A. M., Beuther H., Henning T., Krause O., Launhardt R., Schmiedeke A., Schuller F., Tackenberg J., Vasyunina T.	2013, ApJ 766, 68
1834	A Millimeter-wave Interferometric Search for a Molecular Torus in the Radio Galaxy NGC 4261	Okuda T., Iguchi S., Kohno K.	2013, ApJ 768, 19
1835	Herschel/SPIRE Submillimeter Spectra of Local Active Galaxies	Pereira-Santaella M., Spinoglio L., Busquet G., Wilson C. D., Glenn J., Isaak K. G., Kamenetzky J., Rangwala N., Schirm M. R. P., Baes M., Barlow M. J., Boselli A., Cooray A., Cormier D.	2013, ApJ 768, 55
1836	Laboratory Characterization and Astrophysical Detection of Vibrationally Excited States of Ethyl Cyanide	Daly A. M., Bermúdez C., López A., Tercero B., Pearson J. C., Marcelino N., Alonso J. L., Cernicharo J.	2013, ApJ 768, 81
1837	The Fueling Diagram: Linking Galaxy Molecular-to-atomic Gas Ratios to Interactions and Accretion	Stark D. V., Kannappan S. J., Wei L. H., Baker A. J., Leroy A. K., Eckert K. D., Vogel S. N.	2013, ApJ 769, 82
1838	Interstellar Detection of c-C_3D_2	Spezzano S., Brünken S., Schilke P., Caselli P., Menten K. M., McCarthy M. C., Bizzocchi L., Trevinõ-Morales S. P., Aikawa Y., Schlemmer S.	2013, ApJ 769, L19
1839	Discovery of Methyl Acetate and Gauche Ethyl Formate in Orion	Tercero B., Kleiner I., Cernicharo J., Nguyen H. V. L., López A., Muñoz Caro G. M.	2013, ApJ 770, L13

1840	The Spatial Distribution of Organics toward the High-mass YSO NGC 7538 IRS9	Öberg K. I., Boamah M. D., Fayolle E. C., Garrod R. T., Cyganowski C. J., van der Tak F.	2013, ApJ 771, 95
1841	Detection of the Ammonium Ion in Space	Cernicharo J., Tercero B., Fuente A., Domenech J. L., Cueto M., Carrasco E., Herrero V. J., Tanarro I., Marcelino N., Roueff E., Gerin M., Pearson J.	2013, ApJ 771, L10
1842	Probing the Interstellar Medium of z ~ 1 Ultraluminous Infrared Galaxies through Interferometric Observations of CO and Spitzer Mid-infrared Spectroscopy	Pope A., Wagg J., Frayer D., Armus L., Chary R.-R., Daddi E., Desai V., Dickinson M. E., Elbaz D., Gabor J., Kirkpatrick A.	2013, ApJ 772, 92
1843	Earliest Stages of Protocluster Formation: Substructure and Kinematics of Starless Cores in Orion	Lee K., Looney L. W., Schnee S., Li Z.-Y.	2013, ApJ 772, 100
1844	Uniform Infall toward the Cometary H II Region in the G34.26+0.15 Complex?	Liu T., Wu Y., Zhang H.	2013, ApJ 776, 29
1845	Broad N_2H^+ Emission toward the Protostellar Shock L1157-B1	Codella C., Viti S., Ceccarelli C., Lefloch B., Benedettini M., Busquet G., Caselli P., Fontani F., Gómez-Ruiz A., Podio L., Vasta M.	2013, ApJ 776, 52
1846	A Deep Search for Molecular Gas in Two Massive Lyman Break Galaxies at z =3 and 4: Vanishing CO-emission Due to Low Metallicity?	Tan Q., Daddi E., Sargent M., Magdis G., Hodge J., Béthermin M., Bournaud F., Carilli C., Dannerbauer H., Dickinson M., Elbaz D., Gao Y., Morrison G., Owen F., Pannella M., Riechers D., Walter F.	2013, ApJ 776, L24
1847	The cm-, mm-, and sub-mm-wave Spectrum of Allyl Isocyanide and Radioastronomical Observations in Orion KL and the SgrB2 Line Surveys	Haykal I., Margulès L., Huet T. R., Motyienko R. A., Écija P., Cocinero E. J., Basterretxea F., Fernández J. A., Castaño F., Lesarri A., Guillemin J. C., Tercero B., Cernicharo J.	2013, ApJ 777, 120
1848	Validation of the Equilibrium Model for Galaxy Evolution to z ~ 3 through Molecular Gas and Dust Observations of Lensed Star-forming Galaxies	Saintonge A., Lutz D., Genzel R., Magnelli B., Nordon R., Tacconi L. J., Baker A. J., Bandara K., Berta S., Förster Schreiber N. M., Poglitsch A., Sturm E., Wuyts E., Wuyts S.	2013, ApJ 778, 2
1849	A SiO 2-1 Survey toward Gas-rich Active Galaxies	Wang J., Zhang J., Shi Y., Zhang Z.	2013, ApJ 778, L39
1850	The First Astrophysical Detection, Terahertz Spectrum, and Database for the Monodeuterated Species of Methyl Formate $HCOOCH_2D$	Coudert L. H., Drouin B. J., Tercero B., Cernicharo J., Guillemin J.-C., Motiyenko R. A., Margulès L.	2013, ApJ 779, 119
1851	MUSCLE W49: A Multi-Scale Continuum and Line Exploration of the Most Luminous Star Formation Region in the Milky Way. I. Data and the Mass Structure of the Giant Molecular Cloud	Galván-Madrid R., Liu H. B., Zhang Z.-Y., Pineda J. E., Peng T.-C., Zhang Q., Keto E. R., Ho P. T. P., Rodríguez L. F., Zapata L., Peters T., De Pree C. G.	2013, ApJ 779, 121
1852	Complex, quiescent kinematics in a highly filamentary infrared dark cloud	Henshaw J. D., Caselli P., Fontani F., Jiménez-Serra I., Tan J. C., Hernandez A. K.	2013, MNRAS 428, 3425
1853	CO in late-type galaxies within the central region of Abell 1367	Scott T. C., Usero A., Brinks E., Boselli A., Cortese L., Bravo-Alfaro H.	2013, MNRAS 429, 221
1854	The ATLAS^{3D} Project - XIV. The extent and kinematics of the molecular gas in early-type galaxies	Davis T. A., Alatalo K., Bureau M., Cappellari M., Scott N., Young L. M., Blitz L., Crocker A., Bayet E., Bois M., Bournaud F., Davies R. L., de Zeeuw P. T., Duc P.-A., Emsellem E., Khochfar S., Krajnović D., Kuntschner H., Lablanche P.-Y., McDermid R. M., Morganti R., Naab T., Oosterloo T., Sarzi M., Serra P., Weijmans A.-M.	2013, MNRAS 429, 534
1855	The ATLAS^{3D} project - XVIII. CARMA CO imaging survey of early-type galaxies	Alatalo K., Davis T. A., Bureau M., Young L. M., Blitz L., Crocker A. F., Bayet E., Bois M., Bournaud F., Cappellari M., Davies R. L., de Zeeuw P. T., Duc P.-A., Emsellem E., Khochfar S., Krajnović D., Kuntschner H., Lablanche P.-Y., Morganti R., McDermid R. M., Naab T., Oosterloo T., Sarzi M., Scott N., Serra P., Weijmans A.-M.	2013, MNRAS 432, 1796
1856	ISM chemistry in metal-rich environments: molecular tracers of metallicity	Davis T. A., Bayet E., Crocker A., Topal S., Bureau M.	2013, MNRAS 433, 1659
1857	Molecular gas in type 2 quasars at $z \sim$ 0.2 - 0.3	Villar-Martín M., Rodríguez M., Drouart G., Emonts B., Colina L., Humphrey A., García Burillo S., Graciá Carpio J., Planesas P., Pérez Torres M., Arribas S.	2013, MNRAS 434, 978
1858	Molecular Gas and Star Formation in nearby Disk Galaxies	Leroy A. K., Walter F., Sandstrom K., Schruba A., Munoz-Mateos J.-C., Bigiel F., Bolatto A., Brinks E., de Blok W. J. G., Meidt S., Rix H.-W., Rosolowsky E., Schinnerer E., Schuster K.-F., Usero A.	2013, Astron. Journal 146, 19
1859	Herschel Galactic Cold Cloud Core Analysis	Verebelyi E., Pagani L.	2013, IAU Symp. 292, 115
1860	Different Evolutionary Stages in the Massive Star-forming Complex W3 Main	Wang Y., Beuther H., Zhang Q., Bik A., Rodón J. A., Jiang Z., Fallscheer C.	2013, IAU Symp. 292, 116
1861	Chemical complexity and star-formation in merging galaxies	Davis T. A., Heiderman A., Iono D., VIXENS Team	2013, IAU Symp. 292, 244
1862	Star Formation Efficiency at Intermediate Redshift	Combes F., García-Burillo S., Braine J., Schinnerer E., Walter F., Colina L.	2013, IAU Symp. 292, 303
1863	Revealing the origin of the cold ISM in massive early-type galaxies	Davis T. A., Alatalo K., Bureau M., Young L., Blitz L., Crocker A., Bayet E., Bois M., Bournaud F., Cappellari M., Davies R. L., Duc P.-A., de Zeeuw P. T., Emsellem E., Falcon-Barroso J., Khochfar S., Krajnovic D., Kuntschner H., Lablanche P.-Y., McDermid R. M., Morganti R., Naab T., Sarzi M., Scott N., Serra P., Weijmans A.	2013, IAU Symp. 295, 324
1864	Probing the Cool Outer Envelope of NGC 6826	Verbena J. L., Schröder K., Jeyakumar S., Wachter A.	2013, ASPC 472, 67
1865	Molecular Gas in High Redshift Galaxies	Combes F.	2013, ASPC 476, 23
1866	Fragmentation in High-Mass Star Forming Regions	Rodón J. A., Beuther H., Schilke P., Zhang Q.	2013, ASPC 476, 315
1867	Detection of Formamide in the Solar-Type Protostar IRAS16293-2422	Kahane C., Ceccarelli C., Faure A., Caux E.	2013, ASPC 476, 323
1868	The Mass Loss History of WX Psc	Trejo A., Zhao-Geisler R., Kemper F.	2013, ASPC 476, 395
1869	The Herschel-PACS photometer calibration - Point-source flux calibration for scan maps	Balog Z., Müller T., Nielbock M., Altieri B., Klaas U., Blommaert J., Linz H., Lutz D., Moór A., Billot N., Sauvage M., Okumura K.	2013, Experimantal Astronomy (October), 38
1870	PACS photometer calibration block analysis	Moór A., Müller T. G., Kiss C., Balog Z., Billot N., Marton G.	2013, Experimental Astronomy (October), 50

1871	Intrinsic Brightness Temperature of Compact Radio Sources at 86 GHz	Lee S.-S.	2013, Journal of the Korean Astron. Soc. 46, 243
1872	The "Far Site" Scenario for Gamma-ray Emission in Blazars. A View from the VLBI Observing Perspective	Agudo I.	2013, EPJ Web of Conferences 61, 4002
1873	Dense cores in the dark cloud complex LDN 1188	Verebélyi E., Könyves V., Nikolić S., Kiss C., Moór A., Ábrahám P., Kun M.	2013, Astronomische Nachrichten 334, 920
1874	First unbiased spectral survey of a young and single massive protostar: CygX-N63	Fechtenbaum S., Bontemps S.	2013, SF2A conf. 219
1875	Properties of interstellar filaments as revealed by the Herschel Gould Belt survey	Arzoumanian D.	2013, SF2A conf. 385
1876	The small-scale structure of OMC-2 FIR 4: Interferometric observations of an intermediate-mass protocluster	Lopez-Sepulcre A., Taquet V., Sanchez-Monge A., Kama M., Ceccarelli C., Dominik C., Caux E., Shimajiri Y.	2013, Protostars and Planets VI, 16
1877	Does the Galactic centre cloud G0.253+0.016 violate star formation relations?	Johnston K., Beuther H., Longmore S., Rathborne J., Ragan S.	2013, Protostars and Planets VI, 18
1878	Resolving the Chemical Substructure of Orion-KL	Feng S., Beuther H., Semenov D., Henning T., Palau A.	2013, Protostars and Planets VI, 19
1879	Fragmentation and Deuteration in Massive Star-Forming Regions	Rodón J. A., Beuther H., Schilke P., Zhang Q.	2013, Protostars and Planets VI, 21
1880	Molecular Line Surveys of Nearby T Tauri Stars: Late-time Chemistry of Protoplanetary Disks	Kastner J., Punzi K., Rodriguez D., Sacco G. G., Hily-Blant P., Forveille T., Zuckerman B.	2013, Protostars and Planets VI, 22
1881	The chemical evolution in the early phases of massive star formation	Gerner T., Beuther H., Semenov D., Linz H., Vasyunina T., Dullemond C., Bihr S., Henning T.	2013, Protostars and Planets VI, 26
1882	CO gas kinematics and excitation in a filamentary IRDC: Filament-filament interaction and accretion processes.	Jimenez-Serra I., Caselli P., Fontani F., Tan J. C., Henshaw J. D., Kainulainen J., Hernandez A. K.	2013, Protostars and Planets VI, 34
1883	Dense cavity walls traced by CS in the L1157-B1 protostellar shocked region	Gomez-Ruiz A., Codella C., Lefloch B., Benedettini M., Busquet G., Nisini B., Ceccarelli C., Cabrit S., Viti S.	2013, Protostars and Planets VI, 40
1884	Cosmic-ray ionization of a molecular cloud interacting with the supernova remnant W28	Vaupré S., Ceccarelli C., Hily-Blant P., Dubus G., Montmerle T.	2013, Protostars and Planets VI, 64
1885	Deuterated water in low-mass protostars	Coutens A., Vastel C., Chess Collaboration, Wish Collaboration, Hexos Collaboration	2013, Protostars and Planets VI, 66
1886	Observational constraints on Acrretion disk formation	Harsono D., Jørgensen J., van Dishoeck E., Hogerheijde M., Bruderer S., Persson M., Mottram J.	2013, Protostars and Planets VI, 88
1887	Kinematics of the NGC1333-IRAS2A inner envelope	Maret S., Calypso Team	2013, Protostars and Planets VI, 91
1888	Detection and Formation of Interstellar c-C_3D_2	Spezzano S., Brunken S., Schilke P., Menten K. M., Caselli P., McCarthy M. C., Bizzocchi L., Trevino S., Aikawa Y., Schlemmer S.	2013, 68th Internat. Symp. on Molec. Spectr., #ET108
1889	Spectroscopy of Isocyanides and Their Search in Interstellar Medium	Margules L., Motiyenko R. A., Tercero B., Cernicharo J., Guillemin J.-C.	2013, 68th Internat. Symp. on Molec. Spectr., #ET112
1890	Millimeter Wave Tunneling-Rotational Spectrum of Phenol	Kolesnikova L., Daly A. M., Alonso J. L., Tercero B., Cernicharo J.	2013, 68th Internat. Symp. on Molec. Spectr., #ERK08
1891	Modeling the circumstellar structure of Water Fountain evolved stars	Durán-Rojas M. C., Gómez J. F., Osorio M., Rizzo J. R., Anglada G., Suárez O., Miranda L. F., D'Alessio P., Calvet N., Pérez-Cáceres F. J.	2013, Highlights of Spanish Astron. VII, 648
1892	Molecular complexity in envelopes of evolved Oxygen-rich stars: IK Tauri and OH231.8+4.2	Velilla Prieto L., Sánchez Contreras C., Cernicharo J., Alcolea J., Agúndez M., Pardo J. R., Bujarrabal V., Herpin F., Menten K. M., Wyrowsky F.	2013, Highlights of Spanish Astron. VII, 676
1893	SHAPEMOL: the companion to SHAPE in the molecular era of ALMA and HERSCHEL	Santander-García M., Bujarrabal V., Alcolea J.	2013, Highlights of Spanish Astron. VII, 920
1894	mm-VLBI observations of the active galaxy 3C 111 in outburst	Schulz R. Kadler M., Ros E., Krichbaum T.P., Grossberger C., Müller C., Mannheim K., Agudo I., Aller H. D., Aller M. F.	2013, 11th EVN Symp., Proc. of Science (POS), 107
1895	Giant Molecular Clouds and Star Formation in Nearby Spiral Galaxies	Rebolledo D., Wong T. H., Leroy A. K., Koda J., Donovan Meyer J.	2013, AAS 221, #206.05
1896	Disk Emission Across the Stellar/Substellar Boundary in Taurus	Patience J., Bulger J., Bouy H., Monin J., Pinte C., Menard F., Koda J., Dowell C. D.	2013, AAS 221, #324.04
1897	Structure and Kinematics of the Starless Cores in Orion	Lee K., Looney L.	2013, AAS 221, #332.02
1898	Millimeter-to-Far-Infrared Photometry of Cygnus A	Benford D. J., Staguhn J., Kovacs A., Sharp E., Maher S.	2013, AAS 221, #339.49
1899	First Results from a Radio Emission Line Survey of the Molecular Disk Orbiting LkCa 15	Punzi K. M., Kastner J. H., Hily-Blant P., Forveille T., Sacco G.	2013, AAS 221, #443.13
1900	Analysis of the Herschel/HIFI 1.2 THz Wide Spectral Survey of the Orion Kleinmann-Low Nebula	Crockett N. R.	2013, Thesis

2013 PUBLICATION LIST: IRAM (CO) AUTHORS

1763	Dense gas in M 33 (HerM33es)	Buchbender C., Kramer C., Gonzalez-Garcia M., Israel F. P., García-Burillo S., van der Werf P., Braine J., Rosolowsky E., Mookerjea B., Aalto S., Boquien M., Gratier P., Henkel C., Quintana-Lacaci G., Verley S., van der Tak F.	2013, A&A 549, A17
1764	A λ = 3 mm molecular line survey of NGC 1068. Chemical signatures of an AGN environment	Aladro R., Viti S., Bayet E., Riquelme D., Martín S., Mauersberger R., Martín-Pintado J., Requena-Torres M. A., Kramer C., Weiß A.	2013, A&A 549, A39
1765	NGC 6240: extended CO structures and their association with shocked gas	Feruglio C., Fiore F., Maiolino R., Piconcelli E., Aussel H., Elbaz D., Le Floc'h E., Sturm E., Davies R., Cicone C.	2013, A&A 549, A51
1766	Fueling the central engine of radio galaxies. II. The footprints of AGN feedback on the ISM of 3C 236	Labiano A., García-Burillo S., Combes F., Usero A., Soria-Ruiz R., Tremblay G., Neri R., Fuente A., Morganti R., Oosterloo T.	2013, A&A 549, A58
1767	A sensitive survey for ^{13}CO, CN, H_2CO, and SO in the disks of T Tauri and Herbig Ae stars	Guilloteau S., Di Folco E., Dutrey A., Simon M., Grosso N., Piétu V.	2013, A&A 549, A92
1768	SiO collimated outflows driven by high-mass YSOs in G24.78+0.08	Codella C., Beltrán M. T., Cesaroni R., Moscadelli L., Neri R., Vasta M., Zhang Q.	2013, A&A 550, A81
1769	A precise and accurate determination of the cosmic microwave background temperature at z = 0.89	Muller S., Beelen A., Black J. H., Curran S. J., Horellou C., Aalto S., Combes F., Guélin M., Henkel C.	2013, A&A 551, A109
1770	Pure rotational spectra of TiO and TiO_2 in VY Canis Majoris	Kamiński T., Gottlieb C. A., Menten K. M., Patel N. A., Young K. H., Brünken S., Müller H. S. P., McCarthy M. C., Winters J. M., Decin L.	2013, A&A 551, A113
1771	H_2O emission in high-*z* ultra-luminous infrared galaxies	Omont A., Yang C., Cox P., Neri R., Beelen A., Bussmann R. S., Gavazzi R., van der Werf P., Riechers D., Downes D., Krips M., Dye S., Ivison R., Vieira J. D., Weiß A., Aguirre J. E., Baes M., Baker A. J., Bertoldi F., Cooray A., Dannerbauer H., De Zotti G., Eales S. A., Fu H., Gao Y., Guélin M., Harris A. I., Jarvis M., Lehnert M., Leeuw L., Lupu R., Menten K., Michałowski M. J., Negrello M., Serjeant S., Temi P., Auld R., Dariush A., Dunne L., Fritz J., Hopwood R., Hoyos C., Ibar E., Maddox S., Smith M. W. L., Valiante E., Bock J., Bradford C. M., Glenn J., Scott K. S.	2013, A&A 551, A115
1772	High-pressure, low-abundance water in bipolar outflows. Results from a Herschel-WISH survey	Tafalla M., Liseau R., Nisini B., Bachiller R., Santiago-García J., van Dishoeck E. F., Kristensen L. E., Herczeg G. J., Yıldız U. A.	2013, A&A 551, A116
1773	Improved mm-wave photometry for kinetic inductance detectors	Calvo M., Roesch M., Désert F.-X., Monfardini A., Benoit A., Mauskopf P., Ade P., Boudou N., Bourrion O., Camus P., Cruciani A., Doyle S., Hoffmann C., Leclercq S., Macias-Perez J. F., Ponthieu N., Schuster K. F., Tucker C., Vescovi C.	2013, A&A 551, L12
1774	Radio to gamma-ray variability study of blazar S5 0716+714	Rani B., Krichbaum T. P., Fuhrmann L., Böttcher M., Lott B., Aller H. D., Aller M. F., Angelakis E., Bach U., Bastieri D., Falcone A. D., Fukazawa Y., Gabanyi K. E., Gupta A. C., Gurwell M., Itoh R., Kawabata K. S., Krips M., Lähteenmäki A. A., Liu X., Marchili N., Max-Moerbeck W., Nestoras I., Nieppola E., Quintana-Lacaci G., Readhead A. C. S., Richards J. L., Sasada M., Sievers A., Sokolovsky K., Stroh M., Tammi J., Tornikoski M., Uemura M., Ungerechts H., Urano T., Zensus J. A.	2013, A&A 552, A11
1775	A detailed study of the radio-FIR correlation in NGC 6946 with Herschel-PACS/SPIRE from KINGFISH	Tabatabaei F. S., Schinnerer E., Murphy E. J., Beck R., Groves B., Meidt S., Krause M., Rix H.-W., Sandstrom K., Crocker A. F., Galametz M., Helou G., Wilson C. D., Kennicutt R., Calzetti D., Draine B., Aniano G., Dale D., Dumas G., Engelbracht C. W., Gordon K. D., Hinz J., Kreckel K., Montiel E., Roussel H.	2013, A&A 552, A19
1776	Spectral energy distributions of H II regions in M 33 (HerM33es)	Relaño M., Verley S., Pérez I., Kramer C., Calzetti D., Xilouris E. M., Boquien M., Abreu-Vicente J., Combes F., Israel F., Tabatabaei F. S., Braine J., Buchbender C., González M., Gratier P., Lord S., Mookerjea B., Quintana-Lacaci G., van der Werf P.	2013, A&A 552, A140
1777	Probing the role of polycyclic aromatic hydrocarbons in the photoelectric heating within photodissociation regions	Okada Y., Pilleri P., Berné O., Ossenkopf V., Fuente A., Goicoechea J. R., Joblin C., Kramer C., Röllig M., Teyssier D., van der Tak F. F. S.	2013, A&A 553, A2
1778	A non-LTE radiative transfer model to study ionized outflows and disks. The case of MWC349A	Báez-Rubio A., Martín-Pintado J., Thum C., Planesas P.	2013, A&A 553, A45
1779	The NGC 1614 interacting galaxy. Molecular gas feeding a "ring of fire"	König S., Aalto S., Muller S., Beswick R. J., Gallagher J. S.	2013, A&A 553, A72
1780	Gas and dust cooling along the major axis of M 33 (HerM33es). ISO/LWS [C ii] observations	Kramer C., Abreu-Vicente J., García-Burillo S., Relaño M., Aalto S., Boquien M., Braine J., Buchbender C., Gratier P., Israel F. P., Nikola T., Röllig M., Verley S., van der Werf P., Xilouris E. M.	2013, A&A 553, A114
1781	Towards a resolved Kennicutt-Schmidt law at high redshift	Freundlich J., Combes F., Tacconi L. J., Cooper M. C., Genzel R., Neri R., Bolatto A., Bournaud F., Burkert A., Cox P., Davis M., Förster Schreiber N. M., Garcia-Burillo S., Gracia-Carpio J., Lutz D., Naab T., Newman S., Sternberg A., Weiner B.	2013, A&A 553, A130
1782	Spatial distribution of small hydrocarbons in the neighborhood of the ultra compact HII region Monoceros R2	Pilleri P., Treviño-Morales S., Fuente A., Joblin C., Cernicharo J., Gerin M., Viti S., Berné O., Goicoechea J. R., Pety J., Gonzalez-García M., Montillaud J., Ossenkopf V., Kramer C., García-Burillo S., Le Petit F., Le Bourlot J.	2013, A&A 554, A87
1783	High-angular resolution observations towards OMC-2 FIR 4: Dissecting an intermediate-mass protocluster	López-Sepulcre A., Taquet V., Sánchez-Monge Á., Ceccarelli C., Dominik C., Kama M., Caux E., Fontani F., Fuente A., Ho P. T. P., Neri R., Shimajiri Y.	2013, A&A 556, A62

1784	The simultaneous low state spectral energy distribution of 1ES 2344+514 from radio to very high energies	Aleksić J., Antonelli L. A., Antoranz P., Asensio M., Backes M., Barres de Almeida U., Barrio J. A., Bednarek W., Berger K., Bernardini E., Biland A., Blanch O., Bock R. K., Boller A., Bonnefoy S., Bonnoli G., Borla Tridon D., Bretz T., Carmona E., Carosi A., Carreto Fidalgo D., Colin P., Colombo E., Contreras J. L., Cortina J., Cossio L., Covino S., Da Vela P., Dazzi F., De Angelis A., De Caneva G., De Lotto B., Delgado Mendez C., Doert M., Domínguez A., Dominis Prester D., Dorner D., Doro M., Eisenacher D., Elsaesser D., Ferenc D., Fonseca M. V., Font L., Fruck C., García López R. J., Garczarczyk M., Garrido Terrats D., Gaug M., Giavitto G., Godinović N., González Muñoz A., Gozzini S. R., Hadamek A., Hadasch D., Herrero A., Hose J., Hrupec D., Jankowski F., Kadenius V., Klepser S., Knoetig M. L., Krähenbühl T., Krause J., Kushida J., La Barbera A., Lelas D., Leonardo E., Lewandowska N., Lindfors E., Lombardi S., López M., López-Coto R., López-Oramas A., Lorenz E., Lozano I., Makariev M., Mallot K., Maneva G., Mankuzhiyil N., Mannheim K., Maraschi L., Marcote B., Mariotti M., Martínez M., Masbou J., Mazin D., Meucci M., Miranda J. M., Mirzoyan R., Moldón J., Moralejo A., Munar-Adrover P., Nakajima D., Niedzwiecki A., Nieto D., Nilsson K., Nowak N., Orito R., Paiano S., Palatiello M., Paneque D., Paoletti R., Paredes J. M., Partini S., Persic M., Pilia M., Prada F., Prada Moroni P. G., Prandini E., Puljak I., Reichardt I., Reinthal R., Rhode W., Ribó M., Rico J., Rügamer S., Saggion A., Saito K., Saito T. Y., Salvati M., Satalecka K., Scalzotto V., Scapin V., Schultz C., Schweizer T., Shore S. N., Sillanpää A., Sitarek J., Snidaric I., Sobczynska D., Spanier F., Spiro S., Stamatescu V., Stamerra A., Steinke B., Storz J., Sun S., Surić T., Takalo L., Takami H., Tavecchio F., Temnikov P., Terzić T., Tescaro D., Teshima M., Tibolla O., Torres D. F., Toyama T., Treves A., Uellenbeck M., Vogler P., Wagner R. M., Weitzel Q., Zandanel F., Zanin R., Longo F., Lucarelli F., Pittori C., Vercellone S., Bastieri D., Sbarra C., Angelakis E., Fuhrmann L., Nestoras I., Krichbaum T. P., Sievers A., Zensus J. A., Antonyuk K. A., Baumgartner W., Berduygin A., Carini M., Cook K., Gehrels N., Kadler M., Kovalev Y. A., Kovalev Y. Y., Krauss F., Krimm H. A., Lähteenmäki A., Lister M. L., Max-Moerbeck W., Pasanen M., Pushkarev A. B., Readhead A. C. S., Richards J. L., Sainio J., Shakhovskoy D. N., Sokolovsky K. V., Tornikoski M., Tueller J., Weidinger M., Wilms J.	2013, A&A 556, A67
1785	Explaining two circumnuclear star forming rings in NGC 5248	van der Laan T. P. R., Schinnerer E., Emsellem E., Meidt S., Dumas G., Böker T., Hunt L., Haan S., Mundell C., Wozniak H.	2013, A&A 556, A98
1786	LkHα 101 at millimeter wavelengths	Thum C., Neri R., Báez-Rubio A., Krips M.	2013, A&A 556, A129
1787	Millimetre continuum observations of comet C/2009 P1 (Garradd)	Boissier J., Bockelée-Morvan D., Groussin O., Lamy P., Biver N., Crovisier J., Colom P., Moreno R., Jorda L., Piétu V.	2013, A&A 557, A88
1788	The IRAM-30 m line survey of the Horsehead PDR. III. High abundance of complex (iso-)nitrile molecules in UV-illuminated gas	Gratier P., Pety J., Guzmán V., Gerin M., Goicoechea J. R., Roueff E., Faure A.	2013, A&A 557, A101
1789	Extended rotating disks around post-AGB stars	Bujarrabal V., Alcolea J., Van Winckel H., Santander-García M., Castro-Carrizo A.	2013, A&A 557, A104
1790	ALMA observations of the Red Rectangle, a preliminary analysis	Bujarrabal V., Castro-Carrizo A., Alcolea J., Van Winckel H., Sánchez Contreras C., Santander-García M., Neri R., Lucas R.	2013, A&A 557, L11
1791	High resolution mapping of CO(1-0) in NGC 6240	Feruglio C., Fiore F., Piconcelli E., Cicone C., Maiolino R., Davies R., Sturm E.	2013, A&A 558, A87
1792	Probing the jet base of the blazar PKS 1830-211 from the chromatic variability of its lensed images. Serendipitous ALMA observations of a strong gamma-ray flare	Martí-Vidal I., Muller S., Combes F., Aalto S., Beelen A., Darling J., Guélin M., Henkel C., Horellou C., Marcaide J. M., Martín S., Menten K. M., V-Trung D., Zwaan M.	2013, A&A 558, A123
1793	ALMA observations of feeding and feedback in nearby Seyfert galaxies: an AGN-driven outflow in NGC 1433	Combes F., García-Burillo S., Casasola V., Hunt L., Krips M., Baker A. J., Boone F., Eckart A., Marquez I., Neri R., Schinnerer E., Tacconi L. J.	2013, A&A 558, A124
1794	Large scale IRAM 30 m CO-observations in the giant molecular cloud complex W43	Carlhoff P., Nguyen Luong Q., Schilke P., Motte F., Schneider N., Beuther H., Bontemps S., Heitsch F., Hill T., Kramer C., Ossenkopf V., Schuller F., Simon R., Wyrowski F.	2013, A&A 560, A24
1795	The IRAM-30 m line survey of the Horsehead PDR. IV. Comparative chemistry of H_2CO and CH_3OH	Guzmán V. V., Goicoechea J. R., Pety J., Gratier P., Gerin M., Roueff E., Le Petit F., Le Bourlot J., Faure A.	2013, A&A 560, A73
1796	Near-infrared long-slit spectra of Seyfert galaxies: gas excitation across the central kiloparsec	van der Laan T. P. R., Schinnerer E., Böker T., Armus L.	2013, A&A 560, A99
1797	Detection of circumstellar nitric oxide. Enhanced nitrogen abundance in IRC +10420	Quintana-Lacaci G., Agúndez M., Cernicharo J., Bujarrabal V., Sánchez Contreras C., Castro-Carrizo A., Alcolea J.	2013, A&A 560, L2 0
1798	HerMES: Candidate Gravitationally Lensed Galaxies and Lensing Statistics at Submillimeter Wavelengths	Wardlow J. L., Cooray A., De Bernardis F., Amblard A., Arumugam V., Aussel H., Baker A. J., Béthermin M., Blundell R., Bock J., Boselli A., Bridge C., Buat V., Burgarella D., Bussmann R. S., Cabrera-Lavers A., Calanog J., Carpenter J. M., Casey C. M., Castro-Rodríguez N., Cava A., Chanial P., Chapin E., Chapman S. C., Clements D. L., Conley A., Cox P., Dowell C. D., Dye S., Eales S., Farrah D., Ferrero P., Franceschini A., Frayer D. T., Frazer C., Fu H., Gavazzi R., Glenn J., González Solares E. A., Griffin M., Gurwell M. A., Harris A. I., Hatziminaoglou E., Hopwood R., Hyde A., Ibar E., Ivison R. J., Kim S., Lagache G., Levenson L., Marchetti L., Marsden G., Martinez-Navajas P., Negrello M., Neri R., Nguyen H. T., O'Halloran B., Oliver S. J., Omont A., Page M. J., Panuzzo P., Papageorgiou A., Pearson C. P., Pérez-Fournon I., Pohlen M., Riechers D., Rigopoulou D., Roseboom I. G., Rowan-Robinson M., Schulz B., Scott D., Scoville N., Seymour N., Shupe D. L., Smith A. J., Streblyanska A., Strom A., Symeonidis M., Trichas M., Vaccari M., Vieira J. D., Viero M., Wang L., Xu C. K., Yan L., Zemcov M.	2013, ApJ 762, 59 25
1799	Evidence for CO Shock Excitation in NGC 6240 from Herschel SPIRE Spectroscopy	Meijerink R., Kristensen L. E., Weiß A., van der Werf P. P., Walter F., Spaans M., Loenen A. F., Fischer J., Israel F. P., Isaak K., Papadopoulos P. P., Aalto S., Armus L., Charmandaris V., Dasyra K. M., Diaz-Santos T., Evans A., Gao Y., González-Alfonso E., Güsten R., Henkel C., Kramer C., Lord S., Martín-Pintado J., Naylor D., Sanders D. B., Smith H., Spinoglio L., Stacey G., Veilleux S., Wiedner M. C.	2013, ApJ 762, L16
1800	Illuminating the Darkest Gamma-Ray Bursts with Radio Observations	Zauderer B. A., Berger E., Margutti R., Levan A. J., Olivares E. F., Perley D. A., Fong W., Horesh A., Updike A. C., Greiner J., Tanvir N. R., Laskar T., Chornock R., Soderberg A. M., Menten K. M., Nakar E., Carpenter J., Chandra P., Castro-Tirado A. J., Bremer M., Gorosabel J., Guziy S., Pérez-Ramírez D., Winters J. M.	2013, ApJ 767, 161

1801	A Redline Starburst: CO(2-1) Observations of an Eddington-limited Galaxy Reveal Star Formation at Its Most Extreme	Geach J. E., Hickox R. C., Diamond-Stanic A. M., Krips M., Moustakas J., Tremonti C. A., Coil A. L., Sell P. H., Rudnick G. H.	2013, ApJ 767, L17
1802	Phibss: Molecular Gas Content and Scaling Relations in z ~ 1-3 Massive, Main-sequence Star-forming Galaxies	Tacconi L. J., Neri R., Genzel R., Combes F., Bolatto A., Cooper M. C., Wuyts S., Bournaud F., Burkert A., Comerford J., Cox P., Davis M., Förster Schreiber N. M., García-Burillo S., Gracia-Carpio J., Lutz D., Naab T., Newman S., Omont A., Saintonge A., Shapiro Griffin K., Shapley A., Sternberg A., Weiner B.	2013, ApJ 768, 74
1803	An ALMA Survey of Submillimeter Galaxies in the Extended Chandra Deep Field South: Source Catalog and Multiplicity	Hodge J. A., Karim A., Smail I., Swinbank A. M., Walter F., Biggs A. D., Ivison R. J., Weiss A., Alexander D. M., Bertoldi F., Brandt W. N., Chapman S. C., Coppin K. E. K., Cox P., Danielson A. L. R., Dannerbauer H., De Breuck C., Decarli R., Edge A. C., Greve T. R., Knudsen K. K., Menten K. M., Rix H.-W., Schinnerer E., Simpson J. M., Wardlow J. L., van der Werf P.	2013, ApJ 768, 91
1804	Fueling Active Galactic Nuclei. I. How the Global Characteristics of the Central Kiloparsec of Seyferts Differ from Quiescent Galaxies	Hicks E. K. S., Davies R. I., Maciejewski W., Emsellem E., Malkan M. A., Dumas G., Müller-Sánchez F., Rivers A.	2013, ApJ 768, 107
1805	Water Deuterium Fractionation in the Inner Regions of Two Solar-type Protostars	Taquet V., López-Sepulcre A., Ceccarelli C., Neri R., Kahane C., Coutens A., Vastel C.	2013, ApJ 768, L29
1806	Clumping and the Interpretation of kpc-scale Maps of the Interstellar Medium: Smooth H I and Clumpy, Variable H_2 Surface Density	Leroy A. K., Lee C., Schruba A., Bolatto A., Hughes A., Pety J., Sandstrom K., Schinnerer E., Walter F.	2013, ApJ 769, L12
1807	CO J = 1-0 and J = 2-1 Line Observations of the Molecular-cloud-blocked Supernova Remnant 3C434.1	Jeong I.-G., Koo B.-C., Cho W.-K., Kramer C., Stutzki J., Byun D.-Y.	2013, ApJ 770, 105
1808	ALMA Follows Streaming of Dense Gas Down to 40 pc from the Supermassive Black Hole in NGC 1097	Fathi K., Lundgren A. A., Kohno K., Piñol-Ferrer N., Martín S., Espada D., Hatziminaoglou E., Imanishi M., Izumi T., Krips M., Matsushita S., Meier D. S., Nakai N., Sheth K., Turner J., van de Ven G., Wiklind T.	2013, ApJ 770, L27
1809	Water Vapor in nearby Infrared Galaxies as Probed by Herschel	Yang C., Gao Y., Omont A., Liu D., Isaak K. G., Downes D., van der Werf P. P., Lu N.	2013, ApJ 771, L24
1810	Herschel-ATLAS: A Binary HyLIRG Pinpointing a Cluster of Starbursting Protoellipticals	Ivison R. J., Swinbank A. M., Smail I., Harris A. I., Bussmann R. S., Cooray A., Cox P., Fu H., Kovács A., Krips M., Narayanan D., Negrello M., Neri R., Peñarrubia J., Richard J., Riechers D. A., Rowlands K., Staguhn J. G., Targett T. A., Amber S., Baker A. J., Bourne N., Bertoldi F., Bremer M., Calanog J. A., Clements D. L., Dannerbauer H., Dariush A., De Zotti G., Dunne L., Eales S. A., Farrah D., Fleuren S., Franceschini A., Geach J. E., George R. D., Helly J. C., Hopwood R., Ibar E., Jarvis M. J., Kneib J.-P., Maddox S., Omont A., Scott D., Serjeant S., Smith M. W. L., Thompson M. A., Valiante E., Valtchanov I., Vieira J., van der Werf P.	2013, ApJ 772, 137
1811	Star Formation and Gas Kinematics of Quasar Host Galaxies at z ~ 6: New Insights from ALMA	Wang R., Wagg J., Carilli C. L., Walter F., Lentati L., Fan X., Riechers D. A., Bertoldi F., Narayanan D., Strauss M. A., Cox P., Omont A., Menten K. M., Knudsen K. K., Neri R., Jiang L.	2013, ApJ 773, 44
1812	Phibss: Molecular Gas, Extinction, Star Formation, and Kinematics in the z = 1.5 Star-forming Galaxy EGS13011166	Genzel R., Tacconi L. J., Kurk J., Wuyts S., Combes F., Freundlich J., Bolatto A., Cooper M. C., Neri R., Nordon R., Bournaud F., Burkert A., Comerford J., Cox P., Davis M., Förster Schreiber N. M., García-Burillo S., Gracia-Carpio J., Lutz D., Naab T., Newman S., Saintonge A., Shapiro Griffin K., Shapley A., Sternberg A., Weiner B.	2013, ApJ 773, 68
1813	A Tight Connection between Gamma-Ray Outbursts and Parsec-scale Jet Activity in the Quasar 3C 454.3	Jorstad S. G., Marscher A. P., Smith P. S., Larionov V. M., Agudo I., Gurwell M., Wehrle A. E., Lähteenmäki A., Nikolashvili M. G., Schmidt G. D., Arkharov A. A., Blinov D. A., Blumenthal K., Casadio C., Chigladze R. A., Efimova N. V., Eggen J. R., Gómez J. L., Grupe D., Hagen-Thorn V. A., Joshi M., Kimeridze G. N., Konstantinova T. S., Kopatskaya E. N., Kurtanidze O. M., Kurtanidze S. O., Larionova E. G., Larionova L. V., Sigua L. A., MacDonald N. R., Maune J. D., McHardy I. M., Miller H. R., Molina S. N., Morozova D. A., Scott T., Taylor B. W., Tornikoski M., Troitsky I. S., Thum C., Walker G., Williamson K. E., Sallum S., Consiglio S., Strelnitski V.	2013, ApJ 773, 147
1814	Low-velocity Shocks Traced by Extended SiO Emission along the W43 Ridges: Witnessing the Formation of Young Massive Clusters	Nguyen-Lu'o'ng Q., Motte F., Carlhoff P., Louvet F., Lesaffre P., Schilke P., Hill T., Hennemann M., Gusdorf A., Didelon P., Schneider N., Bontemps S., Duarte-Cabral A., Menten K. M., Martin P. G., Wyrowski F., Bendo G., Roussel H., Bernard J.-P., Bronfman L., Henning T., Kramer C., Heitsch F.	2013, ApJ 775, 88
1815	Laboratory and Astronomical Discovery of HydroMagnesium Isocyanide	Cabezas C., Cernicharo J., Alonso J. L., Agúndez M., Mata S., Guélin M., Peña I.	2013, ApJ 775, 133
1816	The CO-to-H_2 Conversion Factor and Dust-to-gas Ratio on Kiloparsec Scales in Nearby Galaxies	Sandstrom K. M., Leroy A. K., Walter F., Bolatto A. D., Croxall K. V., Draine B. T., Wilson C. D., Wolfire M., Calzetti D., Kennicutt R. C., Aniano G., Donovan Meyer J., Usero A., Bigiel F., Brinks E., de Blok W. J. G., Crocker A., Dale D., Engelbracht C. W., Galametz M., Groves B., Hunt L. K., Koda J., Kreckel K., Linz H., Meidt S., Pellegrini E., Rix H.-W., Roussel H., Schinnerer E., Schruba A., Schuster K.-F., Skibba R., van der Laan T., Appleton P., Armus L., Brandl B., Gordon K., Hinz J., Krause O., Montiel E., Sauvage M., Schmiedeke A., Smith J. D. T., Vigroux L.	2013, ApJ 777, 5
1817	Luminous Infrared Galaxies with the Submillimeter Array. IV. ^{12}CO J = 6-5 Observations of VV 114	Sliwa K., Wilson C. D., Krips M., Petitpas G. R., Iono D., Juvela M., Matsushita S., Peck A., Yun M.	2013, ApJ 777, 126
1818	Unveiling the Dust Nucleation Zone of IRC+10216 with ALMA	Cernicharo J., Daniel F., Castro-Carrizo A., Agundez M., Marcelino N., Joblin C., Goicoechea J. R., Guélin M.	2013, ApJ 778, L25
1819	Gravitational Lens Models Based on Submillimeter Array Imaging of Herschel-selected Strongly Lensed Sub-millimeter Galaxies at $z > 1.5$	Bussmann R. S., Pérez-Fournon I., Amber S., Calanog J., Gurwell M. A., Dannerbauer H., De Bernardis F., Fu H., Harris A. I., Krips M., Lapi A., Maiolino R., Omont A., Riechers D., Wardlow J., Baker A. J., Birkinshaw M., Bock J., Bourne N., Clements D. L., Cooray A., De Zotti G., Dunne L., Dye S., Eales S., Farrah D., Gavazzi R., González Nuevo J., Hopwood R., Ibar E., Ivison R. J., Laporte N., Maddox S., Martínez-Navajas P., Michalowski M., Negrello M., Oliver S. J., Roseboom I. G., Scott D., Serjeant S., Smith A. J., Smith M., Streblyanska A., Valiante E., van der Werf P., Verma A., Vieira J. D., Wang L., Wilner D.	2013, ApJ 779, 25

1820	The PdBI Arcsecond Whirlpool Survey (PAWS). I. A Cloud-scale/Multi-wavelength View of the Interstellar Medium in a Grand-design Spiral Galaxy	Schinnerer E., Meidt S. E., Pety J., Hughes A., Colombo D., García-Burillo S., Schuster K. F., Dumas G., Dobbs C. L., Leroy A. K., Kramer C., Thompson T. A., Regan M. W.	2013, ApJ 779, 42
1821	The Plateau de Bure + 30m Arcsecond Whirlpool Survey Reveals a Thick Disk of Diffuse Molecular Gas in the M51 Galaxy	Pety J., Schinnerer E., Leroy A. K., Hughes A., Meidt S. E., Colombo D., Dumas G., García-Burillo S., Schuster K. F., Kramer C., Dobbs C. L., Thompson T. A.	2013, ApJ 779, 43
1822	Probability Distribution Functions of ^{12}CO (J=1->2) Brightness and Integrated Intensity in M51: The PAWS View	Hughes A., Meidt S. E., Schinnerer E., Colombo D., Pety J., Leroy A. K., Dobbs C. L., García-Burillo S., Thompson T. A., Dumas G., Schuster K. F., Kramer C.	2013, ApJ 779, 44
1823	Gas Kinematics on Giant Molecular Cloud Scales in M51 with PAWS: Cloud Stabilization through Dynamical Pressure	Meidt S. E., Schinnerer E., García-Burillo S., Hughes A., Colombo D., Pety J., Dobbs C. L., Schuster K. F., Kramer C., Leroy A. K., Dumas G., Thompson T. A.	2013, ApJ 779, 45
1824	A Comparative Study of Giant Molecular Clouds in M51, M33, and the Large Magellanic Cloud	Hughes A., Meidt S. E., Colombo D., Schinnerer E., Pety J., Leroy A. K., Dobbs C. L., García-Burillo S., Thompson T. A., Dumas G., Schuster K. F., Kramer C.	2013, ApJ 779, 46
1825	Suzaku reveals X-ray continuum piercing the nuclear absorber in Markarian 231	Piconcelli E., Miniutti G., Ranalli P., Feruglio C., Fiore F., Maiolino R.	2013, MNRAS 428, 1185
1826	Radio and γ-ray follow-up of the exceptionally high-activity state of PKS 1510-089 in 2011	Orienti M., Koyama S., D'Ammando F., Giroletti M., Kino M., Nagai H., Venturi T., Dallacasa D., Giovannini G., Angelakis E., Fuhrmann L., Hovatta T., Max-Moerbeck W., Schinzel F. K., Akiyama K., Hada K., Honma M., Niinuma K., Gasparrini D., Krichbaum T. P., Nestoras I., Readhead A. C. S., Richards J. L., Riquelme D., Sievers A., Ungerechts H., Zensus J. A.	2013, MNRAS 428, 2418
1827	A survey of molecular gas in luminous sub-millimetre galaxies	Bothwell M. S., Smail I., Chapman S. C., Genzel R., Ivison R. J., Tacconi L. J., Alaghband-Zadeh S., Bertoldi F., Blain A. W., Casey C. M., Cox P., Greve T. R., Lutz D., Neri R., Omont A., Swinbank A. M.	2013, MNRAS 429, 3047
1828	Variations in the fundamental constants in the QSO host J1148+5251 at z = 6.4 and the BR1202-0725 system at z = 4.7	Lentati L., Carilli C., Alexander P., Maiolino R., Wang R., Cox P., Downes D., McMahon R., Menten K. M., Neri R., Riechers D., Wagg J., Walter F., Wolfe A.	2013, MNRAS 430, 2454
1829	Probing dust settling in proto-planetary discs with ALMA	Boehler Y., Dutrey A., Guilloteau S., Piétu V.	2013, MNRAS 431, 1573
1830	H-ATLAS: estimating redshifts of Herschel sources from sub-mm fluxes	Pearson E. A., Eales S., Dunne L., Gonzalez-Nuevo J., Maddox S., Aguirre J. E., Baes M., Baker A. J., Bourne N., Bradford C. M., Clark C. J. R., Cooray A., Dariush A., Zotti G. D., Dye S., Frayer D., Gomez H. L., Harris A. I., Hopwood R., Ibar E., Ivison R. J., Jarvis M., Krips M., Lapi A., Lupu R. E., MichaŃowski M. J., Rosenman M., Scott D., Valiante E., Valtchanov I., Werf P. v. d., Vieira J. D.	2013, MNRAS 435, 2753
1831	The B1 shock in the L1157 outflow as seen at high spatial resolution	Benedettini M., Viti S., Codella C., Gueth F., Gómez-Ruiz A. I., Bachiller R., Beltrán M. T., Busquet G., Ceccarelli C., Lefloch B.	2013, MNRAS 436, 179
1832	Far-infrared spectroscopy of a lensed starburst: a blind redshift from Herschel	George R. D., Ivison R. J., Hopwood R., Riechers D. A., Bussmann R. S., Cox P., Dye S., Krips M., Negrello M., Neri R., Serjeant S., Valtchanov I., Baes M., Bourne N., Clements D. L., De Zotti G., Dunne L., Eales S. A., Ibar E., Maddox S., Smith M. W. L., Valiante E., van der Werf P.	2013, MNRAS 436, L99
1833	The awakening of BL Lacertae: observations by Fermi, Swift and the GASP-WEBT	Raiteri C. M., Villata M., D'Ammando F., Larionov V. M., Gurwell M. A., Mirzaqulov D. O., Smith P. S., Acosta-Pulido J. A., Agudo I., Arévalo M. J., Bachev R., Benítez E., Berdyugin A., Blinov D. A., Borman G. A., Böttcher M., Bozhilov V., Carnerero M. I., Carosati D., Casadio C., Chen W. P., Doroshenko V. T., Efimov Y. S., Efimova N. V., Ehgamberdiev S. A., Gómez J. L., González-Morales P. A., Hiriart D., Ibryamov S., Jadhav Y., Jorstad S. G., Joshi M., Kadenius V., Klimanov S. A., Kohli M., Konstantinova T. S., Kopatskaya E. N., Koptelova E., Kimeridze G., Kurtanidze O. M., Larionova E. G., Larionova L. V., Ligustri R., Lindfors E., Marscher A. P., McBreen B., McHardy I. M., Metodieva Y., Molina S. N., Morozova D. A., Nazarov S. V., Nikolashvili M. G., Nilsson K., Okhmat D. N., Ovcharov E., Panwar N., Pasanen M., Peneva S., Phipps J., Pulatova N. G., Reinthal R., Ros J. A., Sadun A. C., Schwartz R. D., Semkov E., Sergeev S. G., Sigua L. A., Sillanpää A., Smith N., Stoyanov K., Strigachev A., Takalo L. O., Taylor B., Thum C., Troitsky I. S., Valcheva A., Wehrle A. E., Wiesemeyer H.	2013, MNRAS 436, 1530
1834	^{13}CO and C^{18}O emission from a dense gas disc at z = 2.3: abundance variations, cosmic rays and the initial conditions for star formation	Danielson A. L. R., Swinbank A. M., Smail I., Bayet E., van der Werf P. P., Cox P., Edge A. C., Henkel C., Ivison R. J.	2013, MNRAS 436, 2793
1835	A dust-obscured massive maximum-starburst galaxy at a redshift of 6.34	Riechers D. A., Bradford C. M., Clements D. L., Dowell C. D., Pérez-Fournon I., Ivison R. J., Bridge C., Conley A., Fu H., Vieira J. D., Wardlow J., Calanog J., Cooray A., Hurley P., Neri R., Kamenetzky J., Aguirre J. E., Altieri B., Arumugam V., Benford D. J., Béthermin M., Bock J., Burgarella D., Cabrera-Lavers A., Chapman S. C., Cox P., Dunlop J. S., Earle L., Farrah D., Ferrero P., Franceschini A., Gavazzi R., Glenn J., Solares E. A. G., Gurwell M. A., Halpern M., Hatziminaoglou E., Hyde A., Ibar E., Kovács A., Krips M., Lupu R. E., Maloney P. R., Martinez-Navajas P., Matsuhara H., Murphy E. J., Naylor B. J., Nguyen H. T., Oliver S. J., Omont A., Page M. J., Petitpas G., Rangwala N., Roseboom I. G., Scott D., Smith A. J., Staguhn J. G., Streblyanska A., Thomson A. P., Valtchanov I., Viero M., Wang L., Zemcov M., Zmuidzinas J.	2013, Nature 496, 329
1836	The rapid assembly of an elliptical galaxy of 400 billion solar masses at a redshift of 2.3	Fu H., Cooray A., Feruglio C., Ivison R. J., Riechers D. A., Gurwell M., Bussmann R. S., Harris A. I., Altieri B., Aussel H., Baker A. J., Bock J., Boylan-Kolchin M., Bridge C., Calanog J. A., Casey C. M., Cava A., Chapman S. C., Clements D. L., Conley A., Cox P., Farrah D., Frayer D., Hopwood R., Jia J., Magdis G., Marsden G., Martínez-Navajas P., Negrello M., Neri R., Oliver S. J., Omont A., Page M. J., Pérez-Fournon I., Schulz B., Scott D., Smith A., Vaccari M., Valtchanov I., Vieira J. D., Viero M., Wang L., Wardlow J. L., Zemcov M.	2013, Nature 498, 338
1837	Results of the IRAM M33 Large Program	Braine J., Schuster K., Gratier P., Druard C.	2013, IAU Symp. 292, 135
1838	An Updated View of Giant Molecular Clouds, Gas Flows and Star Formation in M51 with PAWS	Meidt S. E., Schinnerer E., Hughes A., Colombo D., Pety J., Garcia-Burillo S., Leroy A., Dobbs C. L., Schuster K. F., Kramer C., Dumas G., Thompson T.	2013, IAU Symp. 292, 139

1839	Star Formation in Quasar Host Galaxies at Redshift 6: Millimeter Surveys and New Insights from ALMA	Wang R., Wagg J., Carilli C. L., Walter F., Fan X., Bertoldi F., Riechers D. A., Omont A., Menten K. M., Cox P., Strauss M. A., Narayanan D.	2013, IAU Symp. 292, 184
1840	AGN feedback on the ISM of 3C 236	Labiano A., García-Burillo S., Combes F., Usero A., Soria-Ruiz R., Tremblay G., Neri R., Fuente A., Morganti R., Oosterloo T.	2013, IAU Symp. 292, 374
1841	Feedback Mechanisms of Starbursts and AGNs through Molecular Outflows	Matsushita S., Krips M., Lim J., Muller S., Tsai A.-L.	2013, ASPC 476, 283
1842	Latest NIKA Results and the NIKA-2 Project	Monfardini A., Adam R., Adane A., Ade P., André P., Beelen A., Belier B., Benoit A., Bideaud A., Billot N., Bourrion O., Calvo M., Catalano A., Coiffard G., Comis B., D'Addabbo A., Désert F.-X., Doyle S., Goupy J., Kramer C., Leclercq S., Macias-Perez J., Martino J., Mauskopf P., Mayet F., Pajot F., Pascale E., Ponthieu N., Revéret V., Rodriguez L., Savini G., Schuster K., Sievers A., Tucker C., Zylka R.	2013, Journal of Low Temperature Physics 153
1843	The Herschel PACS photometer calibration. A time dependent flux calibration for the PACS chopped point-source photometry AOT mode	Nielbock M., Müller T., Klaas U., Altieri B., Balog Z., Billot N., Linz H., Okumura K., Sánchez-Portal M., Sauvage M.	2013, Experimental Astronomy 36, 631
1844	Probing Dust Settling in Proto-planetary Disks with ALMA	Boehler Y., Dutrey A., Guilloteau S., Piétu V.	2013, EPJ Web of Conferences 46, 2002
1845	The first two years in the lifetime of the newly born jet associated to Sw J1644+57	Castro-Tirado A. J., Gómez J. L., Agudo I., Guerrero M. A., Bremer M., Winters J. M., Gorosabel J., Sánchez-Ramírez R., Guziy S., Jelinek M., Tello J. C., Pérez-Ramírez D., Reyes-Iturbide J., Park I. H., Jeong S., Bach U., Kraussh A., Krichbaumh T. P., Pozanenko A. S.	2013, EPJ Web of Conferences 61, 1003
1846	The Gamma-ray Activity of the high-*z* Quasar 0836+71	Jorstad S., Marscher A., Larionov V., Gómez J. L., Agudo I., Angelakis E., Casadio C., Gurwell M., Hovatta T., Joshi M., Fuhrmann L., Karamanavis V., Lähteenmäki A., Molina S., Morozova D., Myserlis I., Troitsky I., Ungerechts H., Zensus J. A.	2013, EPJ Web of Conferences 61, 4003
1847	Detection of the tSZ effect with the NIKA camera	Comis B., Adam R., Adane A., Ade P., André P., Beelen A., Belier B., Benoît A., Bideaud A., Billot N., Bourrion O., Calvo M., Catalano A., Coiffard G., D'Addabbo A., Désert F.-X., Doyle S., Goupy J., Kramer C., Leclercq S., Macías-Pérez J. F., Martino J., Mauskopf P., Mayet F., Monfardini A., Pajot F., Pascale E., Pointecouteau E., Ponthieu N., Revéret V., Rodriguez L., Savini G., Schuster K., Sievers A., Tucker C., Zylka R.	2013, SF2A conf. 331
1848	Star formation efficiency at high z and subgalactic scales	Freundlich J., Combes F., Tacconi L. J., Cooper M. C., Genzel R., Neri R.	2013, SF2A conf. 343
1849	The M33 CO(2-1) survey - Star formation and molecular clouds formation	Druard C., Braine J., Schuster K. F.	2013, SF2A conf. 537
1850	Submillimeter ALMA Observations of the Dense Gas in the Low-Luminosity Type-1 Active Nucleus of NGC 1097	Izumi T., Kohno K., Martín S., Espada D., Harada N., Matsushita S., Hsieh P.-Y., Turner J. L., Meier D. S., Schinnerer E., Imanishi M., Tamura Y., Curran M. T., Doi A., Fathi K., Krips M., Lundgren A. A., Nakai N., Nakajima T., Regan M. W., Sheth K., Takano S., Taniguchi A., Terashima Y., Tosaki T., Wiklind T.	2013, PASJ 65, 100
1851	Determination of the Ortho to Para Ratio of H_3Cl^+ and H_2O^+ from Submillimeter Observations	Gerin M., de Luca M., Lis D. C., Kramer C., Navarro S., Neufeld D., Indriolo N., Godard B., Le Petit F., Peng R., Phillips T. G., Roueff E.	2013, The Journal of Phys. Chemistry A 117, 10018
1852	Molecular Line Observations of Protoplanetary Disks	Chapillon E., Dutrey A., Henning T., Guilloteau S., Wakelam V., Hersant F., Gueth F., Piétu V., Ohashi N., Boehler Y., Launhardt R., Semenov D., Schreyer K., Guélin M., Parise B.	2013, Protostars and Planets VI, 23
1853	Study of deuterated molecules in the PDR around the UC HII region Mon R2	Treviño-Morales S. P., Fuente A., Pilleri P., Kramer C., González-García M., Roueff E., Cernicharo J., Pety J.	2013, Protostars and Planets VI, 24
1854	The circumstellar disk of AB Aurigae: evidence for envelope accretion at late stages of star formation?	Tang Y.-W., Guilloteau S., Pietu V., Dutrey A., Ohashi N., Ho P. T. P.	2013, Protostars and Planets VI, 27
1855	High-velocity clumps in the L1157 outflow	Benedettini M., Viti S., Codella C., Gueth F., Gomez-Ruiz A., Bachiller R., Beltran M., Busquet G., Ceccarelli C., Lefloch B.	2013, Protostars and Planets VI, 56
1856	Imaging Techniques in Millimetre Astronomy	Bremer M.	2013, EAS 59, 189
1857	Dust-forming molecules in VY Canis Majoris (and Betelgeuse)	Kamiński T., Gottlieb C. A., Schmidt M. R., Patel N. A., Young K. H., Menten K. M., Brünken S., Müller H. S. P., Winters J. M., McCarthy M. C.	2013, EAS 60, 191
1858	Millimetre Observations of Gamma-ray Bursts at IRAM	Castro-Tirado A. J., Bremer M., Winters J. M., Tello J. C., Pandey S. B., de Ugarte Postigo A., Gorosabel J., Guziy S., Jelinek M., Sánchez-Ramírez R., Pérez-Ramírez D., Castro Cerón J. M.	2013, EAS 61, 279
1859	Radio Interferometric Detection of TiO and TiO_2 in VY Canis Majoris: "seeds" of Inorganic Dust Formation	Brunken S., Muller H. S. P., Kaminski T., Menten K. M., Gott-Lieb C. A., Patel N. A., Young K. H., McCarthy M. C., Winters J. M., Decin L.	2013, Internat. Symp. On Molecular Spectroscopy, Abstr. #ERF02
1860	The first two months in the lifetime of the newly born jet associated to Swift J1644+57	Castro-Tirado A. J., Gómez J. L., Agudo I., Guerrero M. A., Bremer M., Winters J. M., Gorosabel J., Guziy S., de Ugarte Postigo A., Jelínek M., Tello J. C., Sánchez-Ramírez R., Pérez-Ramírez D., Reyes-Iturbide J., Park I. H., Jeong S., Pozanenko A. S., Acosta-Pulido J.	2013, Revista Mexicana de Astron. Y Astrofísica 42, 36
1861	The first months in the lifetime of the newly born jet associated to Swift J1644+57	Castro-Tirado A. J., Gómez J. L., Agudo I., Guerrero M. A., Bremer M., Winters J. M., Gorosabel J., Sánchez-Ramírez R., Guziy S., Jelinek M., Tello J. C., Pérez-Ramírez D., Reyes-Iturbide J., Park I. H., Jeong S., Pozanenko A. S.	2013, Highlights of Spanish Astron. VII, 185
1862	MOPSIC: Extended Version of MOPSI	Zylka R.	2013, Astrophysics Source Code Library, 3011
1863	GILDAS: Grenoble Image and Line Data Analysis Software	Gildas Team	2013, Astrophysics Source Code Library, 5010
1864	Modeling and Measuring the Optical Coupling of Lumped Element Kinetic Inductance Detectors at 120-180 GHz	Roesch M. J., Mattiocco F., Scherer T. A., Siegel M., Schuster K.-F.	2013, IEEE Trans. On Antennas and Propagation 61, 1939

1865	The latest results from the global mm VLBI array	Hodgson J., Krichbaum T. P., Marscher A., Jorstad S., Marti-Vidal I., Bremer M., Lindqvist M., de Vicente P., Zensus A. J.	2013, 11th EVN Symp., Proc. of Science (POS), 096
1866	IRAM-30m Molecular Submm Surveys of Two Very Different Comets: C/2011 L4 (PanSTARRS) and C/2012 F6 (Lemmon)	Biver N., Debout V., Bockelée-Morvan D., Crovisier J., Colom P., Moreno R., Boissier J., Paubert G., Lis D. C., Hartogh P., Dello-Russo N., Vervack R., Weaver H. A.	2013, AAS DPS meeting 45, #502.03
1867	Plateau de Bure Arcsecond Whirlpool Survey (PAWS): Multiscale Analysis of the ISM in the Whirlpool Galaxy	Pardy S., Leroy A. K., Schinnerer E., Pety J., Colombo D., PdBI Arcsecond Whirlpool Survey (PAWS) Collaboration	2013, AAS 221, #146.20
1868	Studies of the Interstellar Medium in z > 5 Star-Forming Galaxies Through the 158 Micron [CII] Line	Riechers D. A., Carilli C. L., Capak P. L., Scoville N., Schinnerer E., Bertoldi F., Smolcic V., Cox P., Yun M.	2013, AAS 221, #150.01
1869	[C II] Line Emission and Star Formation from Quasar Host Galaxies at 6	Wang R., Carilli C. L., Walter F., Fan X., Wagg J., Riechers D. A., Bertoldi F., Omont A., Cox P., Strauss M. A., Menten K., Narayanan D. T., Knudsen K., Jiang L.	2013, AAS 221, #221.04
1870	The PdBI Arcsecond Whirlpool Survey (PAWS) I. Molecular Gas, Dust and Star Formation	Schinnerer E., Meidt S. E., Pety J., Hughes A., Leroy A. K., Colombo D., Dumas G., Dobbs C. L., Garcia Burillo S., Thompson T. A., Schuster K. F., Kramer C.	2013, AAS 221, #349.15
1871	The PdBI Arcsecond Whirlpool Survey (PAWS) II. Resolved properties of Giant Molecular Clouds in M51 and Local Group galaxies	Colombo D., Schinnerer E., Hughes A., Meidt S. E., Leroy A. K., Pety J., Dobbs C., Garcia Burillo S., Dumas G., Thompson T. A., Schuster K. F., Kramer C.	2013, AAS 221, #349.16
1872	The PdBI Arcsecond Whirlpool Survey (PAWS) III. How Dynamical Environments Regulate the Structure of the Molecular Gas and Star Formation in M51	Meidt S., Schinnerer E., Hughes A., Garcia Burillo S., Colombo D., Pety J., Leroy A. K., Dobbs C., Dumas G., Schuster K. F., Thompson T. A., Kramer C.	2013, AAS 221, #349.17
1873	GRB 130518A: mm detection at PdBI.	Castro-Tirado A. J., Bremer M., Winters J.-M.	2013, GCN 14689, 1
1874	GRB 130925A/Sw J0244-2609: mm observations at PdBI.	Castro-Tirado A. J., Bremer M., Winters J.-M.	2013, GCN 15299, 1

Annex III – Committee Members

EXECUTIVE COUNCIL

R. Bachiller, OAN-IGN, Spain
A. Barcia Cancio, CAY, Spain
R. Genzel, MPE, Germany
J. Gomez-Gonzalez, IGN, Spain
S. Guilloteau, CNRS, France
K. Menten, MPIfR, Germany
D. Mourard, CNRS-INSU, France
J.L. Puget, IAS, France
M. Schleier, MPG, Germany

SCIENTIFIC ADVISORY COMMITTEE

Ph. André, CEA, France
L. Tacconi, MPE, Germany
F. Boulanger, IAS, France
M. Tafalla, OAN-IGN, Spain
D. Jaffe, University of Texas, USA
R. Moreno, LESIA, France
P. de Vicente, OAN-IGN, Spain
A. Weiss, MPIfR, Germany
F. Wyrowski, MPIfR, Germany

PROGRAM COMMITTEE

H. Beuther, MPIA, Germany
S. Garcia-Burillo, OAN-IGN, Spain
A. Blain, University of Leicester, UK
J. Goicoechea, CSIC/INTA, Spain
S. Bontemps, Obs. Bordeaux, France
C. Henkel, MPIfR, Germany
V. Bujarrabal, OAN-IGN, Spain
C. Codella, INAF, Italy
E. Sturm, MPE, Germany
R. Dave, Univ. of Western Cape, South Africa
H. Dole, IAS, France
A. Usero, OAN, Spain
R. Davies, MPE, Germany
C. Vastel, IRAP, France

AUDIT COMMISSION

B. Adans, CNRS, France
A. Keil, MPG, Germany
G. Maar, MPG, Germany

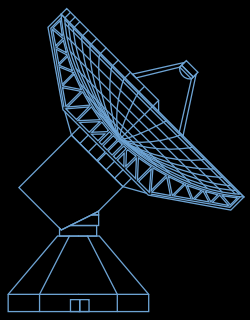

30-meter diameter telescope, Pico Veleta

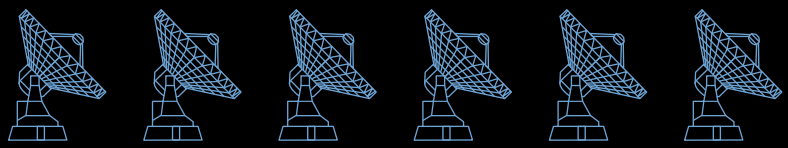

6 x 15-meter interferometer, Plateau de Bure

The Institut de Radioastronomie Millimétrique (IRAM) is a multi-national scientific institute covering all aspects of radio astronomy at millimeter wavelengths: the operation of two high-altitude observatories – a 30-meter diameter telescope on Pico Veleta in the Sierra Nevada (southern Spain), and an interferometer of six 15 meter diameter telescopes on the Plateau de Bure in the French Alps – the development of telescopes and instrumentation, radio astronomical observations and their interpretation. NOEMA will transform the Plateau de Bure observatory by doubling its number of antennas, making it the most powerful millimeter radiotelescope of the Northern Hemisphere.

IRAM was founded in 1979 by two national research organizations: the CNRS and the Max-Planck-Gesellschaft – the Spanish Instituto Geográfico Nacional, initially an associate member, became a full member in 1990.

The technical and scientific staff of IRAM develops instrumentation and software for the specific needs of millimeter radioastronomy and for the benefit of the astronomical community. IRAM's laboratories also supply devices to several European partners, including for the ALMA project.

IRAM's scientists conduct forefront research in several domains of astrophysics, from nearby star-forming regions to objects at cosmological distances.

IRAM Partner Organizations:
Centre National de la Recherche Scientifique (CNRS) – Paris, France
Max-Planck-Gesellschaft (MPG) – München, Deutschland
Instituto Geografico Nacional (IGN) – Madrid, España

iram
Institut de
Radioastronomie
Millimétrique

IRAM Addresses:

Institut de Radioastronomie Millimétrique
300 rue de la piscine,
Saint-Martin d'Hères
F-38406 France
Tel: +33 [0]4 76 82 49 00
Fax: +33 [0]4 76 51 59 38
info@iram.fr www.iram.fr

Observatoire du Plateau de Bure
Saint-Etienne-en-Dévoluy
F-05250 France
Tel: +33 [0]4 92 52 53 60
Fax: +33 [0]4 92 52 53 61

Instituto de Radioastronomía Milimétrica
Avenida Divina Pastora 7, Local 20,
E-18012 Granada, España
Tel: +34 958 80 54 54
Fax: +34 958 22 23 63
info@iram.es

Observatorio Radioastronómico de Pico Veleta
Sierra Nevada,
Granada, España
Tel: +34 958 48 20 02
Fax: +34 958 48 11 49

Designed and produced by rebusparis.com
Printed in France